โพรเพนดีไฮโดรจิเนชันและออกซิเดชันบนตัวเร่งปฏิกิริยาแพลทินัมบนแกมมาและไคอะลูมินาแบบผลึกระดับนาโน

นายธงชัย กลิ่นหรั่น

ศูนย์วิทยทรัพยากร
จุฬาลงกรณ์มหาวิทยาลัย

วิทยานิพนธ์นี้เป็นส่วนหนึ่งของการศึกษาตามหลักสูตรปริญญาวิศวกรรมศาสตรดุษฎีบัณฑิต
สาขาวิชาวิศวกรรมเคมี ภาควิชาวิศวกรรมเคมี
คณะวิศวกรรมศาสตร์ จุฬาลงกรณ์มหาวิทยาลัย
ปีการศึกษา 2553
ลิขสิทธิ์ของจุฬาลงกรณ์มหาวิทยาลัย

PROPANE DEHYDROGENATION AND OXIDATION OVER NANOCRYSTALLINE Pt/γ- AND χ- Al_2O_3 CATALYST

Mr. Thongchai Glinrun

ศูนย์วิทยทรัพยากร
จุฬาลงกรณ์มหาวิทยาลัย

A Dissertation Submitted in Partial Fulfillment of the Requirements
for the Degree of Doctor of Engineering Program in Chemical Engineering
Department of Chemical Engineering
Faculty of Engineering
Chulalongkorn University
Academic Year 2010
Copyright of Chulalongkorn University

Thesis Title	PROPANE DEHYDROGENATION AND OXIDATION OVER NANOCRYSTALLINE Pt/γ- AND χ- Al_2O_3 CATALYST
By	Mr. Thongchai Glinrun
Field of Study	Chemical Engineering
Thesis Advisor	Professor Piyasan Praserthdam, Dr.Ing.
Thesis Co-advisor	Assistant Professor Choowong Chaisuk, Dr.Eng.

Accepted by the Faculty of Engineering, Chulalongkorn University in Partial Fulfillment of the Requirements for the Doctoral Degree

..... Dean of the Faculty of Engineering
(Associate Professor Boonsom Lerdhirunwong, Dr.Ing.)

THESIS COMMITTEE

..... Chairman
(Assistant Professor Montree Wongsri, D. Sc.)

..... Thesis Advisor
(Professor Piyasan Praserthdam, Dr.Ing.)

..... Thesis Co-advisor
(Assistant Professor Choowong Chaisuk, Dr.Eng.)

..... Examiner
(Associate Professor Bunjerd Jongsomjit, Ph.D.)

..... Examiner
(Assistant Professor Anongnat Somwangthanaroj, Ph.D.)

..... External Examiner
(Assistant Professor Okorn Mekasuwandumrong, Dr.Eng.)

ศูนย์วิทยทรัพยากร
จุฬาลงกรณ์มหาวิทยาลัย

ธงชัย กลิ่นหรั่น: โพรเพนดีไฮโดรจิเนชันและออกซิเดชันบนตัวเร่งปฏิกิริยาแพลทินัมบนแกมมาและไคอะลูมินาแบบผลึกระดับนาโน (PROPANE DEHYDROGENATION AND OXIDATION OVER NANOCRYSTALLINE Pt/γ- AND χ- Al_2O_3 CATALYST) อ. ที่ปรึกษาวิทยานิพนธ์หลัก: ศ.ดร. ปิยะสาร ประเสริฐธรรม, อ. ที่ปรึกษาวิทยานิพนธ์ร่วม: ผศ.ดร. ชูวงศ์ ชัยสุข, 110 หน้า.

งานวิจัยนี้ แกมมา(γ) ไค(χ) และเฟสผสมของไคและแกมมา(χ/γ)อะลูมินาเตรียมด้วยวิธีการสลายตัวด้วยความร้อนของสารละลายผสมระหว่างบิวทานอลและโทลูอีน เพื่อใช้เป็นตัวรองรับตัวเร่งปฏิกิริยาแพลทินัม ถึงแม้ว่าแกมมาอะลูมินาจะมีพื้นที่ผิวและความเป็นกรดมากกว่าไคอะลูมินา แต่จากการวัดตำแหน่งที่ว่องไวของแพลทินัมบนไคอะลูมินาและแพลทินัมบนแกมมาอะลูมินา พบว่ามีค่าใกล้เคียงกัน แพลทินัมบนเฟสผสมของไคและแกมมาอะลูมินามีค่าตำแหน่งที่ว่องไวสูงกว่าหรืออาจกล่าวได้ว่า มีการกระจายตัวของแพลทินัมสูงกว่า ในปฏิกิริยาโพรเพนออกซิเดชัน จากผลการทดลองพบว่าตัวเร่งปฏิกิริยาเฟสผสมที่มีปริมาณการกระจายตัวของแพลทินัมสูงกว่า จะให้ค่าการเปลี่ยนโพรเพนสูงกว่าเมื่อเทียบกับแกมมาและไคอะลูมินาบริสุทธิ์ ในกรณีที่มีไฮโดรเจน แพลทินัมบนไคอะลูมินาจะให้ความว่องไวมากกว่าแกมมาอะลูมินาในปฏิกิริยาโพรเพนดีไฮโดรจิเนชัน เนื่องมาจากการคายโมเลกุลของไฮโดรเจนได้ง่ายกว่า ซึ่งแสดงได้ด้วยอุณหภูมิที่ต่ำกว่าจากเทคนิค H_2-TPD ค่าการเลือกเกิดไปเป็นโพรพิลีนในตัวเร่งปฏิกิริยาแพลทินัมบนไคอะลูมินามีค่าต่ำทั้งนี้เนื่องมาจากปฏิกิริยาข้างเคียงของการแตกตัวและปฏิกิริยาไฮโดรจิโนไลซิส มีบทบาทสำคัญสำหรับปฏิกิริยาโพรเพนดีไฮโดรจิเนชัน

ศูนย์วิทยทรัพยากร
จุฬาลงกรณ์มหาวิทยาลัย

ภาควิชา...วิศวกรรมเคมี... ลายมือชื่อนิสิต.....

สาขาวิชา...วิศวกรรมเคมี... ลายมือชื่ออาจารย์ที่ปรึกษา.....

ปีการศึกษา...2553... ลายมือชื่ออาจารย์ที่ปรึกษาร่วม.....

4971812921: MAJOR CHEMICAL ENGINEERING
KEYWORDS: PLATINUM / ALUMINA / PROPANE OXIDATION / PROPANE DEHYDROGENATION / COKE / γ-Al_2O_3 / χ-Al_2O_3 / PHASE COMPOSITION

THONGCHAI GLINRUN : PROPANE DEHYDROGENATION AND OXIDATION OVER NANOCRYSTALLINE Pt/γ- AND χ- Al_2O_3 CATALYST
ADVISOR: PROFESSOR PIYASAN PRASERTHDAM, Dr.Ing.,
CO-ADVISOR: ASSISTANT PROFESSOR CHOOWONG CHAISUK, D.Eng., 110 pp.

In this thesis, gamma(γ), chi(χ) and mixed-phase (χ/γ) alumina supports were prepared by solvothermal method of a mixed solution of toluene and butanol and used as the supports for Pt/Al_2O_3 catalysts. Although, γ-alumina possessed higher BET surface area and higher acidity than χ-phase alumina, the measured amount of active sites for Pt/χ-Al_2O_3 and Pt/γ-Al_2O_3 were quite similar. Pt/χ/γ-Al_2O_3 showed higher active sites or higher Pt dispersion. In propane oxidation, the results showed that the mixed-phase catalysts with higher amount of Pt dispersion exhibited much higher propane conversion than both pure gamma and chi alumina. In the presence of H_2, the propane dehydrogenation activities over Pt/χ-Al_2O_3 were higher than Pt/γ-Al_2O_3 due probably to the easier desorption of H_2 molecule as revealed by lower desorption temperature in the H_2-TPD. The selectivity to propylene was low in Pt/χ-Al_2O_3 catalyst due to the side reactions of cracking and hydrogenolysis were more important for propane dehydrogenation.

ศูนย์วิทยทรัพยากร
จุฬาลงกรณ์มหาวิทยาลัย

Department: Chemical Engineering. Student's signature: Thongchai Glinrun
Field of Study: Chemical Engineering. Advisor's signature: Piyasan Praserthdam
Academic Year: 2010 Co-advisor's signature: Choowong Chaisuk

ACKNOWLEDGEMENTS

The author would like to express my heartfelt thanks to all those individuals whose wisdom, support, and encouragement made my journey possible. Special thanks extended to Professor Dr. Piyasan Praserthdam, my advisor and Associate Professor Dr. Choowong Chaisuk, my co-advisor, who guided me through hurdles, and provided constant support that made my journey completed lot easier than it would have been. Despite their busy schedules, they would always find the time to discuss anything from intriguing experimental results to an issue of surviving in the scientific world. I am also grateful to thank Assistant Professor Dr. Montree Wongsri, as a chairman, Assistant Professor Dr. Bunjerd Jongsomjit, Assistant Professor Dr. Anongnat Somwangthanaroj, and Assistant Professor Dr.Okorn Mekasuwandumrong, as the members of thesis committee for precious time, their valuable suggestions and comments.

The author wishes to thank the members of the Center of Excellence on Catalysis and Catalytic Reaction Engineering (CECC), Chulalongkorn University, Thailand for their assistance. To many others, who have provided her with support and encouragement, please be assured that she is appreciated for your kindly help.

Most of all, I would like to express my greatest gratitude to my parents and my family who always gave me suggestions, support and encouragement.

Finally, I gratefully acknowledge financial supports from the Commission on Higher Education of the Thai, Ministry of Education.

ศูนย์วิทยทรัพยากร
จุฬาลงกรณ์มหาวิทยาลัย

CONTENTS

Page

ABSTRACT (THAI)…… iv

ABSTRACT (ENGLISH)…… v

ACKNOWLEDGEMENTS…… vi

CONTENTS…… vii

LIST OF TABLES…… x

LIST OF FIGURES …… xi

CHAPTER

I INTRODUCTION…… 1

II LITERATURE REVIEWS …… 5

2.1 Chi alumina applications …... 5

2.2 Effect of catalyst and support on propane oxidation …… 7

2.3 Effect of catalyst and support on propane dehydrogenation …… 10

2.4 Coke formation on the catalyst ……. 14

III THEORY …… 17

3.1 The Aluminas …… 17

3.1.1 Properties of Alumina…… 17

3.1.2 Formation and crystal structure of active alumina ……. 17

3.1.3 Dehydration of the trihydroxide ……. 19

3.1.4 Dehydration of oxide hydroxide ……. 19

3.1.5 γ –Al_2O_3……. 21

3.1.6 χ –Al_2O_3……. 22

3.1.7 Preparation of Al_2O_3 by solvothermal method …..……. 22

3.2 Propane oxidation …… 23

3.3 Propane dehydrogenation …… 26

3.4 Catalyst deactivation by coking …… 28

3.5 Coking on noble metal catalyst …… 30

3.5.1 Effects of operation conditions on coking deactivation ….. 30

CHAPTER Page

IV EXPERIMENTAL ……..……..……. 33

4.1 Materials and Chemicals ……..……. 33

4.2 Equipment ……..……..……. 33

4.2.1 The equipment for the synthesis of alumina by solvothermal method …… 33

4.3 Catalyst Preparation ……..……..……. 35

4.3.1 Preparation of various phases Al_2O_3 supports by solvothermal method …… 35

4.3.2 Preparation of Pt/Al_2O_3 Catalysts …… 36

4.4 Catalyst characterization ……..……. 37

4.4.1 X-ray Diffraction ……...…..……. 37

4.4.2 BET Surface Area ……...…..……. 38

4.4.3 Transmission Electron Microscopy (TEM)…...…..……. 39

4.4.4 CO-Pulse Chemisorptions ……..….. 40

4.4.5 Propane Temperature-Programmed Desorption (C_3H_8-TPD)……...……..….. 41

4.4.6 Hydrogen Temperature-Programmed Desorption (H_2-TPD)……...…..….. 41

4.4.7 Ammonia Temperature-Programmed Desorption (NH_3-TPD)…….…..….. 41

4.4.8 Fourier Transform-Infrared Spectroscopy (FT-IR)…….... 42

4.4.9 X-ray photoelectron spectroscopy (XPS) 43

4.5 Reaction Study ……..……...……. 44

4.5.1 Propane Oxidation ……...……. 44

4.5.2 Propane Dehydrogenation ……...……. 47

4.5.3 Characterization of coke measurement ……. 50

V RESULTS AND DISCUSSIONS ……. 53

5.1 The properties of Al_2O_3 supports and Pt/Al_2O_3 catalyst …… 53

5.1.1 The physical properties and crystalline structure of alumina supports ……...……. 53

5.1.2 The Properties of 0.3% Pt/Al_2O_3…...……...……. 55

CHAPTER Page

5.2 Catalytic activities of Pt/Al_2O_3 in propane oxidation …….. 64

5.3 Effect of hydrogen on catalytic activities of Pt/Al_2O_3 in propane dehydrogenation …….....……..…...……...……. 65

5.4 Study of coke formation by FT-IR, TPO, and TGA …… 74

5.5 The effect of mixed γ - and χ -crystalline phase Al_2O_3 on propane dehydrogenation 81

VI CONCLUSIONS AND RECOMMENDATIONS……. 83

6.1 Conclusions…….……...…… 83

6.2 Recommendations……...…….. 84

REFFERENCES…… 85

APPENDICES……...…… 100

APPENDIX A : CALCULATION OF THE CRYSTALLITE SIZE.……... 101

APPENDIX B : CALCULATION FOR METAL ACTIVE SITES AND DISPERSION……...…. 104

APPENDIX C : The sample of chromatogram and the calibration curve…. 105

VITA...……...…… 110

ศูนย์วิทยทรัพยากร
จุฬาลงกรณ์มหาวิทยาลัย

LIST OF TABLES

TABLE		Page
4.1	χ/γ ratio in preparing Al_2O_3 supports of solvothermal method …..…	36
4.2	The details of gases used in propane oxidation …..…….……...	44
4.3	Operating conditions of gas chromatographs for propane oxidation...	45
4.4	The details of gases used in propane dehydrogenation ……...	47
4.5	Operating conditions of gas chromatographs for propane dehydrogenation ……...……...……	48
4.6	Operating conditions of gas chromatographs for propane oxidation...	51
5.1	The physical properties of alumina supports…..……....……	55
5.2	The Catalyst properties of 0.3 wt.% Pt/Al_2O_3……...……..	57
5.3	Areas of peaks identified from H_2 TPD data for $Pt/\gamma Al_2O_3$ and $Pt/\chi Al_2O_3$…….…….	61
5.4	XPS binding energies obtained by deconvolution of the Al 2p manifold …….……	64
5.5	The product selectivity of the dehydrogenation of propane over Pt/C100G0 **(**H_2/C_3H_8 ratios =0:1) …….……..	69
5.6	The product selectivity of the dehydrogenation of propane over Pt/C0G100 (H_2/C_3H_8 ratios =0:1) …….……..	70
5.7	The product selectivity of the dehydrogenation of propane over Pt/C100G0 **(**H_2/C_3H_8 ratios =1:1) …….……..	70
5.8	The product selectivity of the dehydrogenation of propane over Pt/C0G100 **(**H_2/C_3H_8 ratios =1:1) …….……..	71
5.9	The product selectivity of the dehydrogenation of propane over Pt/C100G0 **(**H_2/C_3H_8 ratios =3:1) …….……..	71
5.10	The product selectivity of the dehydrogenation of propane over Pt/C0G100 **(**H_2/C_3H_8 ratios =3:1) …….……..	72

LIST OF FIGURES

FIGURE		Page
3.1	Transformation sequence of aluminum hydroxides ……...	18
3.2	Metastable aluminas formed by dehydration of the trihydroxides …	19
3.3	Phase transformation of metastable aluminas formed from trihydroxides in vacuum …..…….....	20
3.4	Conversion vs. temperature in catalytic combustion …….	24
3.5	Typical influence of pressure on stability ……..……	31
3.6	The deposition of coke on Pt/Al2O3 from various hydrocarbon; T = 500 ℃ …….……...……...	32
3.7	Influence of temperature on rate of coke deposition …….……	32
4.1	Autoclave reactor ……...……	34
4.2	Diagram of the reaction equipment for the synthesis of catalyst …..	35
4.3	X-ray refractometer, SIEMENS XRD D5000.....	38
4.4	Micromeritic ChemiSorb 2020 automated system	39
4.5	Micromeritic ChemiSorb 2750 automated system. ……...	40
4.6	Fourier Transform-Infrared Spectroscopy (FT-IR).....	42
4.7	X-ray photoelectron spectroscopy (XPS).....	43
4.8	Schematic diagram of the reaction line for propane oxidation analyzed by gas chromatographs equipped with porapak QS columns……	46
4.9	Schematic diagram of the reaction line for propane dehydrogenation analyzed by gas chromatographs equipped with VZ-10 column …..	49
4.10	Differential Thermal Analyzer (SDT Q800)……...……	50
4.11	Schematic diagram of for temperature programmed oxidation analyzed by gas chromatographs equipped with porapak QS columns……	52
5.1	X-ray diffraction pattern of alumina supports ……	54
5.2	TEM images of 0.3% Pt/Al_2O_3 catalyst with various phase composition…….…….……	56
5.3	C_3H_8-TPD profiles of catalysts with various phase composition.…...	58

FIGURE		Page
5.4	NH_3 TPD data for the C0G100 (Pt/γ-Al_2O_3) and the C100G0 (χ-Al_2O_3) support.……..…….....…	59
5.5	(a) H_2-TPD data for the Pt/γ-Al_2O_3 catalyst…….	60
	(b) H_2-TPD for the Pt/χ-Al_2O_3 catalyst……	61
5.6	FTIR spectra for Pt/γ-Al_2O_3 and Pt/χ-Al_2O_3 catalysts(fresh)…..……	61
5.7	Al 2p XPS spectra of (a) γ-Al_2O_3 support and (b) χ-Al_2O_3 support…	63
5.8	C_3H_8 conversion profiles of 0.3% Pt/Al_2O_3 for the propane oxidation……..	65
5.9	C_3H_8 conversion profiles of 0.3% Pt/Al_2O_3 for the propane dehydrogenation. (H_2/C_3H_8 ratios =0:1) …….	66
5.10	C_3H_8 conversion profiles of 0.3% Pt/Al_2O_3 for the propane dehydrogenation**.** **(**H_2/C_3H_8 ratios =1:1)……..	67
5.11	C_3H_8 conversion profiles of 0.3% Pt/Al_2O_3 for the propane dehydrogenation**.** **(**H_2/C_3H_8 ratios =3:1) ……..…..	68
5.12	C_3H_6 selectivity of Pt/C100G0 and Pt/C0G100 for the propane dehydrogenation. (H_2/C_3H_8 ratios =0:1)……..	72
5.13	C_3H_6 selectivity of Pt/C100G0 and Pt/C0G100 for the propane dehydrogenation. (H_2/C_3H_8 ratios =1:1)……..	73
5.14	C_3H_6 selectivity of Pt/C100G0 and Pt/C0G100 for the propane dehydrogenation. (H_2/C_3H_8 ratios =3:1)……..	73
5.15	FTIR spectra for spent Pt/γ-Al_2O_3 and Pt/χ-Al_2O_3 catalysts with hydrogen/propane ratio a - Pt/C100G0(H_2/C_3H_8=0), b - Pt C100G0 (H_2/C_3H_8=3), c - Pt/ C0G100 (H_2/C_3H_8=0) and d - Pt/ C0G100 H_2/C_3H_8=3)…….……...……..……	75
5.16	Percentage conversion of propane at 5 and 80 min. for Pt/γ-Al_2O_3 and Pt/χ-Al_2O_3 catalysts with hydrogen/propane feed gas mixture ratios of 0:1, 1;1, and 3:1 .....…….……	76
5.17	(a) TPO chart for catalysts used in a dehydrogenation with a hydrogen/propane ratio of 0:1 (500^oC, 80min) …….……..	77
	(b) TPO chart for catalysts used in a dehydrogenation with a hydrogen/propane ratio of 1:1 (500^oC, 80min) ……...	77
	(c) TPO chart for catalysts used in a dehydrogenation with a hydrogen/propane ratio of 3:1 (500^oC, 80min) …….……..	78

FIGURE		Page
5.18	Coking and propane conversion mechanism for the Pt/γ-Al_2O_3 and Pt/χ-Al_2O_3 catalysts. (a) H_2/C_3H_8 Ratio = 0 (b) H_2/C_3H_8 Ratio = 1,3…….……..…..…..….	79
A.1	The diffraction peak of pure chi alumina for calculation of the crystallite size…….……....	103
A.2	The plot indicating the value of line broadening due to the equipment. The data were obtained by using α-alumina as a standard	103
C.1	The sample of chromatogram (Propane oxidation)……..	105
C.2	The calibration curve of oxygen from TCD of GC8ATP…….……...	105
C.3	The calibration curve of C_3H_8 from TCD of GC 8ATP……..	106
C.4	The sample of chromatogram (Propane dehydrognation)……	107
C.5	The calibration curve of C_3H_8 from FID of GC 14B…….....	108
C.6	The calibration curve of C_3H_6 from FID of GC 14B……...	108
C.7	The calibration curve of %chi alumina phase from XRD data……	109

ศูนย์วิทยทรัพยากร
จุฬาลงกรณ์มหาวิทยาลัย

CHAPTER I

INTRODUCTION

Supported platinum catalysts are widely used in reaction involving hydrocarbon. Some reactions, such as dehydrogenation of saturated hydrocarbons and total oxidation of hydrocarbon, have been classified as structure insentivity, i.e., the activity per surface metal atom does not depend on the size of the metal particle. Platinum alumina catalysts are also used for total hydrocarbon oxidation, for instance in automotive post-combustion catalysts or in the catalytic combustion of nature gas. Moreover, Platinum alumina catalysts are widely used in industries to promote various types of reactions involving carbon-bearing feed stocks. One of the very useful applications is the dehydrogenation of hydrocarbons using the supported Platinum catalysts. As with any other catalyst system, activity, selectivity and life are the three important aspects of the application of these heterogeneous catalyst systems. The life, or the stability of activity, is dictated by the possibility of sintering, poisoning or coking. Catalyst coking is a phenomenon which involves the deposition of carbonaceous species on the catalyst surface. The formation of the carbon deposits blocks the metal and plugs the support porosity leading to catalyst inactivity.

Alimina (Al_2O_3) is used as a common support for total oxidation of hydrocarbon and dehydrogenation of hydrocarbons. It has attracted intensive interest compared to the other oxides because of its fine particle size, high surface area; excellent thermal stability, good catalytic activity and a variety of aluminas having these requisites are commercially available [1-3]. Aluminas have a variety of phases, and they are transformed to‘‘transition’’ β-, γ-, η-, χ-, κ-, δ- and α-Al_2O_3 by dehydration and treatment at high temperatures [4]. Among the various crystalline phases of Al_2O_3, γ -Al_2O_3 has received much attention due to its high surface area and less generation of by product [5, 6]. In addition to the gamma phase, other phases have been also used as the supports. The alpha alumina is usually used as the thermal stabilizing material but it shows low surface area.

The χ-Al_2O_3 is one of the metastable polymorps of transition alumina with relatively high thermal stability compared to γ -Al_2O_3. It can be synthesized directly by the solvothermal using appropriate solvent. The advantages of the solvothermal method are that it gives products with narrow particle size distribution, uniform morphology and well-controlled chemical composition. In our preliminary works [7-9], nanocrystalline transition alumina with high thermal stability and micro spherical particles has been synthesized by decomposition of aluminum isopropoxide (AIP) under solvothermal conditions. Pansanga et al. [10, 11] investigated preparing alumina powder by varying the concentration of AIP in 1-butanol and they found that at low AIP content, Al_2O_3 was formed in wrinked sheets-like structure of γ -Al_2O_3 while at high AIP concentrations they were formed with fine spherical particles of χ -Al_2O_3.

In this research, nanocrystalline γ -Al_2O_3, χ -Al_2O_3, and mixed γ - and χ -crystalline phase Al_2O_3 with various χ / γ ratios were prepared by the solvothermal method. The catalysts to be studied comprise of platinum, the main metallic component, supported on alumina support. The reactions used to test the performance of these catalysts are propane oxidation and propane dehydrogenation.

1.1 Objectives

1. To investigate the effect of mixed γ - and χ -crystalline phase Al_2O_3 with various χ / γ ratios on propane oxidation.

2. To investigate the effect of H_2 on propane dehydrogenation compare between phase composition of χ -Al_2O_3 and γ -Al_2O_3.

3. To investigate coke formation on Pt/ χ -Al_2O_3 and γ -Al_2O_3 in dehydrogenation.

4. To investigate the effect of mixed γ - and χ -crystalline phase Al_2O_3 with various χ / γ ratios on propane dehydrogenation.

ศูนย์วิทยทรัพยากร
จุฬาลงกรณ์มหาวิทยาลัย

1.2 Scope of work

1. Preparation of various ratios of gamma and chi phase of alumina support (0-100% chi) by solvothermal techniques.

2. The prepared platinum catalyst which platinum loading on various χ / γ ratios alumina support was 0.3%wt. by incipient wetness impregnation method.

3. Characterization of the catalyst sample using X- ray diffraction (XRD), BET surface area, pulse CO chemisorption, and temperature programmed study.

4. Study the catalytic behavior in the propane oxidation over a Pt/Al_2O_3 catalyst by various ratios of gamma and chi phase of alumina. Feed gas contained 1% propane and excess oxygen balance in helium with gas hourly space velocity of reactant about 6,000 h^{-1}. The reaction temperature was raised from ambient temperature to 450 °C stepwise.

5. Study the catalytic behavior in the propane dehydrogenation over Pt/χ-Al_2O_3, $Pt/\ \chi\ /\ \gamma$-Al_2O_3 and Pt/γ- Al_2O_3 catalyst. Feed stream in case of operating condition at hydrogen/propane = 0, 1, 3 and 5 with gas hourly space velocity of reactant about 8,000 h^{-1}, the operating temperature was 500 °C, analyzed the result by gas chromatograph.

1.3 Research methodology

1. Searching for involving data and literature review.
2. Preparing raw materials and chemical substances.
3. Synthesizing alumina supports by solvothermal method.
4. Catalysts preparation alumina supports Pt catalysts.
5. Characterize the physical properties of catalysts.
    - Morphology and structure analysis by transmission electron microscopy (TEM), and X-ray diffraction (XRD).

- Surface area measurement by N_2-physisorption (BET).
- Surface analysis by fourier transform-infared spectroscopy (FT-IR).
- Metal dispersion by CO-chemisorption measurement.
- Propane chemisorption by hydrogen temperature program desorption (C_3H_8-TPD).
- Hydrogen chemisoption by hydrogen temperature program desorption (H_2-TPD).
- Acidity of support by ammonia temperature program desorption (NH_3-TPD).

6. Reaction study in the propane oxidation.
7. Reaction study in the propane dehydrogenation.
8. Coke analysis.
9. Analyzing all obtained data to find the conclusion of research.
10. Writing thesis and preparing for presentation.

ศูนย์วิทยทรัพยากร
จุฬาลงกรณ์มหาวิทยาลัย

CHAPTER II

LITERATURE REVIEWS

2.1 Chi alumina applications

M. Inoue et al. [12] have studied thermal decomposition of aluminum sec-alkoxide in inert organic solvents at 300°C yielded a product composed of agglomerates of 4- to 20-nm particles having the χ -alumina structure. The χ -alumina was stable and maintained a surface area above 100 m^2/g until its transformation at 1150°C to α -alumina.

Mekasuwandumrong et al. [13] investigated thermal decomposition of aluminum isopropoxide in toluene at 315°C. The results showed that χ -alumina had high thermal stability, whereas the reaction at lower temperatures resulted in formation of an amorphous product. The χ -alumina thus obtained directly transformed to α -alumina at 1150°C, bypassing the other transition alumina phases, whereas the amorphous product transformed to γ -alumina and then to θ -alumina before final transformation to α -alumina. When the χ -alumina, solvothermally synthesized at 315°C, was recovered by the removal of the solvent at the reaction temperature, thermal stability of the product was improved further. This procedure is convenient because it avoids bothersome work-up processes that yield large-surface-area and large-pore-volume alumina.

Mekasuwandumrong et al. [8] have studied the solvothermal reaction of 20 g aluminum isopropoxide (AIP) in mineral oil at 300 ◦C for 2 h and it gave χ -alumina showing high thermal stability while the reaction with higher amounts of starting AIP (30 and 40 g) contributed contamination of pseudoboehmite. The χ -alumina thus obtained directly transformed into α -alumina completely at approximately 1400 ◦C bypassing the other transition alumina phases whereas some part of the contaminated product transformed to γ -alumina through θ -alumina and finally α -alumina. When silicon was doped in the alumina matrix (5, 10, 20 and 50 at.%) using

tetraethylorthosilicate as the silicon (Si) precursor, χ -alumina was still observed without any contaminations at low concentration doping (5–20 at.%). Amorphous structure was obtained by doping 50 wt % Si. The phase transformation temperature was shifted to the high temperature after loading the Si. The α-phase transformation did not go to completion even after calcinations at 1500 ˚C. This could be due to the incorporation of Si atom in alumina lattice forming SiO_2–Al_2O_3 solid solution.

Pansanga et al. [10] prepared nanocrystalline alumina powders by thermal decomposition of aluminum isopropoxide (AIP) in 1-butanol at 300 ^oC for 2 h and employed as cobalt catalyst supports. The crystallization of alumina was found to be influenced by the concentration of AIP in the solution. At low AIP content, wrinkled sheets-like structure of γ-Al_2O_3 was formed, while at high AIP concentrations, fine spherical particles of χ-Al_2O_3 were obtained. They found that using these fine particles alumina as cobalt catalyst supports resulted in much higher amounts of cobalt active sites measured by H_2 chemisorption and higher CO hydrogenation activities.

Mephoka et al. [14] prepared alumina supports by solvothermal method of a mixed solution of toluene and butan-1-ol for various chi/gamma phase compositions and the Pt/Al_2O_3 catalyst was prepared by the incipient wetness impregnation technique. The catalysts were evaluated in the carbon monoxide oxidation. Increasing amount of %chi phase in the alumina supports has roughly the same BET surface area. The different alumina supports were affected on the Pt dispersion on alumina. The pure chi alumina and pure gamma alumina supports had the same effect of catalyst activity. In the various chi/gamma phase compositions, it was found that Pt dispersion and catalyst activity are lower than pure gamma and chi phases for alumina support with 10% chi. The alumina supports with 30–70% chi gave higher dispersion and activity than pure phase and 10% chi support.

Khom-in et al. [11] investigated dehydration of methanol to dimethyl ether (DME) over a wide range of nanocrystalline Al_2O_3 with mixed γ- and χ-crystalline phases. The catalysts were characterized by X-ray diffraction (XRD), N_2 physisorption, and NH_3-tempearture programmed desorption (NH_3-TPD). It was

found that γ-Al_2O_3 catalyst containing 20 wt% of χ-phase exhibited the highest yield (86%) with good stability for DME synthesis. The NH_3-TPD results revealed that the existence of 20 wt% χ-phase in γ-Al_2O_3 increased significantly both the density and the strength of surface acidity.

2.2 Effect of catalyst and support on propane oxidation

P. Bera et al. [15] have studied the catalytic oxidation of both CH_4 and over combustion synthesized nanosize Pt, Pd, Ag and Au C_3H_8 particles supported on α – Al_2O_3 by using the temperature programmed reaction technique in a packed-bed tubular reactor. Complete CH_4 oxidation occurs over 1% Pt/Al_2O_3 and 1% Pd/Al_2O_3 at 350 ^oC and 425 ^oC, respectively, whereas complete oxidation of C_3H_8 over 1% Pt/Al_2O_3 and 1% Pd/Al_2O_3 gives CO_2 and H_2O at 175 and 300 ^oC. Supported Ag and Au both show CH_4 and C_3H_8 conversion at much higher temperatures. Combustion synthesized Pd/Al_2O_3 is a good catalyst for CH_4 oxidation, whereas Pt/ Al_2O_3 is active for C_3H_8 oxidation. The C_3H_8 reaction occurs at a lower temperature than the CH_4 reaction because C_3H_8 contains an easily abstractable secondary hydrogen. Pt/ Al_2O_3 and Pd/Al_2O_3 show better catalytic activities regarding CH_4 and C_3H_8 oxidation than Ag/ Al_2O_3 and Au/ Al_2O_3.

Y. Yazawa et al. [16] examined the oxidation state of palladium on SiO_2-Al_2O_3 used for propane combustion was by XPS and XRD, and the correlation of the catalytic activity with the oxidation state of palladium was systematically studied. The propane conversion over 5 wt% Pd/ SiO_2-Al_2O_3 was measured in the range $1.0<S<7.2$ (S is defined as $[O_2]/5[C_3H_8]$ based on stoichiometric ratio). The propane conversion strongly depended on the S value and reached the maximum at S.5.5. They found that the oxidation state of palladium also changed with the S value; palladium particles were more oxidized under the reaction mixture of higher S value.On the sample used for the reaction at S.5.5, both of metallic palladium and palladium oxide were found. It is concluded that partially oxidized palladium which has optimum ratio of metallic palladium to palladium oxide shows the highest catalytic

Y. Yazawa et al. [17] investigated the kinetic study of support effect on the low-temperature propane combustion over platinum catalysts. The catalytic activity of

supported platinum catalysts varied with the support material, and $Pt/SiO_2–Al_2O_3$ showed much higher activity than Pt/ZrO_2. The reaction order for oxygen was negative and that for propane was positive. The reaction order for propane and oxygen also greatly depended on the support material: Pt/ZrO_2 gave anomalous reaction orders, i.e., −2.9 for oxygen and 3.4 for propane. Further, oxidized Pt/ZrO_2 showed a long-term change of the catalytic activity with time-on-stream, compared with oxidized $Pt/SiO_2–Al_2O_3$. From the results, they concluded that high catalytic activity of platinum on acidic support is attributed to high ability to maintain the metallic state of platinum with high oxidation-resistance and high reducibility of platinum oxide.

Y. Yazawa et al. [18] studied the support effect on the low temperature catalytic combustion of propane over palladium catalyst was studied by using a series of metal oxides as support materials: MgO, ZrO_2, Al_2O_3, SiO_2, $SiO_2– ZrO_2$, $SiO_2–Al_2O_3$, and $SO_4^{2-}–ZrO_2$. They found that the catalytic activity varied with the kind of the support materials; a support material with moderate acid strength gave maximum conversion. The maximum activity was obtained at high concentration on $Pd/SiO_2–Al_2O_3$, at moderate concentration on Pd/Al_2O_3, and at low concentration on Pd/ZrO_2. This sequence corresponded to that of acid strength of the support materials measured by Hammett indicators.

H. Yoshida et al. [19] have studied the effects of support and additive on the oxidation state and catalytic activity of Pt catalyst in the low temperature propane combustion were systematically investigated on Pt/MgO, Pt/Al_2O_3 and $Pt/SiO_2–Al_2O_3$. The catalytic activity varied much with both support materials and additives. The catalyst on the more acidic support showed higher activity, and the catalytic activity on every support materials increased as the electronegativity of additives increased, while some additives decreased the activity.

G. Corro et al. [20] has investigated the nature of the active sites of non-sulfated and sulfated $1\%Pt/\gamma\text{-}Al_2O_3$ for the combustion of propane. An enhancement in the activity for propane oxidation was confirmed with the sulfated catalyst. FTIR spectroscopy proved the formation of sulfate species in the catalyst surface. XPS results revealed an increased formation of a highly oxidized Pt species over sulfated $1\%Pt/\gamma\text{-}Al_2O_3$ that suggests that the promoting effect on the propane combustion is

due to the interaction of surface sulfates with surface highly oxidized Pt atoms that can be ascribed to Pt^{4+} at the edge of the Pt particles

A.. Gluhoi et al. [21] investigated oxidation of propene and propane to CO_2 and H_2O over Au/Al_2O_3 and two different $Au/CuO/Al_2O_3$ (4 wt.% Au and 7.4 wt.% Au) catalysts and compared with the catalytic behavior of $Au/Co_3O_4/Al_2O_3$ (4.1 wt.% Au) and Pt/Al_2O_3 (4.8 wt.% Pt) catalysts. The various characterization techniques employed (XRD, HRTEM, TPR and DR-UV–vis) revealed the presence of metallic gold, along with a highly dispersed CuO (6 wt.% CuO), or more crystalline CuO phase (12 wt.% CuO). A higher CuO loading does not significantly influence the catalytic performance of the catalyst in propene oxidation, the gold loading appears to be more important. Moreover, it was found that $7.4Au/CuO/Al_2O_3$ is almost as active as Pt/Al_2O_3, whereas $Au/Co_3O_4/Al_2O_3$ performs less than any of the CuO-containing gold-based catalysts. The light-off temperature for C_3H_8 oxidation is significantly higher than for C_3H_6. For this reaction the particle size effect appears to prevail over the effect of gold loading. The most active catalysts are $4Au/CuO/Al_2O_3$ (gold particles less than 3 nm) and $4Au/Co_3O_4/Al_2O_3$ (gold particles less than 5 nm).

B. Solsona et al. [22] have shown the supported and unsupported nanocrystalline cobalt oxides to be extremely efficient catalysts for the total oxidation of propane. Total conversion with a high stability has been achieved at reaction temperatures as low as 250ºC. Their works, a comparison between the catalytic performance of bulk and alumina supported nanocrystalline cobalt oxide catalysts has been made. The influence of crystallite size, nature of the support (alpha, gamma and mesoporous alumina) and cobalt loading, have been probed. Unsupported cobalt oxide catalysts were more active than any supported cobalt oxide catalysts. The catalytic activity was mainly dependant on the crystallite size, decreasing with an increase in the crystallite size.

2.3 Effect of catalyst and support on propane dehydrogenation

O. Barias et al. [23] have studied the catalytic dehydrogenation of propane over Pt and Pt-Sn catalysts supported on γ-Al_20_3 and SiO2. Without the promoter Pt shows the same initial specific activity (TOF) on both supports, but deactivates

rapidly due to coking. The effect of Sn as a promoter depends on the support. On γ-Al_20_3 tin interacts with the support and is stabilized in an oxidation state > 0. The result is an increase in Pt dispersion and reduced deactivation without any change in the initial specific activity in dehydrogenation. The selectivity to propene is strongly enhanced by tin, particularly due to blocking or poisoning of acid sites on the support. On SiO_2 the Sn is more readily reduced, and alloy formation is possible. This leads to a similar increase in Pt dispersion and improved catalytic stability, but also to a strong reduction in the specific activity. The change in catalytic stability on both supports is parallelled by a dramatic change in the hydrogen adsorption properties, as seen from the TPD profiles after reduction.

O. Barias et al. [24] prepared Pt and Pt–Sn catalysts supported on SiO_2 and γ-Al_2O_3 by impregnation and studied temperature programmed reduction (TPR), hydrogen chemisorption, temperature programmed desorption(TPD) and catalytic dehydrogenation of propane. They found that without the promoter Pt shows the same initial specific activity on both supports, but deactivates rapidly due to coking. The effect of Sn as a promoter depends on the support. On γ- Al_2O_3 tin interacts with the support and is stabilized in an oxidation state >0. The result is an increase in Pt dispersion and an improved stability of the catalytic activity without any change in the initial specific activity in dehydrogenation. On SiO_2 the Sn is more readily reduced, and. alloy formation is possible. This leads to a similar increase in Pt dispersion and improved catalytic stability, but also to a strong reduction in the specific activity. The change in catalytic stability on both supports is paralleled by a dramatic change in the hydrogen adsorption properties, as seen from the TPD profiles after reduction.

G. Aguilar-Rios et al. [25] prepared Pt-Sn/$ZnA1_20_4$ catalysts by two-step impregnation (first tin), with a Sn/Pt atomic ratio ranging from zero to 6.72, and characterized by hydrogen chemisorption, temperature-programmed reduction and tested in isobutane dehydrogenation. Metal dispersion correlates linearly with reaction rate; both parameters reach a maximum when the Sn/Pt atomic ratio is about one. The activity of the sites capable of hydrogen chemisorption, as expressed in turnover frequency number, TOF, decrease as the tin concentration is increased. From

theoretical ab-inito calculations, it is proposed that tin reduces the platinum-hydrogen charge transfer responsible for hydrogen dissociation through an orbital overlapping.

E.L. Jablonski et al. [26] have studied the effect of the Ga addition to Pt/Al_2O_3 on the performance in propane dehydrogenation. Mono and bimetallic catalysts were characterized by tests reactions, TPR, H_2 chemisorption, FT-IR of preadsorbed CO, and tested in propane dehydrogenation by using a pulse technique. Results showed that the selectivity to propylene is enhanced by the Ga addition, while the catalyst deactivation and the carbon formation are decreased when the Ga content increased. Ga appears to have a very low effect on the acidity function, but it modified the structure of the metallic phase in a different way according to the previous reduction temperature. Thus, at low reduction temperature (573 K) the action of Ga can be related only to geometric effects, while after reducing at high temperature (773 K), additional effects including Ga blocking, and in a minor extension, an electronic modification of Pt sites, would take place.

J. Salmones et al. [27] prepared bimetallic $Pt–Sn/MgAl_2O_4$ catalysts with different metal concentrations, used for propane dehydrogenation, by the impregnation, coprecipitation–impregnation and sol–gel methods. Pore size distribution and surface acidity of the catalysts were studied by N_2 physisorption and temperature programmed desorption of ammonia (TPD-NH_3), respectively. Reduction behaviors of the catalysts were characterized by temperature programmed reduction (TPR) technique. In the catalysts containing 0.6 wt.% Sn, some platinum-modified by tin crystals were produced by association with acid sites of the support, where hydrogen reduction took place above 500 $^{\circ}$C. These tin-modified platinum species were found to be favorable for propane dehydrogenation reaction and also to be responsible for the improvement of the activity as tin content increases from 0.3 to 0.6 wt.%.Metal dispersion, pore size distribution and acidity of the support strongly impact the selectivity and stability of the catalysts. The sol–gel catalyst showed better selectivity but lower stability compared to other catalysts that can be explained by its very narrow pore size distribution and relatively stronger acidity as well as more homogeneous metal distribution on the support. When the catalysts were pretreated with oxygen and then hydrogen, their catalytic activities were significantly enhanced largely due to a better metal distribution on the support.

L. Bednarova et al. [28] investigated platinum and tin deposited on γ -Al_2O_3, MgO, and Mg(Al)O supports by CO chemisorption and analytical electron microscopy in the scanning transmission electron microscopy with energy-dispersive X-ray spectrometry (STEM/EDX). Composition and size of individual particles in the 1-nm range are presented and results are compared with dispersion measurements obtained from volumetric chemisorption. They demonstrated that dispersion determined by chemisorption measurements can give unrealistically low values, possibly caused by metal–support interaction, while STEM/EDX reveals the correct size of metal particles. The metal–support interaction seems not to be present on γ -Al_2O_3 support but only on Mg(Al)O and MgO supports. The performance of the catalyst in propane dehydrogenation is related to the amount of Pt on the metal particle surface. It is shown that there is a relationship between the composition of metal particles and the activity of the catalyst. The most active is a catalyst that contains metal particles with high Pt content; however, some Sn is necessary for reduced coking and probably for increased stability.

C. Yu et al. [29] have studied the effects of Ce addition on the Pt-Sn/γ-Al_2O_3 catalysts for propane dehydrogenation to propylene by reaction tests. The results showed that the Ce addition could greatly improve the catalytic performance and catalytic stability of the Pt-Sn/γ-Al_2O_3, which is reported as the optimal catalyst for propane dehydrogenation to propylene. We could keep >38% of propane conversion, >98% propylene selectivity and >37% propylene yield over 50 h in the reaction of propane dehydrogenation to propylene over Pt-Sn/Ce- Al_2O_3 catalysts at 576 ^oC, 3800 h^{-1} and $H_2/C_3H_8/Ar$ = 1/1/5. The presence of Ce in the Pt-Sn/Ce- Al_2O_3 catalysts could not only stabilize the active states of Pt, Sn and support, but could also suppress the coke accumulation on the catalyst during reaction, and further improve the catalytic performance of Pt-Sn/γ-Al_2O_3.

Y. Zhang et al. [30] prepared PtSn/ZSM-5 catalyst with different amounts of Sn for propane dehydrogenation. It was found that the addition of Sn not only had ‘‘geometric effect’’, thus decreasing the size of the surface Pt ensembles, but also changed the interfacial character between metal and support. The presence of Sn could facilitate the transfer of the carbon deposits from the active sites to the carrier,

which in consequence improved the catalytic stability. Suitable concentration of Sn on PtSn/ZSM-5 catalyst was preferable for the reaction. With the continuous addition of Sn, more amounts of Sn^0 species could be formed, which was disadvantageous to the reaction. Compared to PtSn/c-Al2O3, the capacity of the catalyst that supported on ZSM-5 zeolite to accommodate the coke was much better. The possible reason may attribute to the larger surface area and the particular character of the channels of ZSM-5 zeolite.

C. Yu et al. [31] studied the influence of the zinc addition to alumina supported Pt and PtSn, not only on the activity, selectivity and deactivation in the propane dehydrogenation reaction, but also on the characteristics of platinum metal phase. Zinc can give a remarkable improvement in dehydrogenation performance of catalysts. High propylene selectivity (≥97%) can be obtained over zinc-doped catalysts. The presence of zinc modifies the metallic phase, mainly by geometric and electronic modifications of the metallic phase. These modifications could be responsible for the improvement of catalytic performance.

2.4 Coke formation on the catalyst

Majority of propane dehydrogenation reaction are affected by a deactivation phenomenon, which results from the coking of catalysts. As the result of this problem, there have been a very large number of experimental and theoretical investigations of catalyst deactivation by coking. In the present work, the coke formation on the catalysts is considered.

Barbier et al. [32] have studied the selective poisoning by coke formation on Pt/Al_2O_3. The thermal programmed oxidation of coke by oxygen mixture was studied in the 0 ^{O}C – 500 ^{O}C range. Two peaks were observed. One could be ascribed to metal deactivation, the other to coke on alumina. The effects on three test reactions by cyclopentane have differed due to the sites deposited by coke.

Barbier et al. [33] have characterized the coke deposited on heterogeneous catalysts by temperature programmed oxidation. The comparison between the amount of CO_2 produced and the amount of O_2 consumed gives the ratio H/C. For Pt/Al_2O_3

catalysts it has been shown the coke deposited on the metal is less dehydrogenated than coke deposited on the support.

Beltramini et al. [34] have studied the deactivating effect of different paraffins, naphthenes and aromatics during their reforming over a Pt/Al_2O_3 catalyst was studied. It was found that coke formation is not directly related to the molecular weight of those hydrocarbons, but to their structure or to those of their principal products. The n-pentane produces more coke than n-hexane or n-heptane, but coke deposition increases with the molecular weight of higher n-paraffin. The five carbon atom ring is the most important coke precursor for naphthenes. For aromatics, the structure and position of the chains joined to the aromatic ring have an important influence on coke formation. The deactivating effect of coke does not only depend on its amount because it affects in different ways the metallic and the acidic functions of the catalyst. The reactions that occur with different feeds are diversely affected according to their particular mechanisms of reforming.

Barbier et al. [35] have studied the effect of metallic dispersion on coke formation from cyclopentane reactions was studied on a series of Pt/Al_2O_3 catalysts of widely varying accessibility. While small metal crystallites presented a strong resistance to coke deposition, the big particles showed a higher sensitivity to this poison. The results can be explained by means of a higher stabilization of the adsorption of the cyclopentadiene produced during the reaction, by the big platinum crystallites than by the small ones which present an electron efficiency due to metal-support interactions.

Marecot et al. [36] investigated coke deposition during cyclopentane reaction on Pt/Al_2O_3 catalysts of varying dispersity. For all working pressures the higher the metallic accessibility, the higher the amount of coke deposited on the catalyst. Nevertheless, coke deposited on the less dispersed catalysts is more toxic for the metallic function. An increasing metal accessibility improves the graphitization of coke on the support and so, prevents the deactivation of the metal of a bifunctional catalyst.

Parera et al. [37] have studied an acidic (Al_2O_3-Cl), a metallic (Pt/SiO_2) and a bifunctional catalyst (Pt/Al_2O_3-Cl) used in naphtha reforming. Temperature programmed oxidation of the coked catalysts shows that the coke on the metal is oxidized at lower temperatures than that on the acid function. According to C_1/C_3 (metal to acid), coke is mainly produced on the metal at the start of the run. At increasingly severe coking conditions, coke is produced on both functions and at higher severities or times it is produced mainly on the acidic function. Coke on the metal is in equilibrium with gaseous hydrogen. On increasing the hydrogen pressure, the coke is eliminated more easily from the metal than from the acid.

Mongkhonsi et al. [38] have investigated temperature programmed oxidation of coke deposited on Pt based propane dehydrogenation catalysts. They found that the deposited coke can be categorized into three groups according to their burning temperatures. When coke was separated from the catalyst, however, only one TPO peak could be observed. Experimental results suggest that gamma $A1_20_3$ enhances the coke burning process by increasing coke surface area contacts to oxygen. Pt may also act as a catalyst for the coke combustion reaction. Experiments also show that changing dehydrogenation reaction temperature, variation of H/HC ratios, addition of only Sn or Sn and an alkali metal (Li, Na and K) can significantly affect the amount of each coke formed. Sample weight used in the temperature programmed oxidation (TPO) experiment also affects the resolution of TPO spectrum.

Xu et al. [39] have studied carbon deposition and migration, as well as their influence on the performances of Pt/Al_2O_3 and $Pt\text{-}Sn/Al_2O_3$ dehydrogenation catalysts. The results showed that carbonaceous precursors first adsorbed at the active metal sites, and then migrated onto the acidic support surface. It was also found that the rate of carbon deposition on the Pt/Al_2O_3 was quicker than that on the $Pt\text{-}Sn/Al_2O_3$ at the initial period during butane dehydrogenation. The coking rate on the Pt catalyst increased slowly with continual reaction, while that on the Pt-Sn catalyst increased linearly, and finally overtook the Pt catalyst. However, the amount of carbonaceous material migrated from the metal to the support was larger on the Pt-Sn catalyst than on the Pt catalyst. For the same amount of carbon deposition, e.g. 8 wt%, on the catalyst surface, 50% of the metal surface on the Pt-Sn catalyst remained uncovered, whereas only 25% of the metal surface of the platinum catalyst was bare. Hence,

addition of tin into the Pt/Al_2O_3 catalyst could increase its catalytic activity and stability for paraffin dehydrogenation.

ศูนย์วิทยทรัพยากร
จุฬาลงกรณ์มหาวิทยาลัย

CHAPTER III

THEORY

Alumina is an important material in many field because of its excellent and wide range properties. Study of Alumina has been a subject of great interest for many decades. It is one of the most common crystalline materials to be used as adsorbent, coating, soft abrasives, catalyst and catalyst support because of its fine particle size, high surface area, and surface catalytic activity.

3.1 The Aluminas [40]

3.1.1 Properties of Alumina

Alumina which is Al_2O_3 is general form is a polymorphic material. Alumina can be easily synthesized small particles and obtained desirous surface area and pore distribution. Commercial alumina have surface area between 100-600 m^2/g. High porosity solid cause high intra surface area, good metal dispersion and increasable effective of catalytic. There are many form of alumina (β-, γ-, η-, χ-, κ-, δ- and α-Al_2O_3) but the α-Al_2O_3 is the only stable form. The thermodynamically stable phase is alpha alumina (α-Al_2O_3, corundum) where all Al ions are equivalent in octahedral coordination in a hep oxide array. α-Al_2O_3, (corundum) powders are applied, in catalysis as supports, for example, of silver catalysts for ethylene oxidation to ethylene oxide, just because they have low Lewis acidity, low catalytic activity, and conversely, they are mechanically and thermally very strong. All other alumina polymorphs are metastable.

3.1.2 Formation and crystal structure of active alumina

Alumina can exist in many metastable phases before transforming to the stable α-alumina (corundum form). There are six principal metastable phases of alumina designated by the Greek letters chi (χ), kappa (κ), eta (η), theta (θ), delta (δ), and gamma (γ), respectively. Although the range of temperature in which each transition

phase is thermodynamically stable has been reported by many researchers, they are inconsistent, depending upon various factors such as degree of crystallinity of sample, amount of impurities in the starting materials, and the subsequent thermal history of sample. Most of the studies on phase transformation of alumina were conducted by calcination of alumina precursor. It was found that difference in the phase transformation sequence is resulted from the difference in the precursor structure [41, 42]. Moreover, the transformation sequence is irreversible. The nature of the product obtained by calcination depends on the starting hydroxide and on the calcination condition (Figure 3.1) . The phase transformation sequences, from metastable Al_2O_3 structures to the final stable α-alumina phase, reported in the literature are also approximates.

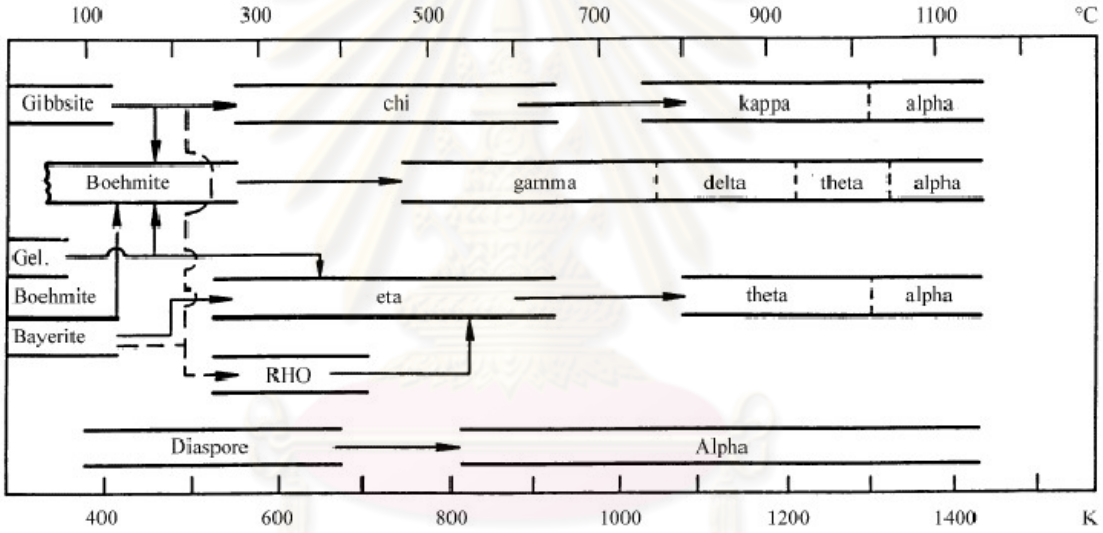

Figure 3.1 Transformation sequence of aluminum hydroxides[43].

The phase transformation sequence normally starts with aluminum hydroxide ($Al(OH)_3$ and AlOOH) transforming to low-temperature phase of alumina (η and χ) at temperature around 150-500^{o}C, and subsequently to high temperature phase (δ,θ,κ) at temperature around 650-1000^{o}C. Finally, the thermodynamically stable phase, α-alumina, is formed at temperature around 1100-1200^{o}C. It is generally believed that α-phase transformation takes place through the nucleation and growth mechanism.

Aluminas are usually obtained by dehydration of various hydroxides. Much controversy exits about the dehydration of various sequences, even in recent work [43, 44]. Apart from difficulties in characterization of the obtained forms, most of the confusion arises from insufficient information concerning the reaction conditions.

3.1.3 Dehydration of the trihydroxide

The dyhydration of gibbsite in air and nitrogen gives the sequence of products different from dehydration of bayerite or nordstrandite (Figure 3.2) . Both crystallinity and particle size of gibbsite are much greater than those of bayerite and nordstrandite. Up to 25% of boehmite can be contaminated by the intergranular hydrothermal reactions in the product from the dehydration of gibbsite, whereas less than 5% is usually formed from bayerite and nordstrandite. However, very fine powders of bayerite [45] and gibbsite do not form any boehmite at all. Detailed phase transformations starting from the trihydroxides are shown in Figure 3.2.

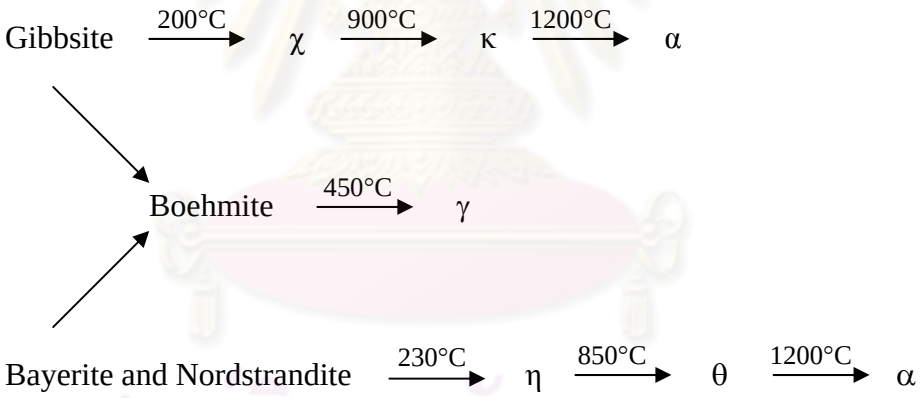

Figure 3.2 Metastable aluminas formed by dehydration of the trihydroxides.

In vacuum (Figure 3.3) , three kinds of trihydroxide decompose at low temperatures into almost completely amorphous product (ρ-alumina), which changes into γ- and η- alumina and further into θ-alumina upon the calcination at high temperature, as shown in Figure 3.3.

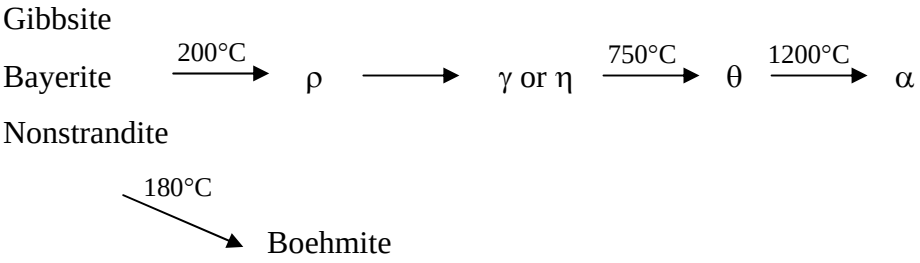

Figure 3.3 Phase transformation of metastable aluminas formed from trihydroxides in vacuum.

3.1.4 Dehydration of oxide hydroxide

Diaspore is the only aluminum hydroxide that transforms directly into α-alumina [46], which initially has high surface area before recrystallization.

The dehydration sequence of boehmite depends on its crystallinity. Well crystallized boehmite (crystal sizes > 1 μ) decomposes according to :

Well crystallized boehmite $\xrightarrow{450°C}$ γ $\xrightarrow{700°C}$ δ $\xrightarrow{1050°C}$ θ+α $\xrightarrow{1200°C}$ α-Al_2O_3

Formation of δ-phase strongly depends on impurities and crystallinity of boehmite. Small amount of Na favors the formation of θ-alumina, whereas Li and Mg stabilize δ-alumina and can prevent the formation of θ-alumina. If boehmite has low crystallinity, the formation of δ-alumina is retarded.

Gelatinous boehmite (pseudoboehmite) decomposes at temperature around 300°C into alumina. Due to the poor crystallinity of the pseudoboehmite, formation of δ-alumina is hardly observed. Thus the dehydration scheme is :

Gelatinous boehmite $\xrightarrow{300°C}$ γ $\xrightarrow{900°C}$ δ $\xrightarrow{1000°C}$ θ+α $\xrightarrow{1200°}$ α-Al_2O_3

Gamma alumina is an enormously important material in catalysis. It is used as a catalyst in hydrocarbon conversion (petroleum refining), and as a support for

automative and industrail catalysts. It is one of the metastable polymorphs of transition alumina, which is normally obtained by decomposition of boehmite. Boehmite transforms to γ-alumina at temperature in the range of 500-800°C and consequently to δ-alumina at 900°C.

3.1.5 γ –Al_2O_3 [47]

γ –Al_2O_3 which is the most used form of alumina in industry and any field of technologies is mostly obtained by decomposition of the boemite oxyhydroxide γ-AlOOH (give medium surface area lamellar powders , ~ 100 m^2/g) or of a poorly crystallizied hydrous oxyhydroxide called “pseudobomite” at 327 to 527 ^oC, giving high surface area materials (~ 500 m^2/g). However, the details of its structure are still matter of controversy. It has a cubic structure describe by Lippens [47] and de Boer [47] to be a defective spinel, although it can be tetragonally distorted. Being the stoichiometry of the “normal” spinel $MgAl_2O_4$ (with Al ions virtually in octahedral coordination and Mg ions in tetrahedral coordination) the presence of all trivalent cations in γ–Al_2O_3 implies the presence of vacancies in usually occupted tetrahedral or octahedral coordination sites. Soled proposed that the cation charge can be balanced, more than by vacancies, by hydroxyl ions at the surface. In fact, γ-Al_2O_3 is always hydroxylated; dehydroxylation occurring only at a temperature where conversion to other alumina forms is obtained. XRD studies using the Rietveld method, performed by Zhou [47]and Snyder[47], suggested that Al^{3+} cations can be in positions different from those of spinels, that is, in trigonal coordination. The possibility of a structure of γ-Al_2O_3, as “hydrogen-spinel” has been proposed based on IR spectroscopy. Calculations based on the composition HAl_5O_4 have been performed but found that this structure is very unstable. Sohlberg et al. [47] arrived to a structure very similar to that proposed by Zhou and Snyder, based on spinel but with occupation of extraspinel sites. On the contrary, Digne et al. [47] and Krokidis et al [47] proposed a structure based on ccp oxide lattice but different from that of a spinel, with 25% of Al ions in tetrahedral interstice and no structural vacancies. According to these authors, this structure, although unstable with respect to corundum, is more stable than that of the spinel based structures. γ-Al_2O_3 is also active as an acidic catalyst. As for example it is very active in the dehydration of alcohols to olefins and

to ether as well as both in double bond isomerization and in skeletal isomerization of olefins.

3.1.6 χ –Al_2O_3

χ-alumina is a modification of transition alumina [43, 48]. It is characterized by the appearance of a diffraction peak at d = 0.212 nm, which cannot be explained by the spinel structure proposed for other transition aluminas, such as γ- and η- phases. χ-alumina is a crystallographic from of transition alumina, normally obtained by dehydration of gibbsite (<200 nm) [49, 50]. Dollimore [51]et al. have reported that χ-alumina is formed by thermal decomposition of aluminum oxalate and that aluminum oxalate has a crystal structure similar to that of gibbsite. Normally, χ-alumina transforms into κ- alumina at temperature around 650-750 ^{o}C with a loss in surface area by phase transformation. There are three different unit cells suggested for χ-alumina structure : cubic and two forms of hexagonal close packing with different lattice parameters[52].

3.1.7 Preparation of Al_2O_3 by solvothermal method

The synthesis method for producing Al_2O_3 has many methods, which are under intensive worldwide investigation for powder preparation. Solvothermal method has been developed from hydrothermal method for synthesis of metal oxide and binary metal oxide, by using solvent as the reaction medium under pressure and at temperatures above its normal boiling point. The advantages of the solvothermal method are given products with uniform morphology, well-controlled chemical composition, narrow particle size distribution, controlled crystal structures, and controlled grain sizes and morphologies can be controlled by process conditions such as solute concentration, reaction temperature, reaction time and the type of solvent [10].

3.2 Propane oxidation

The catalytic combustion of hydrocarbons has been widely used for the power generation in gas turbine combustors and for emission control of automotive exhausts. For the catalytic combustion, supported noble metal catalysts, mostly supported platinum catalysts are recognized to be the most active for the catalytic combustion of lower alkanes such as propane, excepting for supported palladium catalysts in case of methane oxidation [15, 53-57].

Catalytic combustion of alkane is a complex reaction and the literature on catalytic combustion is plentiful in seemingly contradictory results. The reaction mechanism of alkane oxidation over the precious metal on alumina has been reported as under oxygen rich conditions [58-61], oxygen can adsorb much more effectively than alkane resulting on the high coverage of chemisorbed oxygen on metal surface. The slowest step of reaction has been postulated as the dissociative chemisorption of the alkane on the bare metal surface with the breakage of the weakest C-H bond [62-65] followed by its interaction with oxygen adsorbed on an adjacent site. If the metal surface atoms are sites for both hydrocarbon chemisorption and oxygen, then they compete with each other and the surface coverage of both reactants is interdependent. The nature of some basic phenomena of catalytic combustion still remains controversial, many researchers report conclusions on the “structure-sensitiveness” of the reaction in the case of methane and propane combustion over supported metal catalysts [53, 66-69].

The general pattern of catalytic combustion of hydrocarbons is well established (Figure 3.4). As temperature is increased, oxidation is initiated at a temperature that depends on the hydrocarbon and the catalyst. A further increase in temperature leads to an exponential increase in rate (area B in Figure 3.4) to the point where heat generated by combustion is much greater than heat supplied. The reaction becomes mass transfer controlled (area C) until the reactants are depleted (area D). One important factor in the catalytic combustion of hydrocarbons is ‘light off’. This can be defined in various ways but refers to the temperature at which mass transfer control becomes rate controlling. Because of the shape of the curve (Figure 3.4), the

definition of light-off temperatures as the temperature at which conversion reaches10%, 20% or 50% makes little difference [70].

It is also seen that the kinetics of catalytic combustion are only relevant to parts A and B of Figure 3.4. Once light-off occurs, mass and heat transfer are the important parameters. The geometry of the catalytic combustor together with the porosity of the catalyst/support have much more effect in this region.

The reaction rapidly approaches complete conversion of one or both reactants and the heat generated from the combustion results in a significant increase in catalyst temperature. Thus, the stability of catalysts at high temperatures is also of considerable interest. It is possible to design devices in which efficient heat transfer is used to minimize temperature rise (e.g. the catalytic boiler) but particular attention must be paid in all cases to the temperature stability of materials. Thus, it is clear that considerations of catalytic combustion must include the chemical reactivity of the catalyst and the hydrocarbon (areas A and B), mass and heat transfer effects (area C) and maximum temperatures reached (relevant to area D).

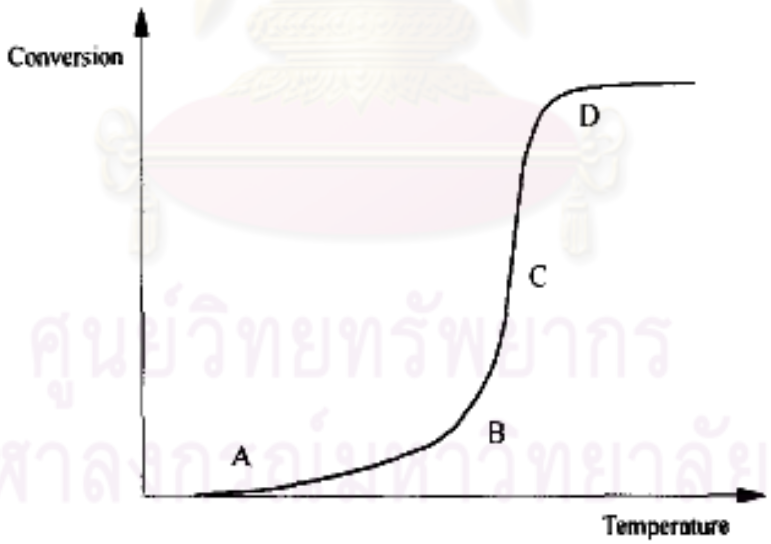

Figure 3.4 Conversion vs. temperature in catalytic combustion [70].

In some cases, further complexity may result from the initiation of homogeneous combustion by overheating the catalyst [71] . The present article considers mass and heat transfer effects only briefly, but relevant references are provided. Rather, attention is focused on the oxidation of methane on various catalysts

in the absence and presence of supports. Finally, the performance of catalyst with respect to deactivation and sintering is examined.

The production of energy by the combustion of propane and natural gas is well established. Overall, the reaction may be represented by the equation

$$C_3H_8 + 5O_2 \longrightarrow 3CO_2 + 4H_2O \qquad (3.1)$$

This overall equation is, however, a gross simplification with the actual reaction mechanism involving very many free radical chain reactions . Gas-phase combustion can only occur within given flammability limits, and the temperatures produced during combustion can rise to above ca. 1600 ^{o}C, where the direct combination of nitrogen and oxygen to unwanted nitrogen oxides can occur.

Catalytic combustion offers an alternative means of producing energy. A wide range of concentrations of hydrocarbon can be oxidized over a suitable catalyst, and it is possible to work outside the flammability limits of fuel. Reaction conditions can usually be controlled more precisely, with reaction temperatures being maintained below 1600°C. This may be important both to minimize the production of nitrogen oxides and also to avoid thermal sintering of the catalyst.

Catalysts and catalytic oxidation

Metal oxides and noble metals such as Pt, Rh and Pd have been used as catalysts for the catalytic oxidation of methane. Noble metal catalysts show higher activity than metal oxide catalysts [72, 73]. They can be used either with or without a support, but supported catalysts are favored for the oxidation. One particular advantage of supported metal catalysts is that the metal is dispersed over a greater surface area of the support and shows different activity from the unsupported metals due to interactions of the metal with the support. The support also reduces thermal degradation. The application of noble metals other than Pt and Pd in catalytic combustion is limited practically because of their high volatility, ease of oxidation and limited supply. Palladium and platinum have been the most widely used catalysts for the catalytic oxidation of propane.

3.3 Propane dehydrogenation

The dehydrogenation of paraffin gases to the corresponding olefins is still a problem of fundamental importance to the oil industry, though the technical problem of efficiently converting gaseous olefins into liquid motor fuel has been solved within recent years by both catalytic (solid phosphoric, cold and hot sulfuric acids) and purely thermal process. Therefore, a process for the conversion of paraffin into olefins would put to good use all the paraffin gasses except methane. These gases are available in enormous quantities from such sources as natural gas and gasoline, petroleum distillation gas, gas from the cracking processes, coke-oven gas and refinery gasoline. A catalytic dehydrogenation process has been developed for converting normal and isobutene, propane and ethane to the corresponding olefins.

For the past several years the demand for propylene has been increasing due to its important role in a myriad of (petro) chemical applications such as in the production of polypropylene, cumene, etc. [74-76]. So far, a major part of the propylene demand has been supplied by conventional crackers such as steam and fluid catalytic (FC) crackers where propylene is produced as a by-product [77-79]. Due to the growing demand, the high severity crackers were optimized to increase the production of propylene; however they are governed by the gasoline demand. As a result of this, the rate of propylene recovery from FCC has been increased today to ~ 80% as compared to 29% in 1980 [77, 78]. Nevertheless, these conventional crackers are not keeping up with the propylene demand resulting in a gap between demand and supply. Therefore, on-purpose propylene production technologies such as dehydrogenation of propane (DHP) [79, 80] has been developed. Since then, these technologies have received a great deal of attention due to their potential to make-up the shortfall of propylene supply left by conventional crackers.

Dehydrogenation of hydrocarbons on metals is exemplified by the reaction

$$C_3H_8 \rightleftharpoons C_3H_6 + H_2 \qquad (3.2)$$

The reaction (3.1) did not go by the simple removal of two hydrogen atoms togive propylene, since there was extensive H-D exchange between the hydrogen of

C_3H_6 and D_2 from the research by Turkvich [81] et al . This exchange indicates that the elementary reaction steps are reversible and forms the basis of the following propose reaction mechanism(asterisks represent surface sites) :

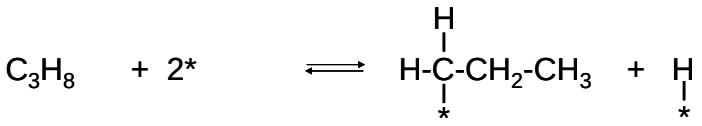
(3.3)

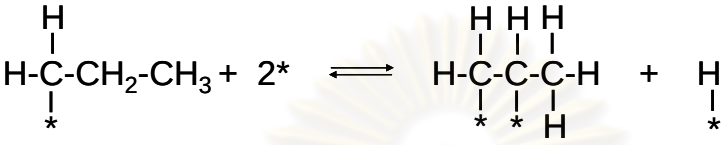
(3.4)

(3.5)

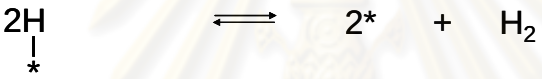
(3.6)

There is another type of dehydrogenation, illustrated by the surface – reaction step:

(3.7)

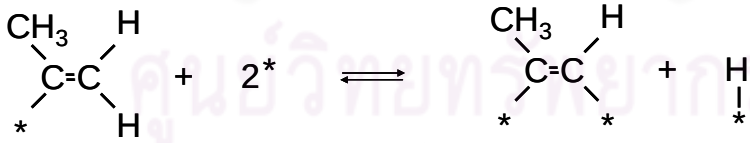
(3.8)

Here there is further C-H bond scission, leading to what is essentially an adsorbed propyne molecule. This was shown to be the cause of a self-poisoning of the catalyst. Since propyne is more strongly adsorbed than propylene, propylene formed on the surface wound have a short residence time before adsorbing because of competition with the more strongly adsorbed propyne. This wound keep the surface concentration of propylene low, consequently propylene will be produced under the dehydrogenation conditions.

3.4 Catalyst deactivation by coking

A catalyst may lose its activation or its selectivity for a wide variety of reason. The caused may be grouped loosely in poison , fouling , reduction of active area by sintering or migration and loss of active species [82]. One of these deactivation which was mainly focused on the present work is the deactivation by fouling. The term fouling is generally used to describe a physical blockage such as the deposit of fine powder or carbonaceous deposit (coke). In the latter case activity can usually be restored by removal of the coke by burning. The deactivation by fouling have been paid attention by researchers for long times. Hughs et al. [83] has mentioned that the catalyst deactivation by fouling usually involves significant amounts of deposition by an impurity in the feed stream.

The first is typified by coke or carbon deposition on catalyst which occurs under certain conditions when hydrocarbon streams are proceed. Since the deposit originates from a cracking type reaction either the feed stream or in the various products, it can not be completely eliminated. On the other hand, the latter is typified by poisoning so that the feed may, in principle, be purified to remove the impurities. The fouling by coke deposition is always associated with the main reaction. Therefore, it is usually not possible to eliminate the coke deposition totally, but the process of coking can often be substantially reduced by modifying the catalyst so as to improve its selectivity. An example of this is the addition of small amounts of alkali to stream reforming and dehydrogenation catalysts. This reduces the acidity of the catalyst and tends to reduce the cracking type reactions that may occur.

Examples of reactions that produce carbonaceous deposits are extremely numerous. Virtually any process having carbon atoms in the feed or product molecules can, under appropriate condition, give rise to deposition of coke. Naturally, molecules with large numbers of carbon atom/or those with aromatic or naphthenic rings ten to produce coke deposits more easily. Both aromatics and olefins are the immediate coke precursors which readily yield coke deposits.

Butt et al. [84] has started that on the deactivation by fouling the strongly adsorbed carbonaceous deposits could form large polynuclear aromatic structures,

apparently through polymerization and condensation. However, coke is not a well-defined substance; normally it has an empirical formula approximating CH, but the chemical nature depends very much on how it is formed. For, example, coke is known to develop in filamentous or whisker-like structures of encapsulating-type structures on metal and in pyrolytic-type structures on acidic surface. The coke also varies depending on reaction temperature and pressure. Moreover, these structures change as they age on the catalyst surface. Thus, it is apparent that they are great variations in the morphology of the coke depending on the catalyst and its history. Butt et al. [84] has commented that industrial hydrocarbon feeds are complex mixtures of compounds and products formed. The activity of the catalyst depends on the number of active centers that are available to carry out the main reactions.

3.5 Coking on noble metal catalyst

The coke of catalysts containing noble metals has long been of interest, primarily as a result of the industrial importance of reforming catalysts and their deactivation as a result of coke formation. Platinum, other metals and binary and ternary alloys are of particular interest and have been studied in detail

There are several unusual features associated with coking of noble metals and several differences from transition metals. Most studies have been carried out using a Pt/Al_2O_3 reforming catalyst and it is important to remember that both metal and support can coke.

3.5.1 Effects of operation conditions on coking deactivation

Operating conditions have an extremely important influence on the deactivation of reforming catalysts. Franck and Martino [85] and Figuli et al. [86] give excellent summaries as follows:

3.5.1.1 Hydrogen and hydrocarbon pressures

From thermodynamics, dehydrogenation will be the best to operate at he lowest possible hydrogen pressure but it is well known that the catalysts are unstable

under these conditions because of enhanced coking [87]. Figure 3.5 shows the evolution of the temperature needed at the inlet of the reators in order to maintain a constant level of performance during operation according to different hydrogen pressure, it can be seen that although deactivation is relatively slow under 50 bar, it becomes very fast even under 10 bar of hydrogen pressure. It is noted that when H_2/HC ratio is below 10, the effect is extremely important.

It is interest to note that a decrease in hydrogen pressure not only promotes aging but also modified the reaction rate. At low hydrogen pressure, there are many highly unsaturated species on the surface of the catalyst which are precursors of coke, whereas at high hydrogen pressure there is less mobile coke but fewer of the intermediates which are needed for reaction.

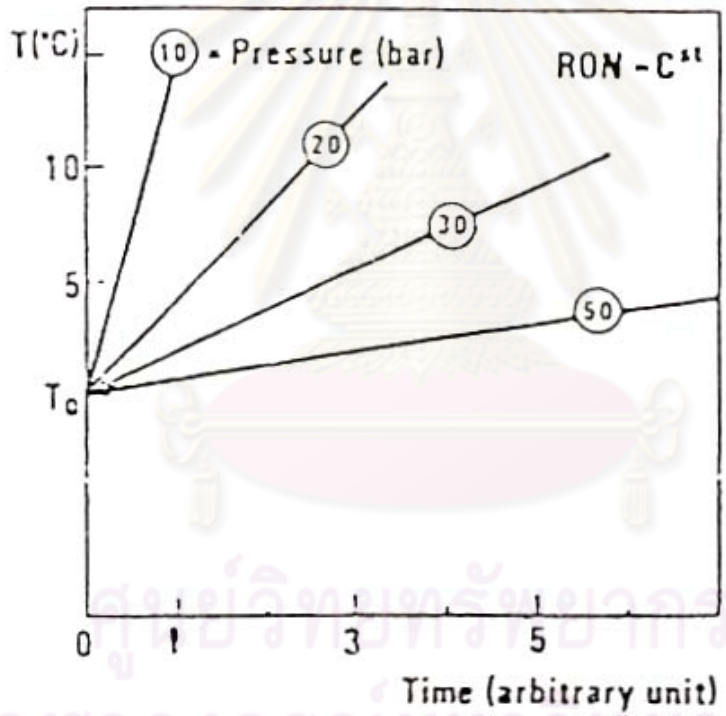

Figure 3.5 Typical influence of pressure on stability [87].

3.5.1.2 Nature of hydrocarbon

Cooper and Trimm [88] showed that the coke evaluation on Pt/Al_2O_3 catalyst for number of different hydrocarbon have 6 carbon atoms. The initial deposition is on the metal site while that at latter times is on the alumina. It is obvious from Figure 3.6 that the rate of coke decreases in the following order for both metal an alumina sites:

Methyl cyclopentane > 3-methylpentane > n-hexane > 2-methylpentane > benzene > cyclohexane

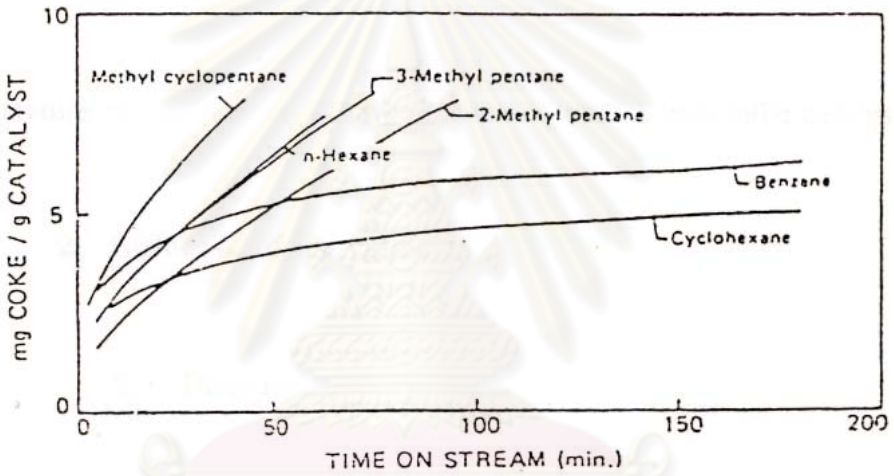

Figure 3.6 The deposition of coke on Pt/Al2O3 from various hydrocarbon; T = 500 ^{o}C [88].

ศูนย์วิทยทรัพยากร
จุฬาลงกรณ์มหาวิทยาลัย

3.5.1.3 Temperature

Temperature is the only possible operating variable for activity maintenance in an industrial unit. Figure 3.7 shows the influence of temperature on the amount of coke contained with a bimetallic catalyst.

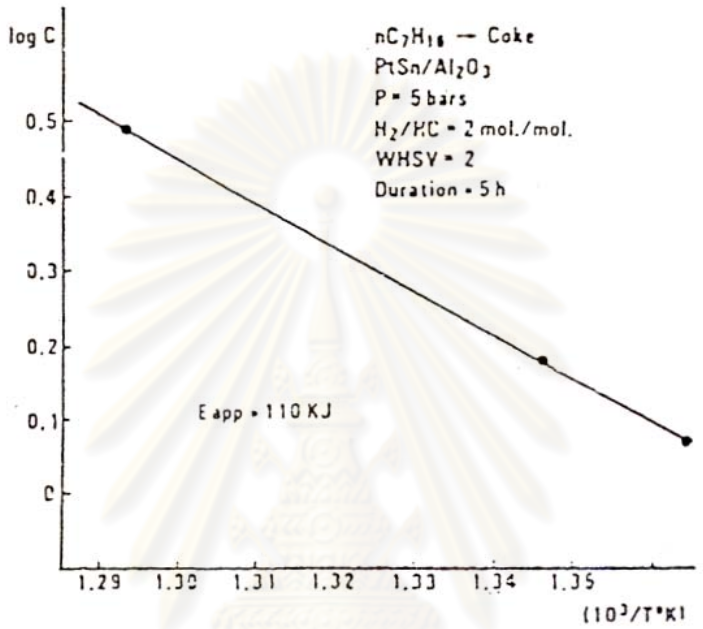

Figure 3.7 Influence of temperature on rate of coke deposition [85].

ศูนย์วิทยทรัพยากร
จุฬาลงกรณ์มหาวิทยาลัย

CHAPTER IV

EXPERIMENTAL

This chapter consists of experimental systems and procedures used in this work which is divided into five parts. The chemicals and equipment for preparation and reaction are shown in section 4.1 and section 4.2, respectively and the preparation of Al_2O_3 supports and Pt/Al_2O_3 catalysts are shown in section 4.3. Section 4.4 describes the details of catalyst characterization by various techniques. The last part (section 4.5) describes the catalytic test in propane dehydrogenation and propane oxidation . In each part the details of procedure, chemicals and apparatus were described as the following:

4.1 Materials and Chemicals

The details of chemicals for preparation of various phases Al_2O_3 catalysts and catalytic reaction are as follows:

1. Aluminum Isopropoxide: AIP, ($[(CH_3)_2CHO]_3Al$) from Aldrich.
2. Chloroplatinic acid hexahydrate ($H_2PtCl_6 \cdot 6H_2O$) from Aldrich.
3. 1-Butanol, (C_4H_9OH) from Fluka.
4. Toluene, ($C_6H_5CH_3$) from Fisher Scientific.
5. Methanol, (CH_3OH) from Merck.
6. De-ionized water.

4.2 Equipment

4.2.1 The equipment for the synthesis of alumina by solvothermal method consisted of:

4.2.1.1 Autoclave reactor

- Made from stainless steel.

- Pressure gauge was connected.
- Relief valve used to prevent runaway reaction.
- Test tube was used to contain the reagent and solvent.

Autoclave reactor used for the experiment is shown in Figure 4.1.

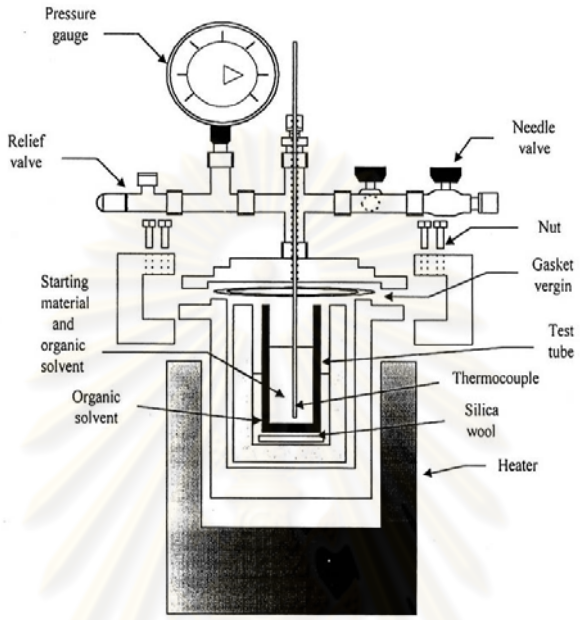

Figure 4.1 Autoclave reactor.

Experiments

- Thermocouple is attached to the reagent in the autoclave.
- Amount of starting material = 25 g
- Amount of organic solvent in the test tube = 100 ml and amount of organic solvent in the gap between test tube and autoclave wall = 30 ml

4.2.1.2 Temperature program controller

A temperature program controller was connected to a thermocouple attached to the autoclave.

4.2.1.3 Electrical furnace (Heater)

Electrical furnace supplied the required heat to the autoclave for the reaction.

4.2.1.4 Gas controlling system

Nitrogen was set with a pressure regulator (0-150 bar) and needle valves were used to release gas from autoclave. The diagram of the reaction equipment for the synthesis of catalyst is shown in Figure 4.2

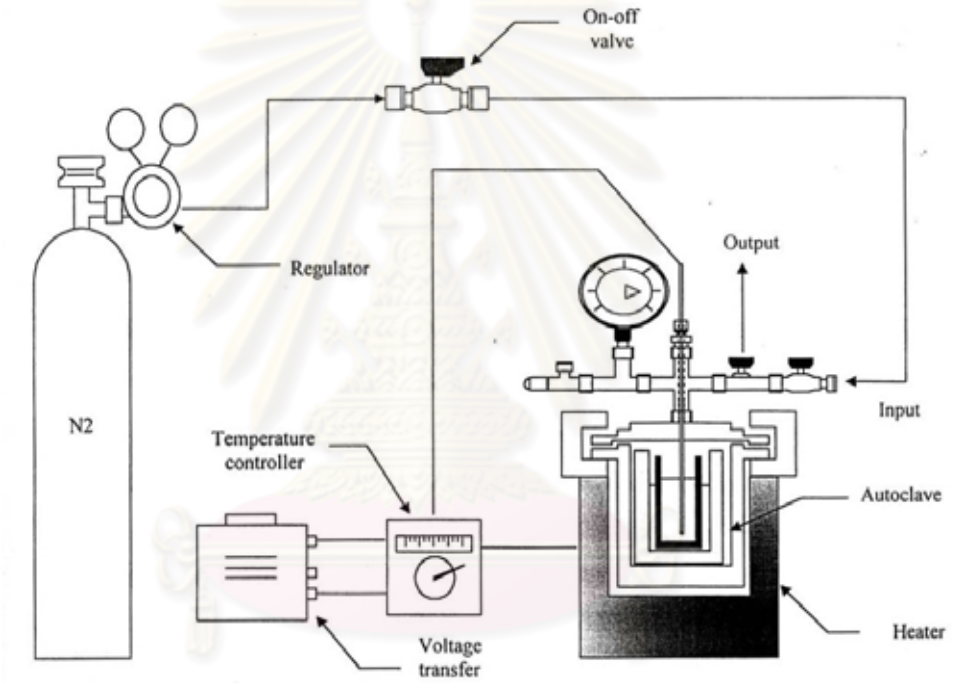

Figure 4.2 Diagram of the reaction equipment for the synthesis of catalyst.

4.3 Catalyst Preparation

4.3.1 Preparation of various phases Al_2O_3 supports by solvothermal method

Nanocrystalline transition Al_2O_3 catalysts with various χ/γ phase compositions were prepared by using solvothermal method. 25 g of aluminum isopropoxide (AIP) was suspended in 100 ml of desired organic solvent in a test tube, and then the test

tube was placed in a 300-ml autoclave. An additional 30 ml of same solvent was placed in the gap between the autoclave wall and the test tube. The autoclave was completely purged with nitrogen, heated to a desired temperature at a rate of 2.5°C min^{-1} and kept at that temperature for 2 h. After the autoclave was cooled to room temperature, the resulting product was repeatedly washed with methanol by vigorous mixing and centrifuging and then dried in air. The organic solvents used in this study were toluene, 1-butanol, and the mixed solvents between toluene and 1-butanol with various compositions. The as-synthesized powders were calcined in air at 600°C for 6 h with a heating rate of 10°C/min. The obtained Al_2O_3 supports comprised of 0, 30, 50, 70 and 100% χ-phase.

Table 4.1 χ/γ ratio in preparing Al_2O_3 supports of solvothermal method.

χ/γ ratio	In test tube (ml)		In the gap between the autoclave wall and the test tube (ml)	
	Toluene	1-Butanol	Toluene	1-Butanol
0/100	0	100	0	30
30/70	30	70	9	21
50/50	50	50	15	15
70/30	70	30	21	9
100/0	100	0	30	0

ศูนย์วิทยทรัพยากร
จุฬาลงกรณ์มหาวิทยาลัย

4.3.2 Preparation of Pt/Al_2O_3 Catalysts

Pt/Al_2O_3 was prepared by the impregnation technique detailed as follows:

1. The amount of platinum was calculated just enough for 2 g of the alumina support and then de-ionized water was added until the total volume of the solution became 2 ml for alumina.

2. 2 g of alumina support was impregnated with aqueous solution of chloroplatinic acid hexahydrate. The impregnation solution was gradually dropped into this support using a dropper. Mixing the support continuously during impregnation was required to ensure the homogenous distribution of metal component on the support.

3. After the incipient wetness impregnation, the mixture of the impregnation solution and the alumina support was left in the atmosphere for 6 hours to make a good distribution of metal complex. Subsequently, the impregnated sample was dried at 110 °C overnight in an oven.

4. The dried sample was purged under nitrogen at a flow rate of 60 ml/min with a heating rate of 10°C/min from room temperature to 500°C. When the temperature was reached to 500°C, 100 ml/min of air flow was instead of nitrogen in order to make silver complex become silver oxide, which was in a stable form. The temperature was held at 500°C for 3 h in air atmosphere.

4.4 Catalyst characterization

This section explains the characterization of catalyst including the crystal structure by XRD analysis, BET Surface Area, Transmission electron microscope (TEM), the metal active sites by CO chemisorptions, hydrogen chemisorptions by Hydrogen Temperature-Programmed Desorption (H_2-TPD), the acidity measurement by NH_3-TPD procedure and the structural properties of catalyst and carbonaceous deposition by Fourier Transform-Infrared Spectroscopy (FT-IR).

4.4.1 X-ray Diffraction

X-ray diffraction analysis was used to analyze the crystallinity and the structure of a catalyst. The refraction or diffraction of the X-rays was monitored at various angles with respect to the primary beam X-ray diffraction analysis using an X-ray refractometer, SIEMENS XRD D5000 (Figure 4.3) , with Ni-filtered CuKα radiation in the 2θ range of 20 to 80°.

Figure 4.3 X-ray refractometer, SIEMENS XRD D5000

ศูนย์วิทยทรัพยากร
จุฬาลงกรณ์มหาวิทยาลัย

4.4.2 BET Surface Area

Surface area, pore volume, average pore diameter, and pore size distribution of catalysts will measured by the BET method, with nitrogen as the adsorbate using a micrometritics model ASAP 2020 (Figure 4.4) at liquid-nitrogen point temperature (-196° C) at the Analysis Center of Department of Chemical Engineering, Faculty of Engineering, Chulalongkorn University.

Figure 4.4 Micromeritic ChemiSorb 2020 automated system

4.4.3 Transmission Electron Microscopy (TEM)

Transmission Electron Microscopy (TEM) will be used to investigate morphology and crystallography of the catalyst particles. Model of TEM: JEOL JEM-2010 employs a LaB_6 electron gun operating in the voltage range of 80 to 200 kV, with an optimal point-to-point resolution of 0.23 nm. Facilities available on this instrument at National Metals and Materials Technology Center (MTEC) include a maximum specimen tilt of 30 degrees along both axes, single-tilt and double-tilt specimen holders, Oxford Instruments Link ISIS 300 X-ray microanalysis system, and Scanning Transmission Electron Microscopy (STEM) attachment.

4.4.4 CO-Pulse Chemisorptions

CO-Pulse Chemisorptions of Pt/ were performed in a Micromeritic ChemiSorb 2750 (Figure 4.5) automated system attached with ChemiSoft TPx software.Platinum dispersion will be determined by pulsing carbon monoxide over the reduce catalyst. Approximately 0.2 g of catalyst is filled in a quartz tube, incorporated in a temperature-controlled oven and connected to a thermal conductivity detector (TCD). Prior to chemisorptions, the catalyst was reduced in a flow of hydrogen (50cc/min) at 500 °C for 1 h, afterward; the sample was purged with helium to cool down to room temperature. Carbon monoxide is pulse at room temperature over the reduced catalyst until the TCD signal is constant.

Figure 4.5 Micromeritic ChemiSorb 2750 automated system.

4.4.5 Propane Temperature-Programmed Desorption (C_3H_8-TPD)

Temperature programmed desorption of C_3H_8 study was performed in a Micromeritic ChemiSorb 2750 automated system attached with ChemiSoft TPx software. A 0.2 g of catalyst was placed in a quartz u-tube in a temperature-controlled oven and connected to a thermal conductivity detector (TCD). The catalyst was first purged under 50 $cm^3 \cdot min^{-1}$ of H_2 flow at 500 °C for 1 h (using a ramp rate of 10 °C·min^{-1}) and cooled down to room temperature with He gas. The C_3H_8 flowed pass the sample at 30 $cm^3 \cdot min^{-1}$ for 30 minutes. Then the sample was passed by He gas until base line was stable. The temperature programmed desorption was performed with a constant heating rate of at 10 °C·min^{-1} from room temperature to 600 °C.

4.4.6 Hydrogen Temperature-Programmed Desorption (H_2-TPD)

Temperature programmed desorption of H_2 study was performed in a Micromeritic ChemiSorb 2750 automated system attached with ChemiSoft TPx software. A 0.2 g of a calcined catalyst was placed in a quartz u-tube in a temperature-controlled oven and connected to a thermal conductivity detector (TCD). The catalyst was first purged under 50 $cm^3 \cdot min^{-1}$ of H_2 flow at 500 °C for 1 h (using a ramp rate of 10 °C·min^{-1}) and cooled down to room temperature in H_2 gas. Then H_2 gas was replaced by He with the flow rate 30 $cm^3 \cdot min^{-1}$ and passed the sample until base line was stable. The temperature programmed desorption was performed with a constant heating rate of at 10 °C·min^{-1} from room temperature to 800 °C.

4.4.7 Ammonia Temperature-Programmed Desorption (NH_3-TPD)

The acidity of the catalyst samples was determined by temperature programmed desorption of ammonia using a Micromeritics Chemisorp 2750 with a computer. In an experiment, about 0.10 gram of the catalyst sample was placed in a quartz tube and pretreated at 500 °C in a flow of helium. The sample was saturated with 15%NH_3/He at 100°C. After saturation, the physisorbed ammonia was desorped in a helium gas flow at that temperature until base line was stable. Then the sample

was heated from 100°C temperature to 550 °°C at a heating rate 10 °°C /min. The amount of ammonia in effluent was measured via TCD signal as a function of temperature.

4.4.8 Fourier Transform-Infrared Spectroscopy (FT-IR)

For FT-IR technique, we used this method to characterize the structural properties of catalyst and carbonaceous deposition by the lattice vibration. The vibration bands between 400 and 4000 cm^{-1} can indicate the structural framework of catalyst and coke catalyst. Approximately 0.08 g of sample was recorded IR spectra by Nicolet mode Impact 400 (Figure 4.6) equipped with a deuterated triglycine sulfate (DTGS) detector and supported with omnic version 1.2a on windows software.

Figure 4.6 Fourier Transform-Infrared Spectroscopy (FT-IR)

4.4.9 X-ray photoelectron spectroscopy (XPS)

Surface-oriented characterization to identify Al coordination on the support relies on X-ray photoelectron spectroscopy (XPS) methods. . XPS analysis was performed using an AMICUS photoelectron spectrometer (Figure 4.7) equipped with a Mg K_α X-ray as a primary excitation and a KRATOS VISION2 software. XPS elemental spectra were acquired with 0.1 eV energy step at a pass energy of 75 kV. The C 1s line was taken as an internal standard at 285.0 eV.

Figure 4.7 X-ray photoelectron spectroscopy (XPS)

4.5 Reaction Study

4.5.1 Propane Oxidation

4.5.1.1 Materials

The gases used in the catalytic activity test are listed in Table 4.2. They were all supplied by Thai Industrial Gas Limited.

Table 4.2 The details of gases used in propane oxidation.

Gases	Formula	Grade
Helium	He	Ultra high purity
Oxygen	O_2	10% in He
Propane	C_3H_8	3% in He

4.5.1.2 Apparatus

A flow diagram of the system for testing the catalytic activity is shown in Figure 4.8. A quartz flow reactor with 0.6 cm inside diameter was used in this experiment. Feed and effluent gases were analyzed by TCD gas chromatographs, SHIMADZU GC-8AIT. An operating condition used in this experiment is given in Table 4.3.

ศูนย์วิทยทรัพยากร
จุฬาลงกรณ์มหาวิทยาลัย

4.5.1.3 Procedure

Catalytic runs were performed in a quartz tube with 6 mm inside diameter, approximately 0.2 gram of catalyst was loaded in this tube. Composition of products was analyzed on-line using a gas chromatograph with a TCD detector (SHIMADZU GC 8A) with a Porapak QS column. Temperature programmed reaction was performed to observe the catalyst activity as a function of temperature. The gas feed

was obtained by mixing three gas sources. The concentrations of propane and oxygen in the reaction mixture were 1.0 and 7.0%, respectively. Helium was used as a balance gas, and the total volumetric flow rate of 100 cm^3 min^{-1} was corresponding with GSHV of 16,000 h^{-1}. The reaction gases were raised stepwise from ambient temperature to 450 ^oC. At each step, after the catalyst bed temperature attained the desired value, the reaction condition was kept for 20 min. The apparatus consists of a reactor, and automatic temperature controller, and electrical furnace and gas controlling system are shown in Figure 4.8.

Table 4.3 Operating conditions of gas chromatographs for propane oxidation.

Gas Chromatograph	SHIMADZU GC8A-AIT
Detector	TCD
Packed column	Porapak QS
Carrier gas	He (UHP)
Flow rate of carrier gas	30 ml/min
Injector temperature	110°C
Column temperature	90°C
Detector temperature	110°C
Current	90 mA
Analyzed gas	C_3H_8, H_2O

ศูนย์วิทยทรัพยากร
จุฬาลงกรณ์มหาวิทยาลัย

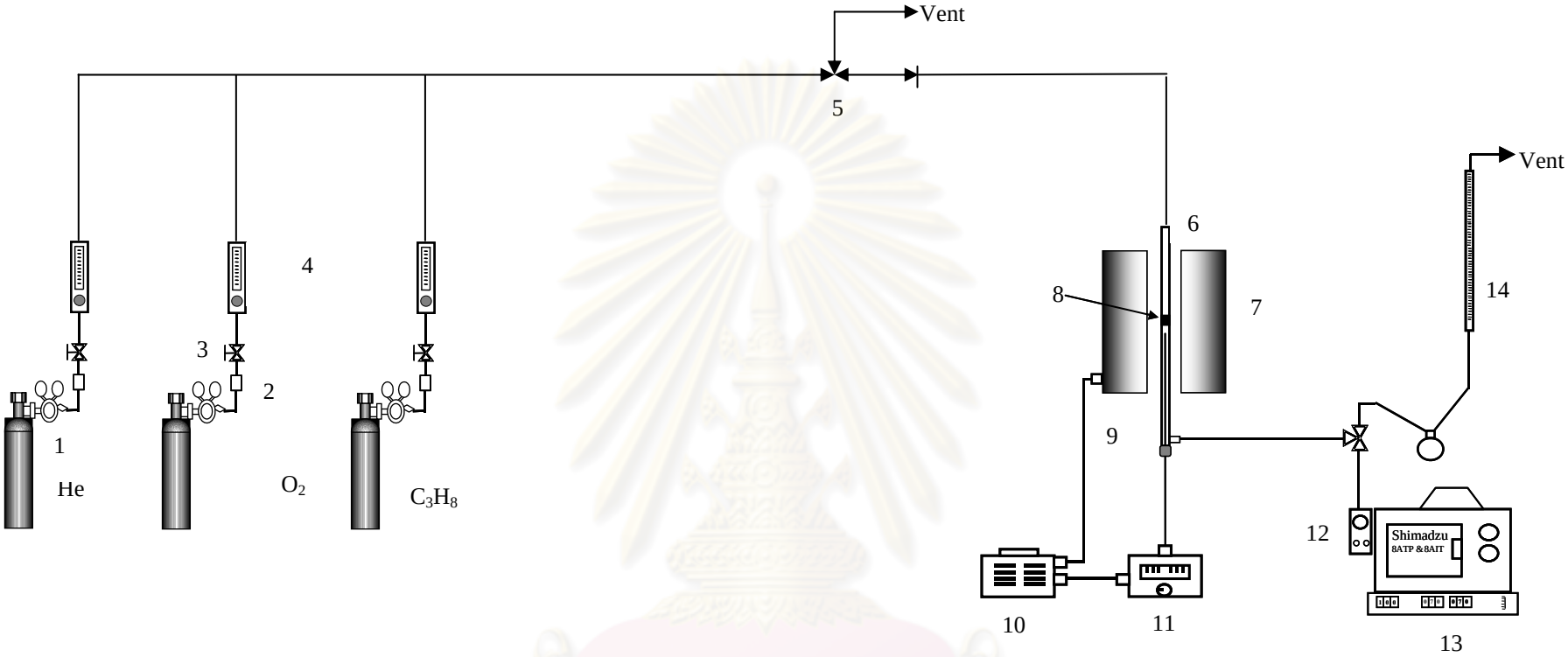

1. Pressure Regulator 2. Gas Filter 3. On-Off Valve 4. Flow meter 5. Three-way Valve
6. Reactor 7. Furnace 8. Catalyst Bed 9. Thermocouple 10. Variable Voltage Transformer
11. Temperature Controller 12. Sampling Valve 13. Gas Chromatography 14. Bubble Flow Meter

Figure 4.8 Schematic diagram of the reaction line for propane oxidation analyzed by gas chromatographs equipped with porapak QS columns.

4.5.2 Propane Dehydrogenation

4.5.2.1 Materials

The gases used in the catalytic activity test are listed in Table 4.4. They were all supplied by Thai Industrial Gas Limited.

Table 4.4 The details of gases used in propane dehydrogenation.

Gases	Formula	Grade
Helium	He	Ultra high purity
Hydrogen	H2	Ultra high purity
Propane	C_3H_8	Ultra high purity

4.5.2.2 Apparatus

A flow diagram of the system for testing the catalytic activity is shown in Figure 4.9. A quartz flow reactor with 0.6 cm inside diameter was used in this experiment. Feed and effluent gases were analyzed by Shimadzu GC-14B flame ionization detector (FID) gas chromatograph with a VZ-10 column. An operating condition used in this experiment is given in Table 4.4.

4.5.2.3 Procedure

The apparatus used was an ordinary atmospheric flow system consisting of a quartz reactor. The reactor temperature was controlled by an electric furnace. A schematic diagram of the apparatus is shown in Figure 4.5. 0.1 gram of catalyst (Pt/ χ -Al_2O_3 or γ -Al_2O_3) was packed in the middle of quartz reactor. The reactor was placed in the furnace and then hydrogen gas was introduced into the reactor at a flow rate of 100ml./min. The reactor was heated up at an increasing rate of 10 ^oC/min until the temperature reached 500 ^oC and held at this temperature for 1 hour. When the reduction time was completed, the hydrogen gas was changed to the helium gas for 5

min. To start the propane dehydrogenation reaction, the helium gas was changed to the feed stream in case of operating condition at hydrogen/hydrocarbon(propane) = 0, 1, and 3 at a flow rate of 30 ml/min. The first sampling was started at 5 minutes, next was 20 min, 35 min, 50 min and finished at 80 min (0.3%Pt/50%χ- Al_2O_3 and 0.3%Pt/70%χ- Al_2O_3 were selected to investigate the effect of mixed γ - and χ - phase on propane dehydrogenation at the ratio hydrogen/propane = 1, 3). The gas compositions were analyzed during the process with a Shimadzu GC-14B flame ionization detector (FID) gas chromatograph with a VZ-10 column. The operating condition of gas chromatograph used for analyzing the effluent stream is shown in Table 4.5.

Table 4.5 Operating conditions of gas chromatographs for propane dehydrogenation.

Gas Chromatograph	SHIMADZU GC-14B
Detector	FID
Packed column	VZ-10
Carrier gas	N_2 (UHP)
Flow rate of carrier gas	250 kpa
Column temperature	
- initial	70°C
- final	70°C
Injector temperature	100 ^oC
Detector temperature	150 ^oC
Analyzed gas	Hydrocarbon C1-C4

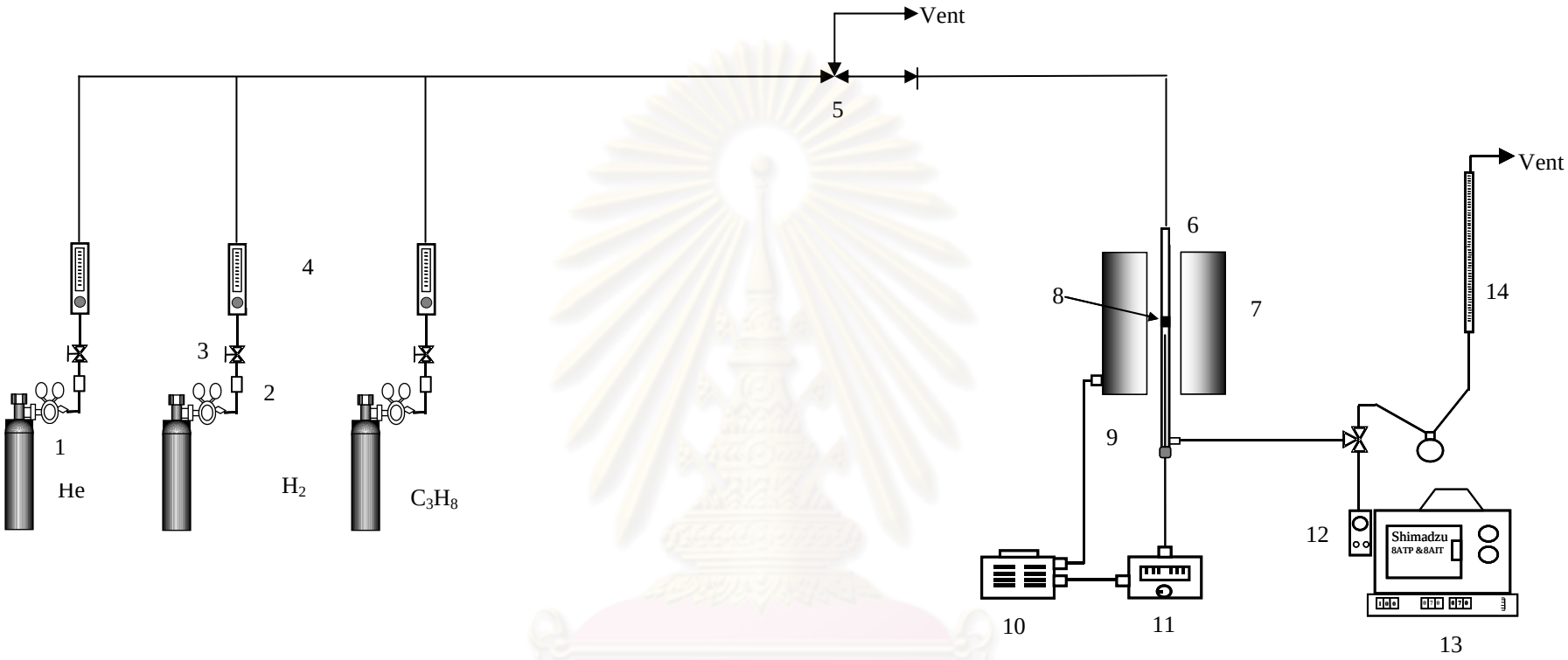

1. Pressure Regulator 2. Gas Filter 3. On-Off Valve 4. Flow meter 5. Three-way Valve
6. Reactor 7. Furnace 8. Catalyst Bed 9. Thermocouple 10. Variable Voltage Transformer
11. Temperature Controller 12. Sampling Valve 13. Gas Chromatography 14. Bubble Flow Meter

Figure 4.9 Schematic diagram of the reaction line for propane dehydrogenation analyzed by gas chromatographs equipped with VZ-10 column.

ศูนย์วิทยทรัพยากร
จุฬาลงกรณ์มหาวิทยาลัย

4.5.3 Characterization of coke measurement

4.5.3.1 Weight of coke measurement

In this section, the weight of coke formed on catalyst was measured by Differential Thermal Analyzer (SDT Q800) Figure 4.10. The deactivated catalyst was placed in ceramic cell. To remove moisture of samples, nitrogen gas was introduced at a flow rate 30 ml/min. The temperature was increased at the rare of 10 ^{o}C/min up to 200 ^{o}C and held at this temperature for 1 hour before cooled down to room temperature. Then the nitrogen gas was switched to the air zero supplied by Thai Industrial Gas at a flow rate of 30 ml/min. The temperature was increased at 5 ^{o}C/min up to 700 ^{o}C. The weight loss of the catalyst was measured.

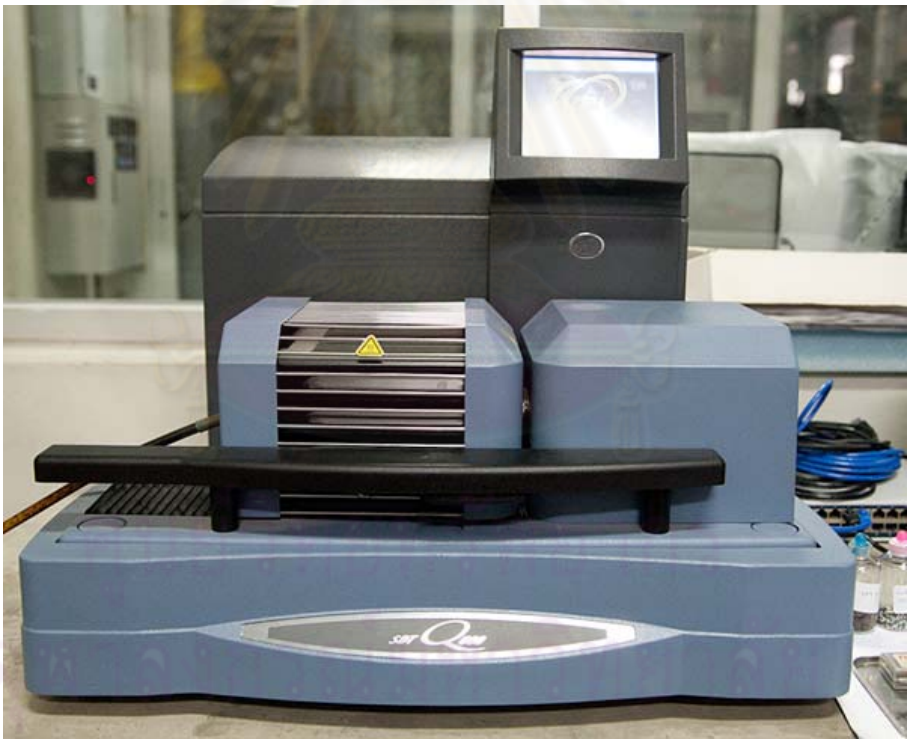

Figure 4.10 Differential Thermal Analyzer (SDT Q800).

4.5.3.2 Temperature programmed oxidation (TPO)

After the dehydrogenation of propane reaction was finished, the coked catalyst were cooled down in He flowing. The amount of coke on the catalyst was determined from the oxygen consumed and carbondioxide formed during the temperature programmed oxidation in 1% O_2 in He at the flow rate of 30 ml/min. CO_2 produced was measured with a gas chromatography equipped with a TCD (GC-8AIT) with a Porapak QS column. and an on-line gas sampling valve. The heating rate was 5 ^oC / min until the temperature reached 700 ^oC. The flow diagram of this system is shown in Figure 4.11.

The operating condition of gas chromatograph used for analyzing the effluent stream is shown in Table 4.6.

Table 4.6 Operating conditions of gas chromatographs for propane oxidation.

Gas Chromatograph	SHIMADZU GC8A-AIT
Detector	TCD
Packed column	Porapak QS
Carrier gas	He (UHP)
Flow rate of carrier gas	30 ml/min
Injector temperature	100°C
Column temperature	70°C
Detector temperature	70°C
Current	80 mA
Analyzed gas	O_2, CO_2

ศูนย์วิทยทรัพยากร
จุฬาลงกรณ์มหาวิทยาลัย

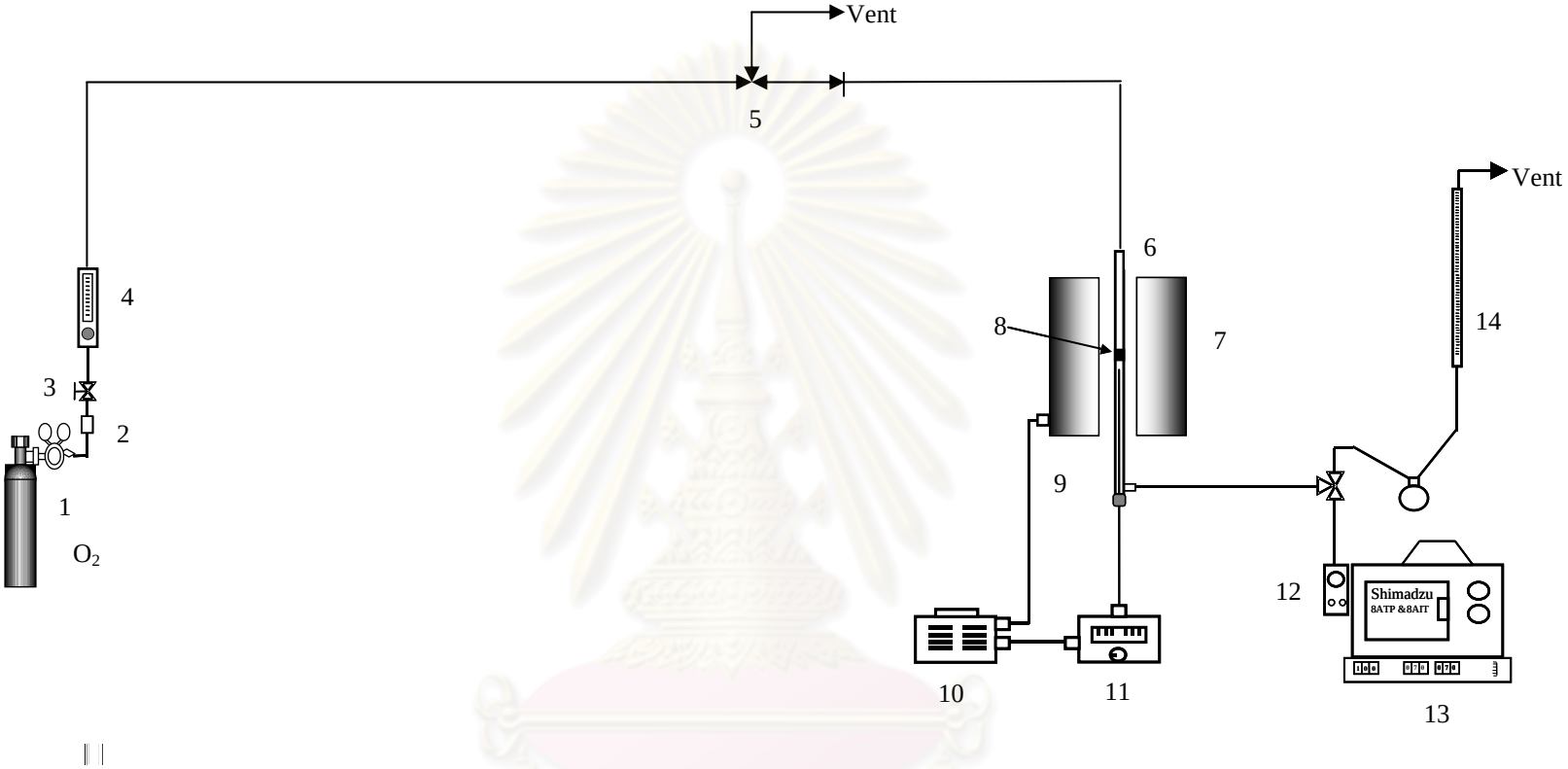

1. Pressure Regulator 2. Gas Filter 3. On-Off Valve 4. Flow meter 5. Three-way Valve
6. Reactor 7. Furnace 8. Catalyst Bed 9. Thermocouple 10. Variable Voltage Transformer
11. Temperature Controller 12. Sampling Valve 13. Gas Chromatography 14. Bubble Flow Meter

Figure 4.11 Schematic diagram of for temperature programmed oxidation analyzed by gas chromatographs equipped with porapak QS columns.

ศูนย์วิทยทรัพยากร
จุฬาลงกรณ์มหาวิทยาลัย

CHAPTER V

RESULTS AND DISCUSSIONS

In preliminary experiments, the study was conducted so as to investigate the physical and chemical properties of support Al_2O_3 and Pt/Al_2O_3 catalyst in various alumina phases. These Al_2O_3 supports were synthesized by solvothermal technique, various χ/γ phase compositions are 0/100, 30/70, 50/50, 70/30 and 100/0. The catalytic properties were evaluated using propane oxidation and propane dehydrogenation. The results in this chapter are divided into four main parts. The first part describes the characteristics of Al_2O_3 and Pt/Al_2O_3 catalyst consisting of various phase compositions between gamma and chi alumina (section 5.1). The second part describes the activities of Pt/Al_2O_3 in propane oxidation (section 5.2). The third part explains the effect of hydrogen on activities of Pt on gamma and chi phase alumina supports in propane dehydrogenation (section 5.3). The final part (section 5.4) describes the total amounts of coke and the location of coke deposited on the catalyst by the amount of CO_2 production from TPO method.

5.1 The properties of Al_2O_3 supports and Pt/Al_2O_3 catalyst

5.1.1 The physical properties and crystalline structure of alumina supports

The XRD pattern of the alumina support with various χ- and γ-phase compositions are shown in Figure 5.1. Nanocrystalline Al_2O_3 supports with pure χ- and γ-phase are obtained by the reaction of AIP in toluene and 1-butanol, respectively. While the Al_2O_3 support with various phase compositions are obtained by the reaction in the mixed solvents. The calculation method for determination of phase composition in a mixed-phase Al_2O_3 support has also been reported previously in other Al_2O_3 systems such as χ/γ Al_2O_3 Meephoka et al.[14] and Khom-in et al.[11]. For the pure gamma phase, XRD peaks at 32°, 37°, 39°, 45°, 61° and 66° were evident. The peak at 43^o shows characteristics of the chi phase and thus the larger

peak area at 43^{o} indicated that the increasing of %chi alumina phase. In this study, alumina samples comprise of 0%, 30%, 50%, 70% and 100% chi phase are referred herein as C0G100, C30G70, C50G50, C70G30 and C100G0, respectively.

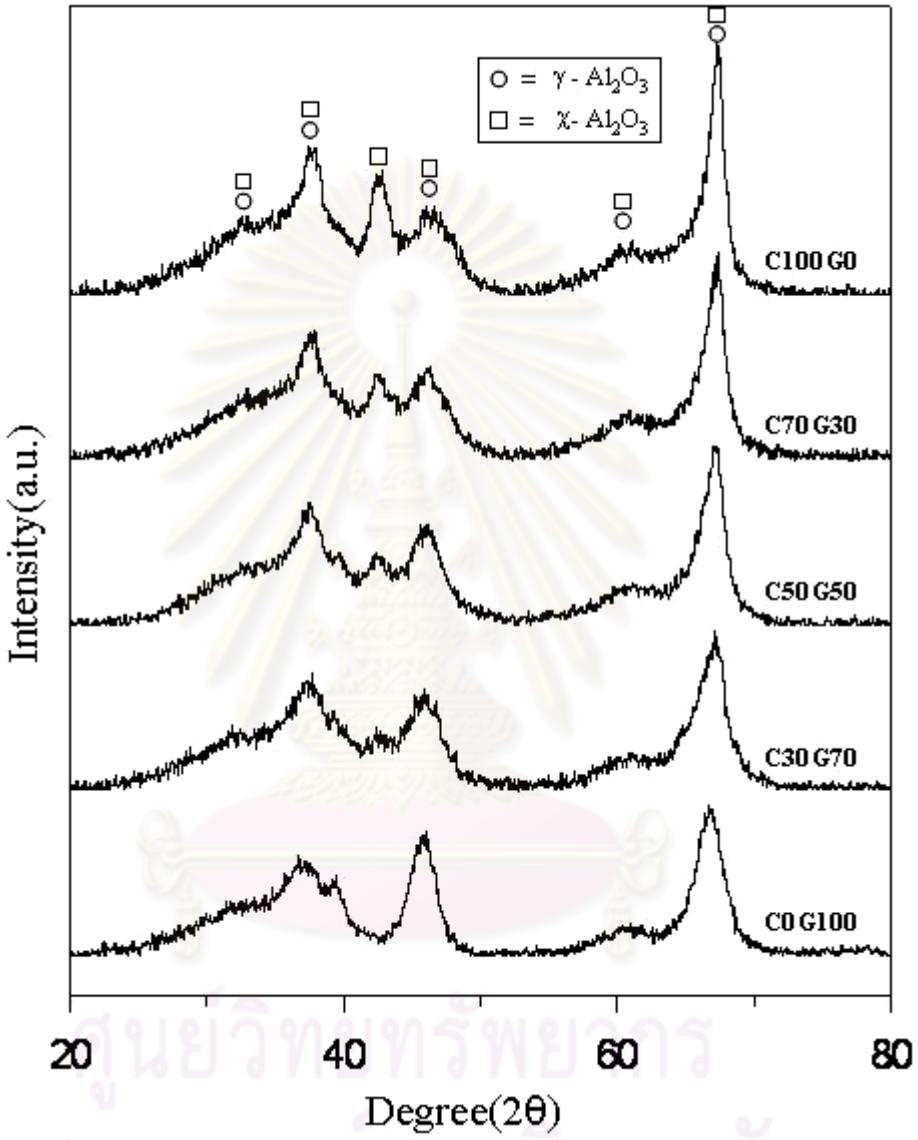

Figure 5.1 X-ray diffraction pattern of alumina supports.

The physical and chemical properties of the alumina supports are summarized in Table 5.1. The BET surface area and pore volume of various alumina decrease from 215 to 142 m^2/g and 0.63-0.51 , respectively as the chi-phase content increases from 0 to 100 % . The average crystallite size of chi, gamma and chi/gamma phase

compositions Al_2O_3 support prepared by using solvothermal method determined from the half-width of peaks using Scherrer's formula ($d = 0.9\lambda/\beta \cos\theta$) is between 5-7 nm.

Table 5.1 The physical properties of alumina supports.

Sample	Crystallite size (nm),d*	BET surface area (m^2g^{-1})	Pore Volume ($cm^3.g^{-1}$)	Avg. Pore Diameter (nm)
C0G100	5	215	0.63	8
C30G70	5	185	0.53	9
C50G50	6	172	0.49	7
C70G30	6	165	0.50	6
C100G0	7	142	0.51	9

* d - Calculate from XRD

5.1.2 The Properties of 0.3% Pt/Al_2O_3

TEM images of 0.3 wt% of Pt on alumina supports containing different compositions of γ and of χ phases are shown in Figure 5.2. In all the TEM figures, the absence of Pt particles on the 0.3% Pt/Al_2O_3 catalyst indicated that platinum were well dispersed. For γ-Al_2O_3 (Pt/C0G100), the wrinkled sheets morphology is observed but the χ-Al_2O_3 (Pt/C100G0) particles have a spherical shape and they were found to be similar to those obtained from [7], [10], [89]. As the χ-Al_2O_3 increased, the wrinkled sheets morphology became less apparent and spherical particles were observed . The presence of spherical particles structure was probably due to the formation of χ- Al_2O_3.

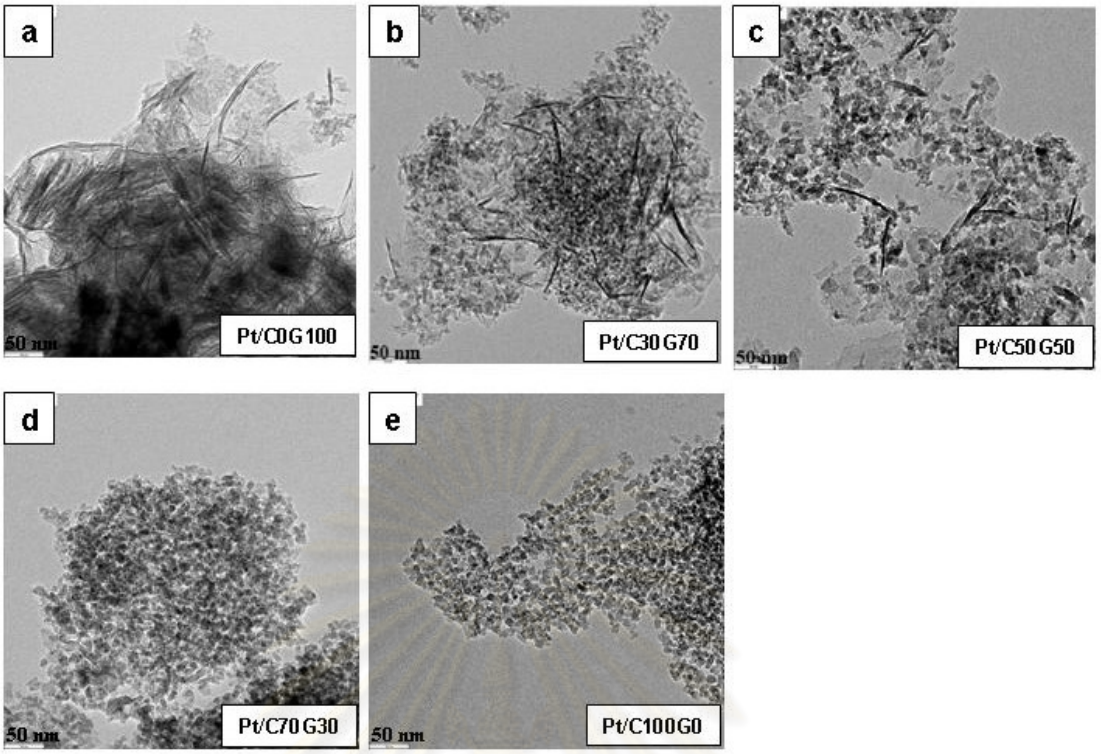

Figure 5.2 TEM images of 0.3% Pt/Al_2O_3 catalyst with various phase composition.

The platinum 0.3wt% was impregnated on various alumina supports comprise of 0%, 30%, 50%, 70% and 100% χ-phase content. The obtained catalysts are named as Pt/C0G100, Pt/C30G70, Pt/C50G50, Pt/C70G30 and Pt/C100G0, respectively. The physical properties of Pt catalysts are given in Table 5.2. The BET surface areas of the alumina supported Pt catalysts were slightly less than those of the original alumina supports. This indicates plugging of the loaded platinum on some of the alumina pores. The metal active sites on the aluminas with pure phase were rather equivalent at approximately 3.5×10^{18} molecule $CO\cdot g^{-1}$ catalyst. The mixed phase aluminas can assist high dispersion of platinum on them. Surprisingly, the metal dispersion was maintained constant in a wide range between 30 and 70% chi phase composition.

Table 5.2 The Catalyst properties of 0.3 wt.% Pt/Al_2O_3.

Sample	BET surface area ($m^2.g^{-1}$)	CO chemisorption x 10^{-18} (molecule $CO.g^{-1}$ catalyst)	% Pt dispersion * (%)
Pt/C0G100	198	3.45	37.30
Pt/C30G70	176	4.26	46.05
Pt/C50G50	161	4.37	47.24
Pt/C70G30	155	4.38	47.35
Pt/C100G0	134	3.56	38.40

* Calculate based on CO Chemisorption

The characteristics of the surface active sites of Pt/Al_2O_3 catalysts were studied by means of the temperature programmed desorption of C_3H_8 from 50-500^oC and the results are shown in Figures 5.3. The major C_3H_8 desorption peak appeared at ca. 425$^{\circ}C$ (C_3H_8 was cracked to CH_4) for those supported on the single phase Al_2O_3 (either pure γ- or χ-Al_2O_3). It is clearly seen that such peak was significantly shifted towards lower temperature (to ca. 320$^{\circ}C$) for the Pt/Al_2O_3 catalysts containing mixed γ- and χ-Al_2O_3 supports. It is suggested that the Pt may interact more strongly on the mixed Al_2O_3 structures than on the single phase ones so that the adsorption strength of C_3H_8 was altered (lower).

ศูนย์วิทยทรัพยากร
จุฬาลงกรณ์มหาวิทยาลัย

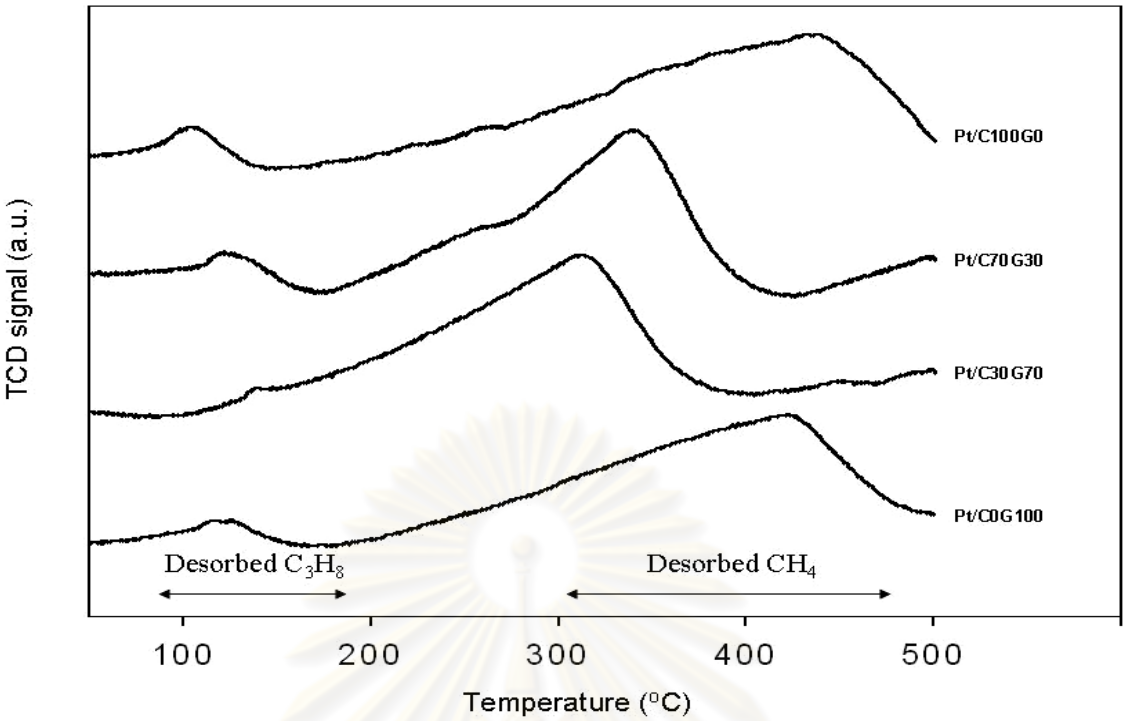

Figure 5.3 C_3H_8-TPD profiles of catalysts with various phase composition

In general, strong bases, as adsorbates, should in principle be suitable probes for the evaluation of the overall acidity of catalysts, as well as to distinguish between protonic (Bronsted) acidity and aprotic (Lewis) acidity. In this work, ammonia is independently used as probe molecules for acidity measurement. The total concentration of acid centers at the alumina supports are measured by ammonia temperature programmed desorption (NH_3-TPD) method. Although this procedure can not resolve to discriminate between different types of acid sites, it is routinely used to evaluate the total acidity of alumina supports. The acidity of the two supports were examined by temperature-programmed desorption of ammonia experiments, and the NH_3-TPD profiles of the C0G100 and C100G0 are depicted in Figure 5.4. On C100G0, a broad desorption peak with a maximum temperature at about 225 °C can easily be seen. Based on Narayanan's definition [90], the amounts of ammonia desorbed in the temperature regions of 120–250 °C, 250–350 °C and 350–450 °C were taken as a measure of weak, medium, and strong acid sites. C0G100 shows the different TPD characteristic: a dominant desorption peak at 225 °C, 300 °C and 425 °C is observed. These are considered to represent desorption of NH_3 from weak, medium, and strong acid sites on the alumina surface. According the total desorption peak area, it can infer that the order of total acid content on C0G100 is higher than

C100G0. Thus, it can be considered that the acidic centers of C100G0 are related to weak acid sites. And as for C0G100, the medium and strong acidic centers are essential.

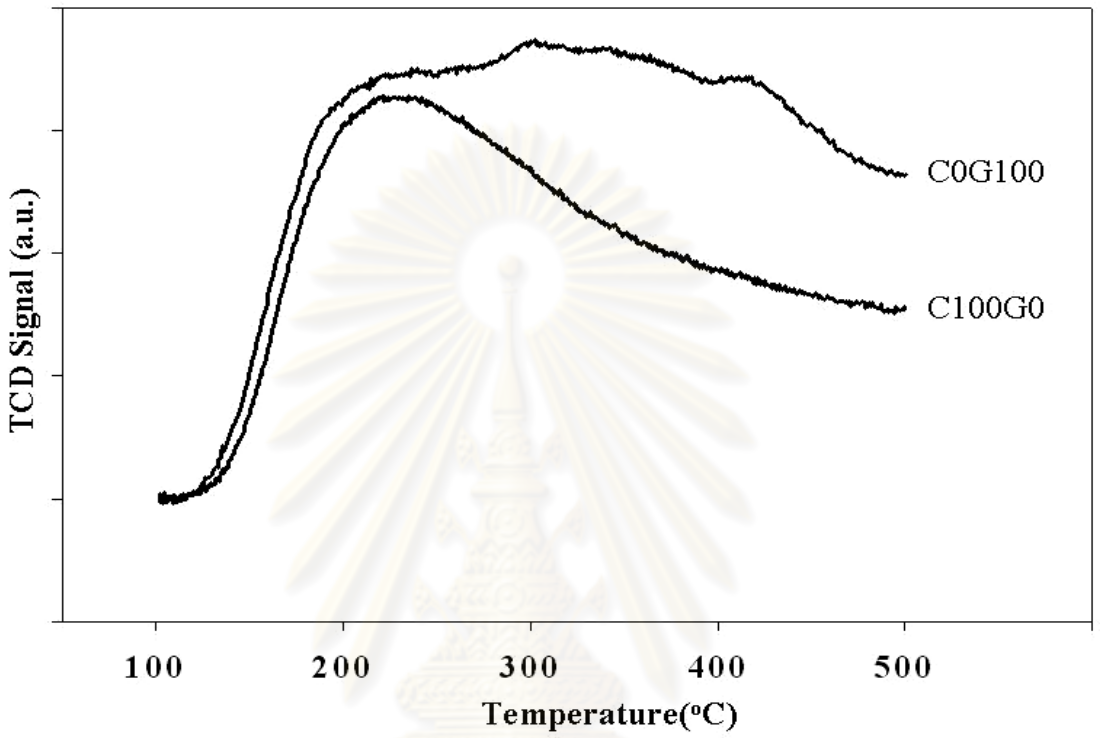

Figure 5.4 NH_3 TPD data for the C0G100 (Pt/γ-Al_2O_3) and the C100G0 (χ-Al_2O_3) support

The H_2-TPD profiles of both catalysts are shown in Figures 5.5(a) to 5.5(b). The raw data was split into separate peaks by deconvolution using proprietary software. The allocation of the fourth peak is due to the onset of the isothermal stage in the TPD test at 800°C and so can be discounted as a separate curve. The main peaks which fall well below this isothermal range, having peak temperatures of approximately 400 and 675°C, can be considered as reliable representations of true modes of hydrogen adsorption. Lower temperature desorption peaks below 300°C are commonly assigned to hydrogen on Pt metal [91]. Higher temperature desorption peaks (350°C - 500°C) have been attributed to spillover hydrogen [92-94], strongly chemisorbed hydrogen [95], hydrogen in subsurface layers of the Pt [96] and spillover hydrogen at the interface between the Pt and support [97]. The peak at approximately

450°C could be attributed to interface adsorption, strong chemisorption hydrogen or hydrogen in subsurface layers of the platinum [98]. Desorption peaks at approximately 650-700°C have previously been attributed to spillover hydrogen stabilized by physically bonding with existing hydroxyl groups or by the formation of hydroxyl groups [99].

The peak areas from H_2-TPD profiles are given in Table 5.3. It is shown that the Pt/χ-Al_2O_3 has considerably more hydrogen adsorption sites desorbing at lower temperatures, with the area of peak I being 0.17 and 0.93 for Pt/γ-Al_2O3 and Pt/χ-Al_2O_3 respectively. When normalized with regards to surface area, the values are approximately 0.009 and 0.069 au/m^2 for Pt/γ-Al2O3 and Pt/χ-Al2O3 respectively. Considering peaks II, III and IV as strongly adsorbing sites, their combined areas for Pt/γ-Al2O3 and Pt/χ-Al2O3 catalysts are 2.61 and 2.32 respectively, indicating that there are more strong hydrogen adsorption sites per unit mass for the Pt/γ-Al2O3 catalyst, when normalizing for surface area

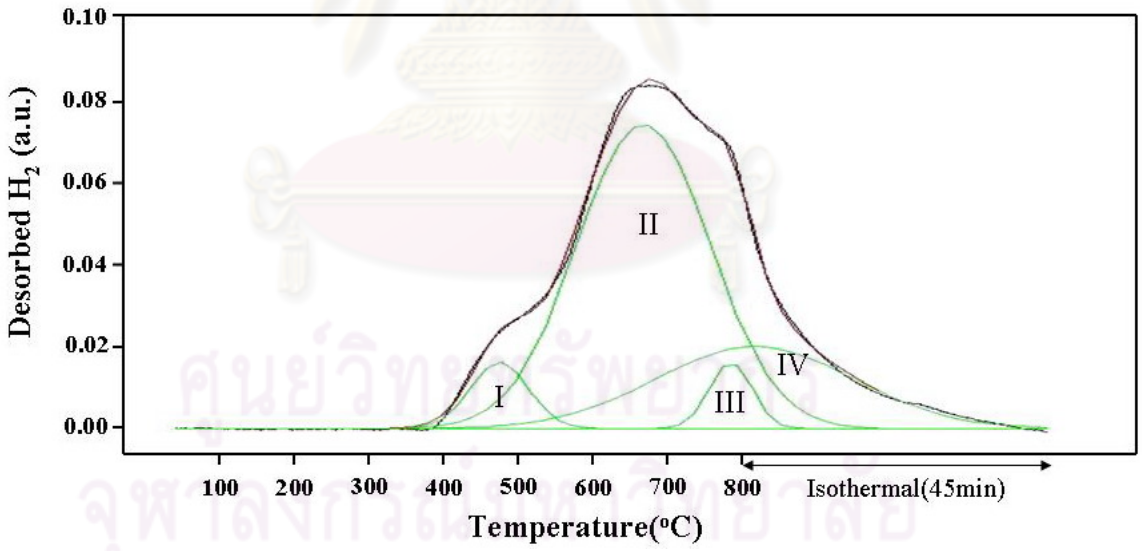

Figure 5.5 (a) H_2-TPD data for the Pt/γ-Al_2O_3 catalyst.

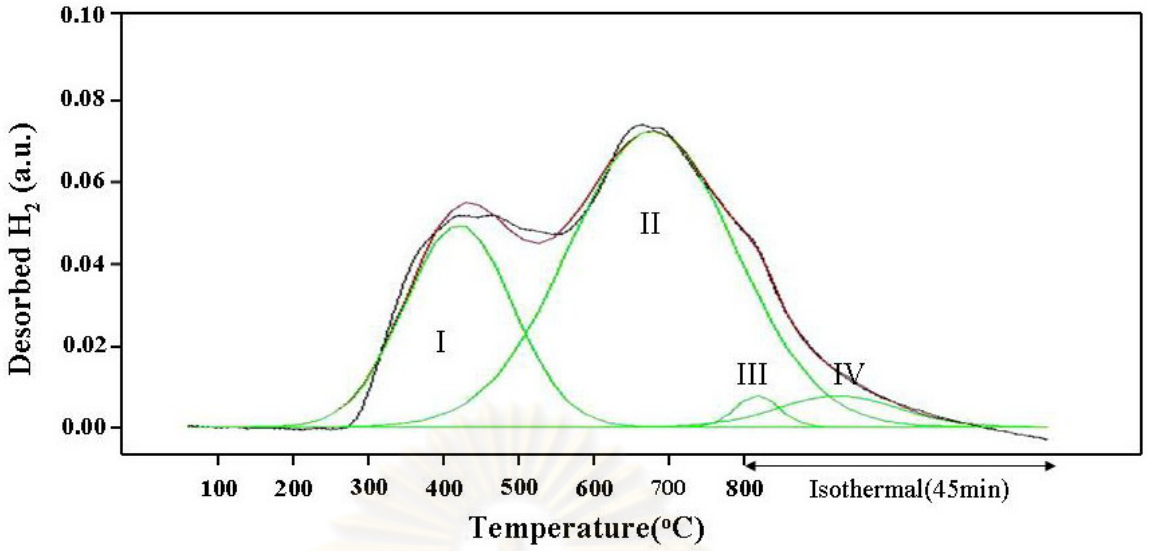

Figure 5.5(b) H_2-TPD for the Pt/χ-Al_2O_3 catalyst.

Table 5.3 Areas of peaks identified from H_2 TPD data for Pt/γAl_2O_3 and Pt/χAl_2O_3.

Catalyst	Area of identified peaks (au.°C)			
	I	II	III	IV
Pt/ C0G100	0.169 (480 °C)	1.774 (670 °C)	0.125 (780 °C)	0.711 (800 °C)
Pt/ C100G0	0.932 (420 °C)	2.106 (670 °C)	0.058 800 °C)	0.160 (800 °C)

Alumina, acid groups exist in the form of uncoordinated Al^{3+} ion Lewis acid sites and Al-OH Brønsted acid sites [100]. Lower coordination Al^{3+} sites acts as stronger Lewis acid sites and OH groups bonded to octahedrally coordinated Al atoms act as weaker Brønsted acid sites [101]. Likewise, hydroxyl groups bond more strongly to lower coordination aluminium atoms and so act as more thermally stable hydrogen adsorption sites [101, 102].

Recently, molecular computational studies carried out by Ahmed *et al.* [103] have shown the collision between an adsorbed hydrogen species on alumina and a diffusing free radical hydrogen species will result in the formation of a hydrogen

molecule, that will subsequently desorb into the gas phase. One could therefore expect that where the hydrogen adsorption sites are located within relatively close proximity, as with the Pt/χ-Al_2O_3 catalyst, there will be higher rate of hydrogen desorption due to these collisions.

The FTIR adsorption spectra obtained for fresh Pt/χ-Al_2O_3 and Pt/γ-Al_2O_3 catalysts are shown in Figure 5.6. There is no significant difference in the broad peak bands within the 3400–3750 cm^{-1} region, which are identified as isolated hydroxyl group vibrations. A distinctive difference between the spectra of the Pt/γ-Al_2O_3 and Pt/χ-Al_2O_3 catalysts is the peak located at 2350 cm^{-1}. This wave number is characteristic of adsorption CO_2 at room temperature. The spectra of both the catalysts also show a peak at 1040 cm^{-1}. Peaks in the range of 1040-1050 cm^{-1} have previously been attributed to Al-O-Al bonds [104-106] and the peaks of both catalysts at 1660 cm^{-1} and 1410 cm^{-1} are related to the hydroxyl group vibrations too .

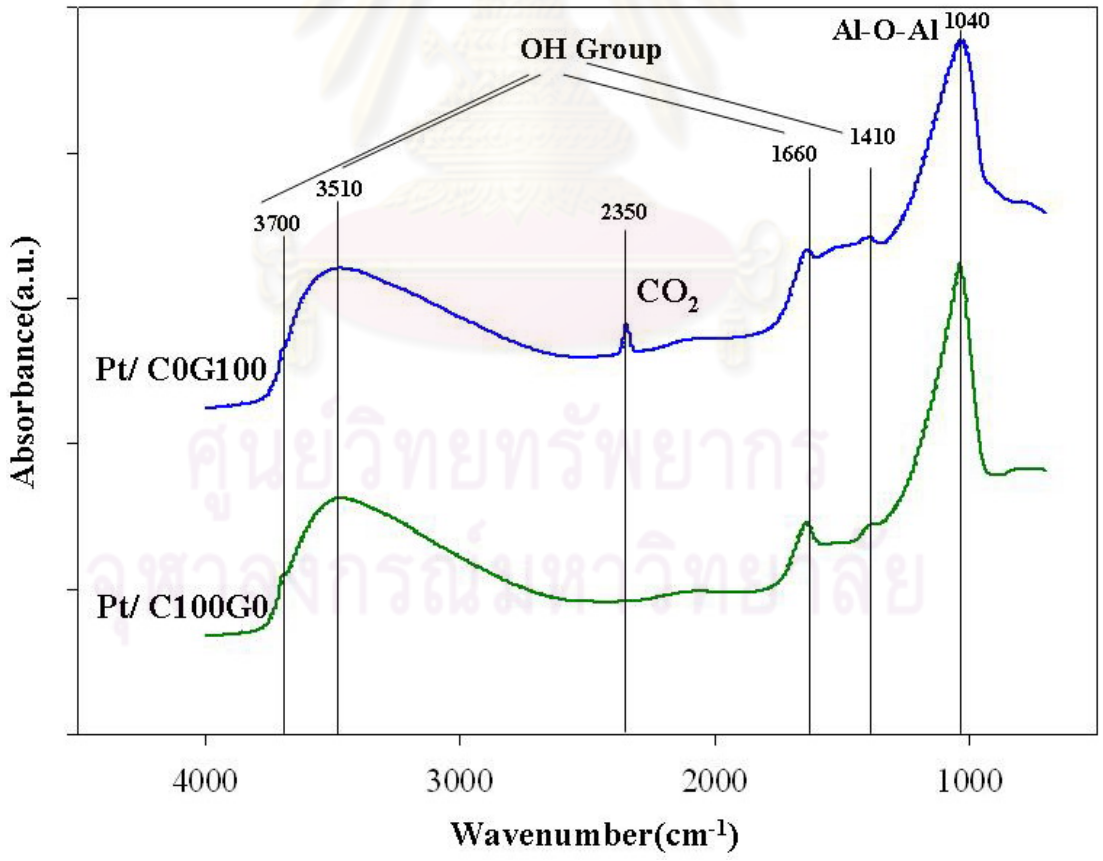

Figure 5.6 FTIR spectra for Pt/γ-Al_2O_3 and Pt/χ-Al_2O_3 catalysts (fresh).

The Al coordination on the surface of gamma and chi alumina support was investigated by X-ray photoelectron spectroscopy (XPS) in Figure 5. The "Fityk" fitting program allowed us to deconvolute peaks by specifying the peaks position, height, width and shape from XPS data. The XPS elemental scan peak for Al 2p was observed at 73.9 ± 0.3eV for gamma and chi alumina which has binding energy very similar to many workers[107-110]. Literature data [110] report Al 2p binding energy values ca. 73.5 in the tetrahedral Al coordination and ca. 74.5 eV in the octahedral Al coordination. Surface compositions in term of octahedrally/ tetrahedrally coordinated alumina ratio of the Gamma $A1_20_3$ and Chi Al_2O_3 were determined by deconvolution yields and the results are given in Table 5.4**.** It was found that the Al_{Tet}/Al_{Oct} ratio was 2.66 and 2.14 for the gamma alumina and Chi alumina, respectively. This lower ratio of Al_{Tet}/Al_{Oct} in chi alumina reveals that the octahedral Al coordination in chi alumina structure was higher than gamma alumina structure.

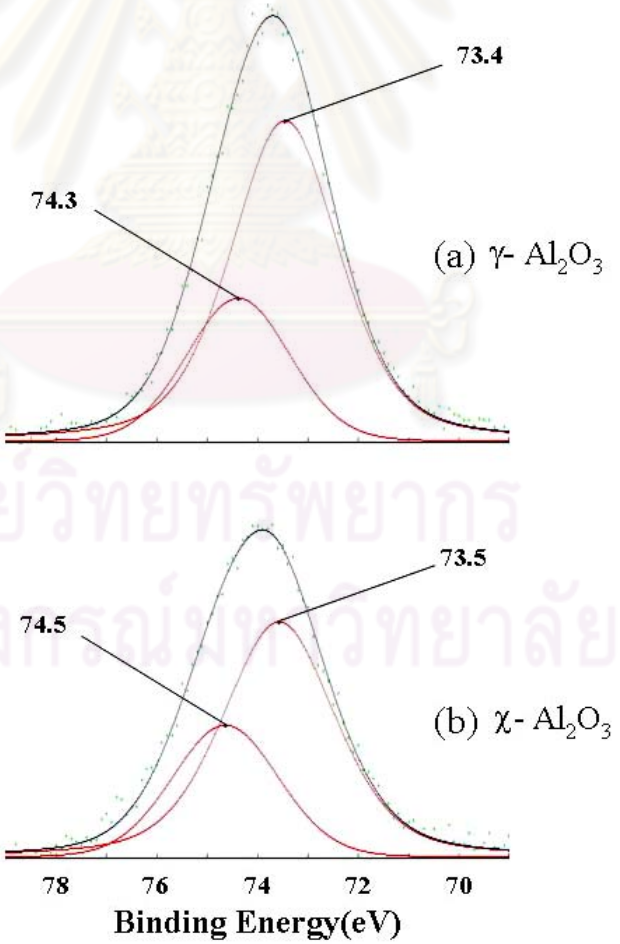

Figure 5.7 Al 2p XPS spectra of (a) γ-Al_2O_3 support and (b) χ-Al_2O_3 support

Table 5.4 XPS binding energies obtained by deconvolution of the Al 2p manifold

Support	Binding energy(eV)		Area(au)		Ratio
	Al_{Tet}	Al_{Oct}	Al_{Tet}	Al_{Oct}	Al_{Tet}/Al_{Oct}
γ- Al_2O_3	73.5	74.3	3904	1469	2.66
χ- Al_2O_3	73.4	74.5	2986	1395	2.14

Tet - Tetrahedral coordination
Oct - Octahedral coordination

5.2 Catalytic activities of Pt/Al_2O_3 in propane oxidation

Figure 5.8 shows the activities of Pt/Al_2O_3 catalysts in propane oxidation as a function of reaction temperature. The catalytic activity of supported platinum catalyst depended on the platinum dispersion. The presence of 30-70% chi phase composition can lower the light-off temperature by 50 °C or it can also be said that the presence of 30-70% χ-phase showed much higher activities. Since the C_3H_8-TPD experiments showed that propane desorption behaviors were different between the mixed phase Al_2O_3 supported Pt catalysts and the single phase supported ones. Faster desorption of C_3H_8 from Pt surface would, therefore, result in more active Pt surface available for reaction to proceed; as a consequence an increase in oxidation activity was obtained. According to the reaction mechanism in the literature, rate of propane oxidation increases by increasing the active sites for both dissociation of C–H bond and oxygen adsorption [60, 62, 112]. The advantages of mixed phase composition effect on the activity and selectivity characteristics have also been reported for other catalyst systems [14, 111-113].

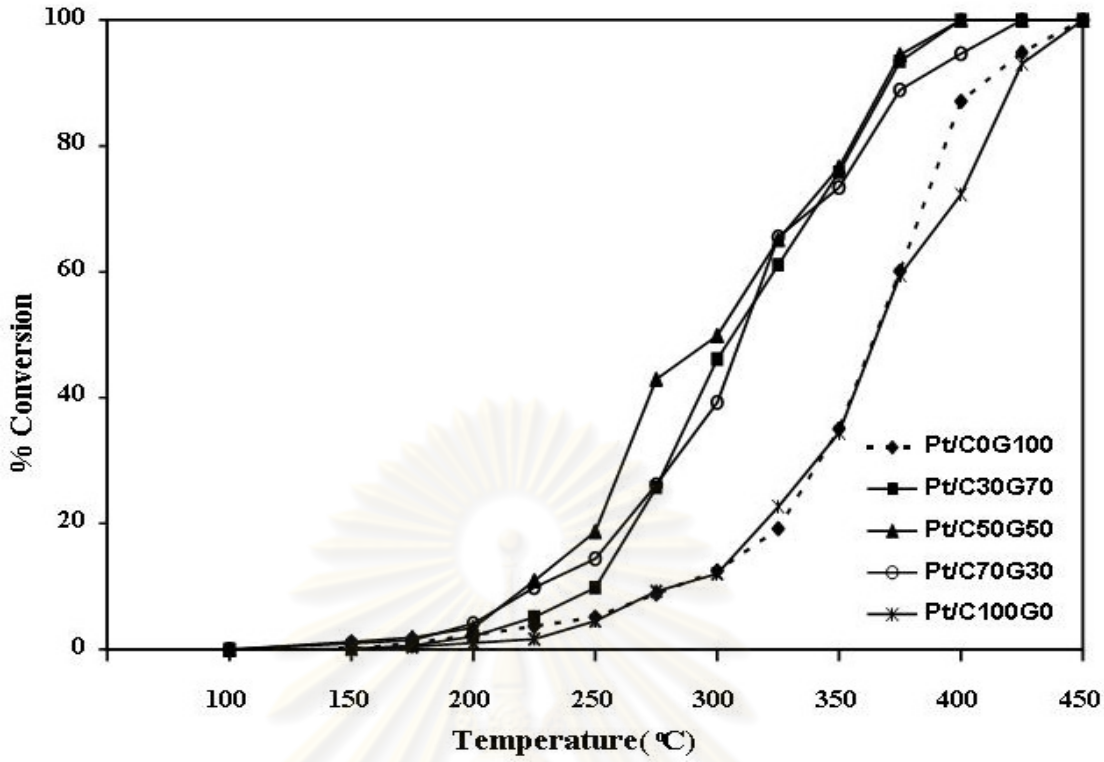

Figure 5.8 C_3H_8 conversion profiles of 0.3% Pt/Al_2O_3 for the propane oxidation.

5.3 Effect of hydrogen on catalytic activities of Pt/Al_2O_3 in propane dehydrogenation

The conversions of propane over Pt/Al_2O_3 catalysts at 500 ^oC during 5 - 80 min on stream with different H_2/C_3H_8 ratios are shown in Figure 5.9-5.11. Figure 5.9 represents greater efficiency of $Pt/\gamma\text{-}Al_2O_3$ catalyst for the conversion of propane in the absence of hydrogen. This may be due to on the dual-functional alumina supported catalysts, the side reactions, such as cracking/hydrogenolysis take place on the acid site[114]. Without hydrogen in feed, acid-catalyzed cracking is important , the high acidity on $Pt/\gamma\text{-}Al_2O_3$ can also account for the higher conversion than $Pt/\chi\text{-}Al_2O_3$. The low conversion of the $Pt/\chi\text{-}Al_2O_3$ may be due to the close proximity of the active sites results in a greater crowding and interference with coke deposits.

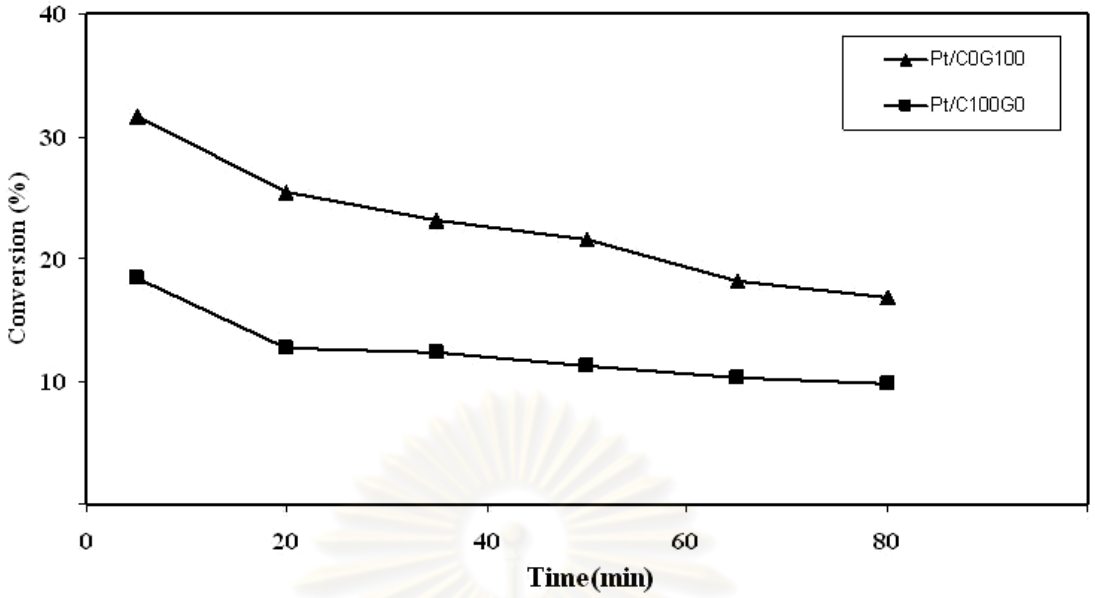

Figure 5.9 C_3H_8 conversion profiles of 0.3% Pt/Al_2O_3 for the propane dehydrogenation**. (**H_2/C_3H_8 ratios =0:1)

Upon the introduction of hydrogen into the feed stream with a propane/hydrogen ratio of 1/1, the conversion of propane on the Pt/χ-Al_2O_3 catalyst significantly increases to be greater than that of the Pt/γ-Al_2O_3 catalyst (Figure 5.10). The hydrogen acts to reduce the coking on the Pt by hydrogenation, which is particularly important for the Pt/χ-Al_2O_3 catalyst as a result of the close proximity between sites. Due to the higher population of weak adsorption sites, the hydrogen species is more mobile over the χ-Al_2O_3, allowing for more hydrogenation of adsorbed hydrocarbons, for example by reverse spillover onto the Pt sites. The supply of spillover hydrogen may also act to increase the population of thermally unstable acid sites, leading to more acid catalysed conversion of propane. Moreover, the spillover hydrogen is helpful for the migration of the coke deposition from the metal sites to the supports [39, 115] and then is beneficial to the stability of the catalysts. As a result, the alumina supports must have a certain pore volume to accommodate the coke that formed or migrated. Furthermore, the catalytic dehydrogenation reaction rate is limited by the intra-particle mass transfer rate; thus, if the mass transfer rate is relatively slow, the activity are lowered [116]. The change in conversion rate from 5 to 80 minutes is similar for both catalysts indicating that the increased inhibition of

the propane conversion for the Pt/γ-Al_2O_3 catalyst is taking place at an early stage in the cycle (less that 5 minutes), i.e. the fast formation of coke on the Pt sites.

A further increase in the ratio of H_2/C_3H_8 to 3:1 (Figure 5.11) results in a decrease in the conversion rate after 5 and 80 minutes on stream. For the χ-Al_2O_3 catalyst, the decrease in conversion rate with increasing hydrogen partial pressure for a 5 minute, is reciprocated in the 80 minute. This implies that the decreased conversion rate is due to a decrease in propene formation as a result of dehydrogenation. For the Pt/γ-Al_2O_3 catalyst however, the change in conversion rate over this same time period, decreases. This is explained as being due to the rate of coke formation reaching a plateau before the end of the run, where the formation rate is balanced by dehydrogenation reactions. Thus the formation of coke is inhibited by the precursors reacting with hydrogen spillover and hydrogen gas.

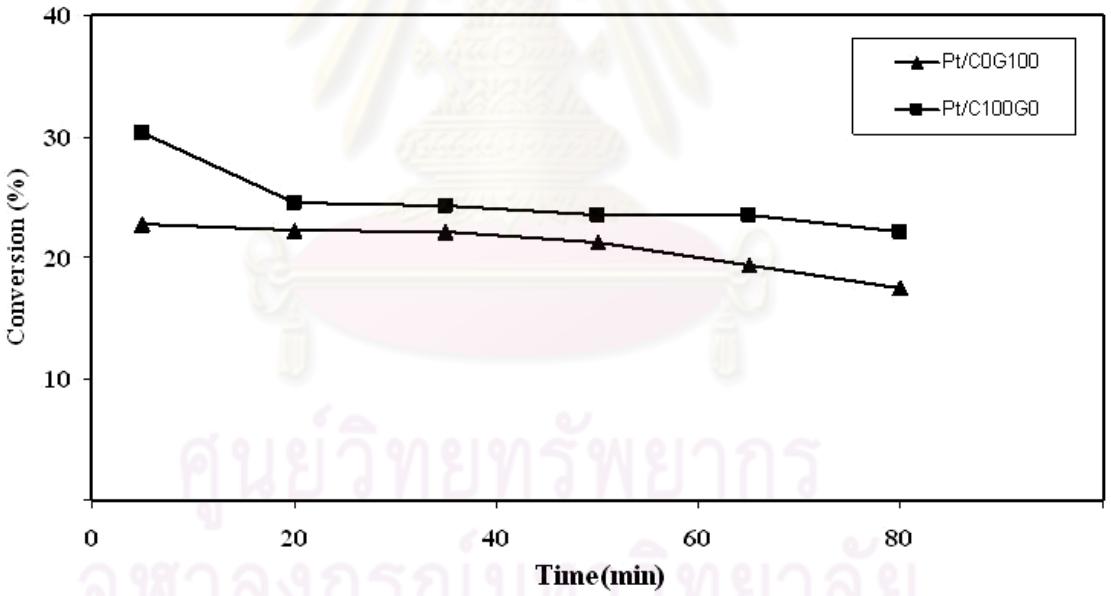

Figure 5.10 C_3H_8 conversion profiles of 0.3% Pt/Al_2O_3 for the propane dehydrogenation**. (**H_2/C_3H_8 ratios =1:1)

ศูนย์วิทยทรัพยากร
จุฬาลงกรณ์มหาวิทยาลัย

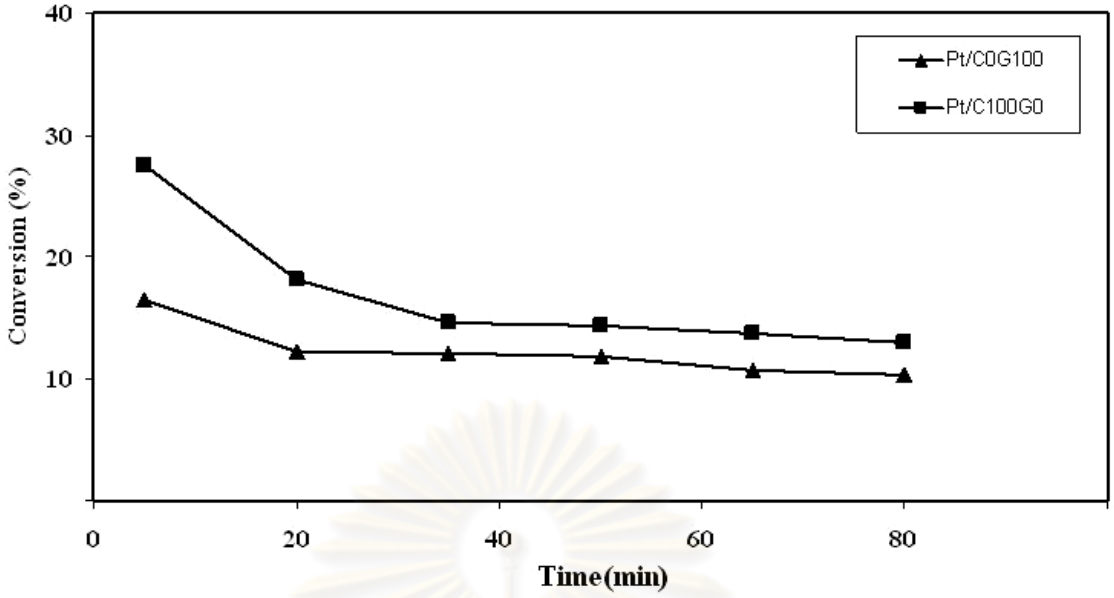

Figure 5.11 C_3H_8 conversion profiles of 0.3% Pt/Al_2O_3 for the propane dehydrogenation**. (**H_2/C_3H_8 ratios =3:1)

In the case of propane dehydrogenation process, side reactions like hydrogenolysis, cracking and coke formation compete with dehydrogenation reaction. Propylene is the major product of the reaction, whereas methane, ethane and ethylene are by-products. Platinum is the only active metal and propylene is only formed on the metal by dehydrogenation. Methane is generated by cracking of propane (acid sites) or by hydrogenolysis of propane on Pt sites. Ethylene is mainly formed from cracking on the carrier. Ethane is the product of propane hydrogenolysis and ethylene hydrogenation on Pt sites. As can be observed in Figure 5.12-5.14, the selectivity to propylene followed the same trend for all catalysts. That is, the selectivity to propylene increased as time on stream. This is most likely due to the rapid coking occurring in the metallic sites that were active for hydrogenolysis and cracking reactions in the beginning of the reaction, which caused a gradual blocking of the active sites by carbon deposition. This means that coke acts as a promoter to improve the selectivity by deactivating those sites that are active for C–C bond activation.

The product distributions of the dehydrogenation of propane over $Pt/\gamma\text{-}Al_2O_3$ and $Pt/\ \chi\text{-}Al_2O_3$ catalysts at the various ratio of H_2/C_3H_8 are listed in Table 5.5-5.10. In this way, the dehydrogenated products such as CH_4, C_2H_6 and C_2H_4 are detected, while C_3H_6 occurred is the main product. Figure 5.12, the $Pt/\gamma\text{-}Al_2O_3$ and $Pt/\ \chi\text{-}Al_2O_3$

catalysts shows a much greater capacity for the selectivities of propylene in the absence of hydrogen. There is no significant different in the selectivity for propylene for all the Pt/γ-Al_2O_3 and Pt/ χ-Al_2O_3 catalysts (propylene selectivity ≈ 94-98%). The introduction of hydrogen into the feed stream with a hydrogen/propane ratio of 1/1 and 3/1 (Figure 5.13-5.14) results in a decrease in the propylene selectivity due to the decreased in conversion rate of propane dehydrogenation. For the Pt/χ-Al_2O_3 catalyst, the selectivity to propylene was lower than Pt/ γ -Al_2O_3 catalyst in particular at the hydrogen /propane ratio of 3/1.The selectivity to propylene on Pt/χ-Al_2O_3 catalyst was very low (average 25% difference in selectivity) compared to Pt/γ-Al_2O_3, the minor products in this case for Pt/χ-Al_2O_3 catalyst were ethane and ethylene. The selectivity to propylene was low in Pt/χ-Al_2O_3 catalyst, indicating that the side reactions of cracking and hydrogenolysis were more important for propane dehydrogenation.

Table 5.5 The product selectivity of the dehydrogenation of propane over Pt/C100G0 **(**H_2/C_3H_8 ratios =0:1)

Time(min)	Selectivity (%)		
	C_3H_6	CH_4	C_2H_6,C_2H_4
5	96.64	0.87	2.49
15	98.13	0.43	1.44
35	98.32	0.39	1.29
50	98.43	0.38	1.19
65	98.27	0.43	1.30
80	98.04	0.47	1.49

Table 5.6 The product selectivity of the dehydrogenation of propane over Pt/C0G100 **(**H_2/C_3H_8 ratios =0:1)

Time(min)	Selectivity (%)		
	C_3H_6	CH_4	C_2H_6,C_2H_4
5	94.41	1.28	4.31
15	97.47	0.57	1.96
35	97.91	0.48	1.61
50	98.09	0.44	1.47
65	98.07	0.45	1.48
80	98.18	0.43	1.39

Table 5.7 The product selectivity of the dehydrogenation of propane over Pt/C100G0 **(**H_2/C_3H_8 ratios =1:1)

Time(min)	Selectivity (%)		
	C_3H_6	CH_4	C_2H_6,C_2H_4
5	84.09	3.90	12.01
15	92.51	1.78	5.70
35	94.63	1.27	4.10
50	95.47	1.06	3.46
65	95.76	1.00	3.24
80	96.07	0.92	3.00

Table 5.8 The product selectivity of the dehydrogenation of propane over Pt/C0G100 **(**H_2/C_3H_8 ratios =1:1)

Time(min)	Selectivity (%)		
	C_3H_6	CH_4	C_2H_6,C_2H_4
5	91.62	2.01	6.37
15	95.92	0.97	3.11
35	96.80	0.75	2.45
50	97.23	0.65	2.12
65	97.41	0.61	1.99
80	97.58	0.57	1.85

Table 5.9 The product selectivity of the dehydrogenation of propane over Pt/C100G0 **(**H_2/C_3H_8 ratios =3:1)

Time(min)	Selectivity (%)		
	C_3H_6	CH_4	C_2H_6,C_2H_4
5	43.70	13.92	42.38
15	66.61	8.00	25.40
35	74.17	6.13	19.70
50	77.69	5.29	17.03
65	79.63	4.84	15.53
80	81.28	4.45	14.27

Table 5.10 The product selectivity of the dehydrogenation of propane over Pt/C0G100 **(**H_2/C_3H_8 ratios =3:1)

Time(min)	Selectivity (%)		
	C_3H_6	CH_4	C_2H_6,C_2H_4
5	59.94	9.73	30.33
15	75.65	5.96	18.38
35	83.75	3.92	12.33
50	86.28	3.29	10.42
65	87.79	2.95	9.27
80	88.69	2.73	8.58

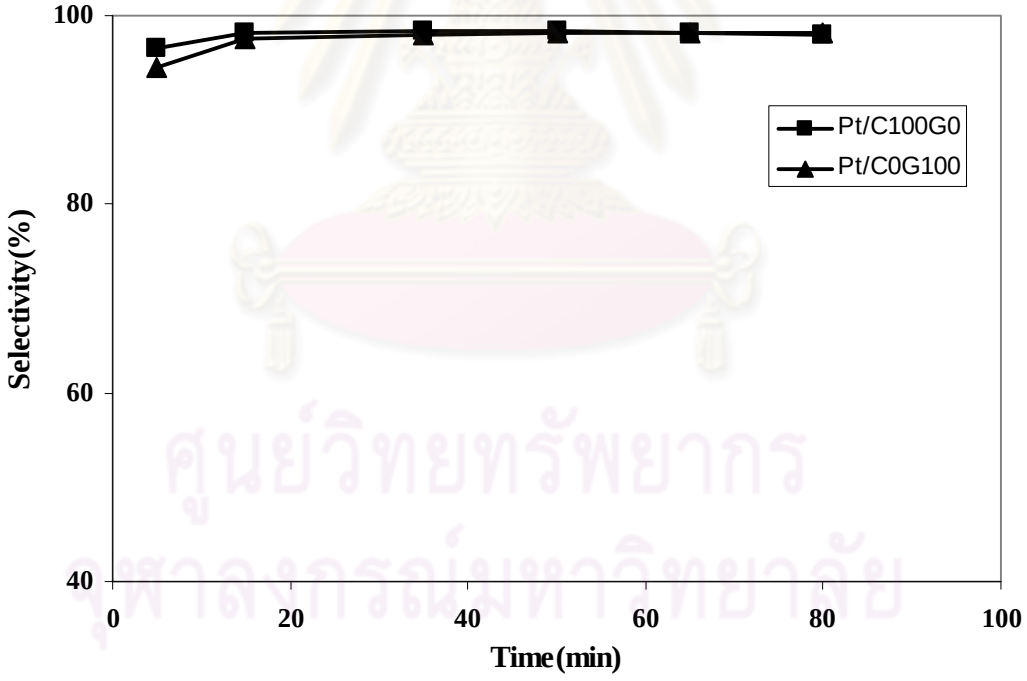

Figure 5.12 C_3H_6 selectivity of Pt/C100G0 and Pt/C0G100 for the propane dehydrogenation. (H_2/C_3H_8 ratios =0:1)

ศูนย์วิทยทรัพยากร
จุฬาลงกรณ์มหาวิทยาลัย

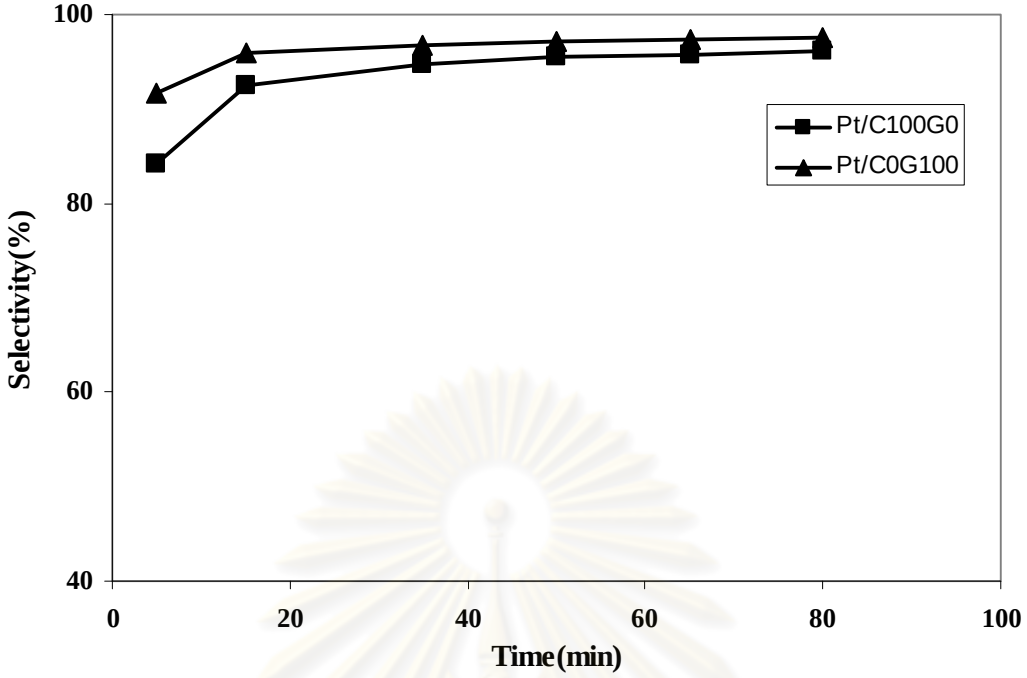

Figure 5.13 C_3H_6 selectivity of Pt/C100G0 and Pt/C0G100 for the propane dehydrogenation. (H_2/C_3H_8 ratios =1:1)

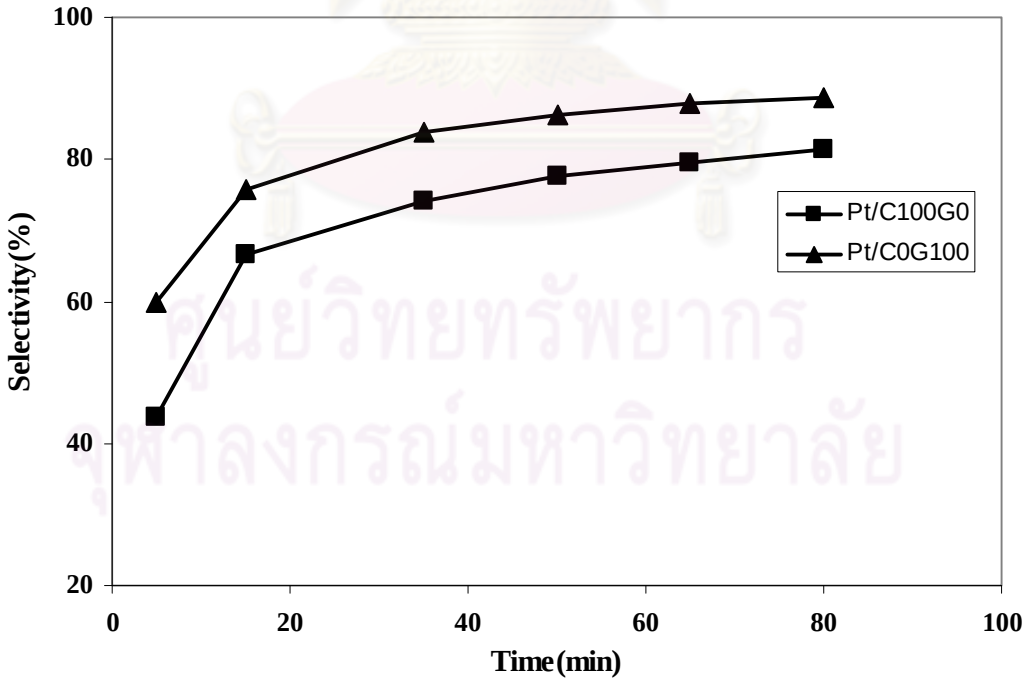

Figure 5.14 C_3H_6 selectivity of Pt/C100G0 and Pt/C0G100 for the propane dehydrogenation. (H_2/C_3H_8 ratios =3:1)

5.4 Study of coke formation by FT-IR, TPO, and TGA

The FTIR spectra for both spent catalysts, represented in Figure 5.15**,** show the presence of coke deposits after the dehydrogenation reaction after 80 min, indicated by the peaks at 2880 and 2950 cm^{-1}, representing the bending vibration modes of CH_3 and CH_2 groups. Referring to the FTIR spectra for Pt/χ-Al_2O_3, one can see the formation of peaks at 1580 and 1470 cm^{-1}, which are identified as the stretching of aromatic C-C and C-H bonds respectively [117], evidence of acid catalysed reactions on the support. With the introduction of hydrogen, the strength of these peaks reduces significantly, whereas the strength of the peaks at 2880 and 2950 cm^{-1} remain relatively unchanged. This is evidence of the preferential hydrogenation of aromatic hydrocarbon precursors.

For the Pt/γ-Al_2O_3 spent catalysts a shoulder can be seen on the left side of the peak at 1040 cm^{-1}, which has previously identified as the in plane vibrations of hydrogen bonded (bridged) hydroxyl groups [106]. The shoulder on the right side of the peak at 1040 cm^{-1} has previously been identified as interference on the Al-O bond vibrations from hydrogen bonding between the OH groups [118]. The Pt/χ-Al_2O_3 catalyst has a higher narrower peak at 1040 cm^{-1} when in the fresh condition, but significantly reduces in height after exposure to a H/C feed gas ratio of 0:1, but less so when this ratio changes to 3:1. The peak does not undergo any other significant change in width or formation of shoulders. This indicates that in this case the shape is only affected mainly by the deposition of coke.

ศูนย์วิทยทรัพยากร
จุฬาลงกรณ์มหาวิทยาลัย

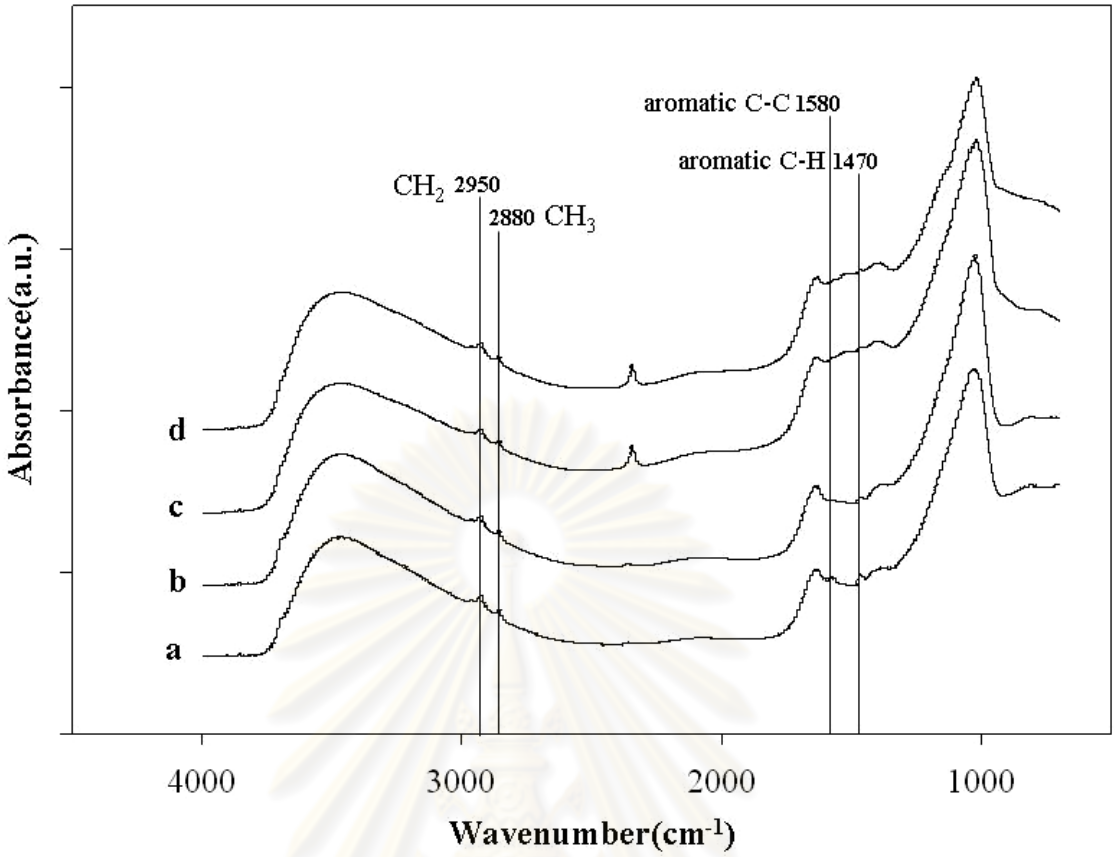

Figure 5.15 FTIR spectra for spent Pt/γ-Al_2O_3 and Pt/χ-Al_2O_3 catalysts with hydrogen/propane ratio a - Pt/C100G0(H_2/C_3H_8=0), b - Pt C100G0 (H_2/C_3H_8=3), c - Pt/ C0G100 (H_2/C_3H_8=0) and d - Pt/ C0G100 (H_2/C_3H_8=3).

Figures 5.14 (a) to 5.14(c) show TPO profiles of the spent Pt/γ-Al_2O_3 and Pt/χ-Al_2O_3 catalysts with H_2/C_3H_8 ratios 0:1, 1:1 and 3:1. Carbon depositions on all spent catalysts were not completely oxidized by oxygen, indicated by the existence of a signal at the end of the run. The TPO charts do provide enough information for a qualitative comparison between the catalysts. TGA data is also provided for spent catalysts after 5 and 80 minutes time on stream, for hydrogen/propane ratios of 0:1, 1:1 and 3:1 providing more accurate measures of the total mass of coke deposited on the catalyst (see Figure 5.16(b)). The data clearly shows the mass of carbon deposited to decrease with increasing partial pressure of hydrogen in the feed stream. This is a result of hydrogenation of unsaturated hydrocarbons, as well as the increased competition for adsorption sites on platinum and alumina.

However, as shown in Figure 5,16(b), for a similar H_2/C_3H_8 ratio, the amount of coke on Pt/γ-Al_2O_3 was higher than for the Pt/χ-Al_2O_3 catalyst which is in line with the higher amount of acid sites on Pt/γ-Al_2O_3 catalyst.

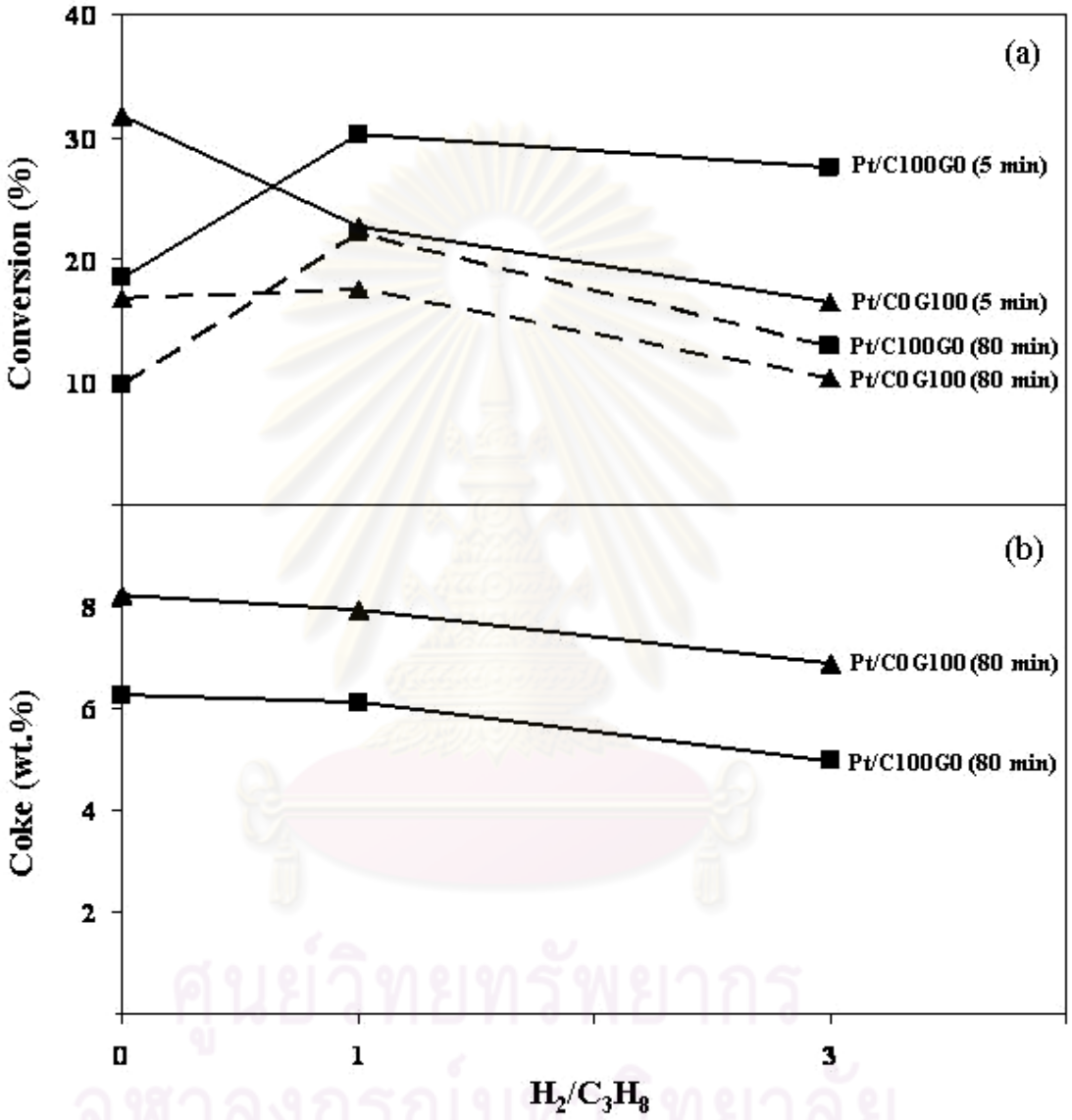

Figure 5.16 (a) Percentage conversion of propane at 5 and 80 min. for Pt/γ-Al_2O_3 and Pt/χ-Al_2O_3 catalysts with hydrogen/propane feed gas mixture ratios of 0:1, 1;1, and 3:1. (b) Coke of spent catalysts from TGA at 80 minutes.

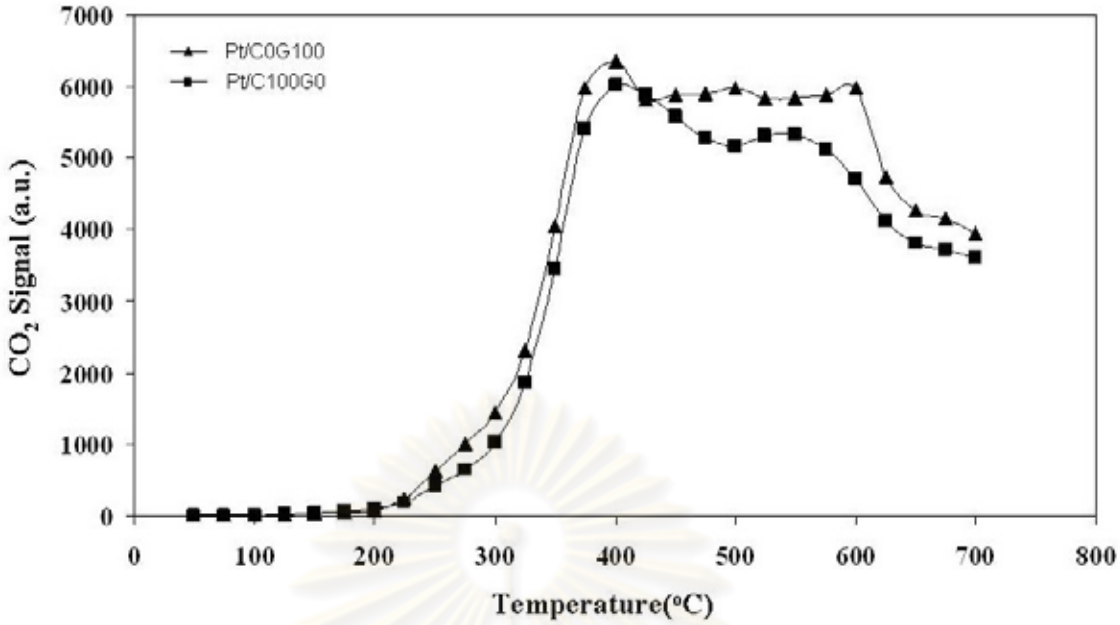

Figure 5.17 (a) TPO chart for catalysts used in a dehydrogenation with a hydrogen/propane ratio of 0:1(500°C, 80min).

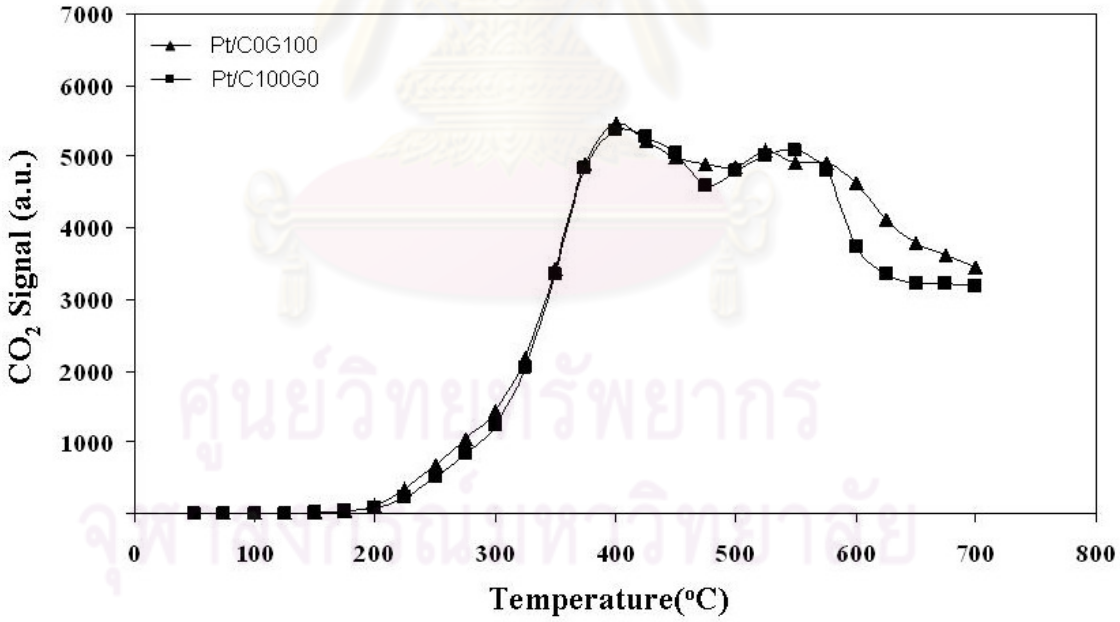

Figure 5.17 (b) TPO chart for catalysts used in a dehydrogenation with a hydrogen/propane ratio of 1:1(500°C, 80min).

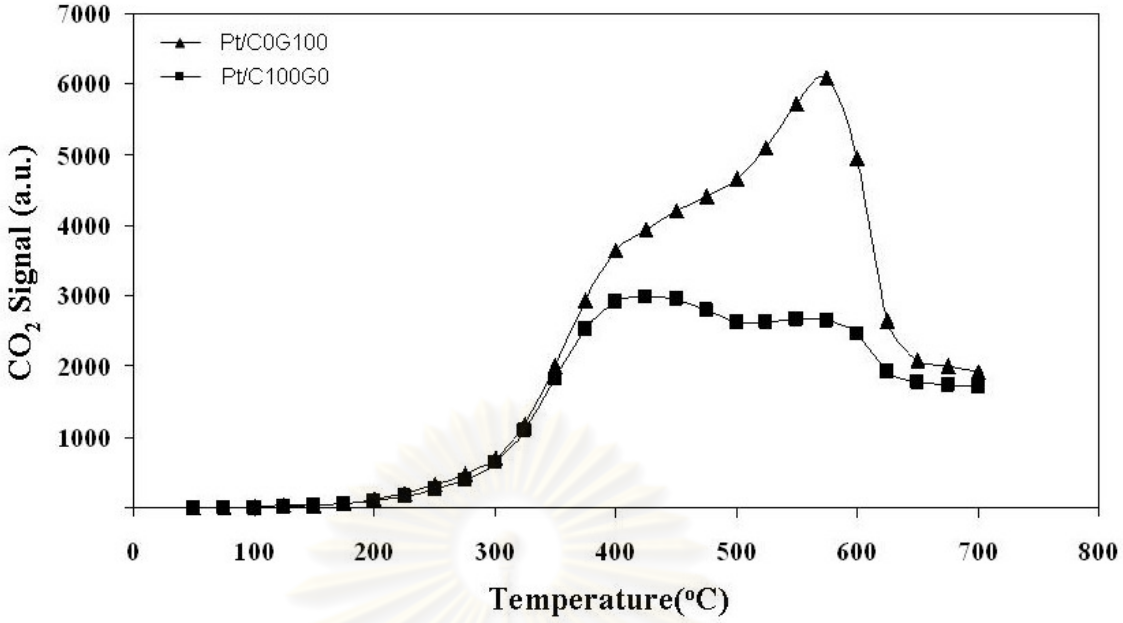

Figure 5.17 (c) TPO chart for catalysts used in a dehydrogenation with a hydrogen/propane ratio of 3:1(500°C, 80min).

As revealed by the TPO profiles, two main peaks exist, one at around 400°C and another exceeding 550°C attributed to two types of coke: (i) coke deposited directly on the metal, and (ii) coke on the support, either at the platinum interface or isolated from the platinum [119, 120]. A particularly noticeable characteristic of all the curves is a large shoulder on the right of the second peak, at temperatures approximately > 620°C. The coke attributed to this shoulder is most likely coke with low hydrogen content and a more graphitic structure, derived from aromatic species formed as part of the acid catalysed conversion of propylene [121].

The TPO profile of at the hydrogen/propane ratio of 0: 1 in Figure 5.17 (a) . For both spent catalysts, the first peak shows the same amount of coke on the metal but for second peak the amount of coke on Pt/γ-Al_2O_3 was higher than for the Pt/χ-Al_2O_3 catalyst which is due to the higher amount of acid sites on Pt/γ-Al_2O_3 catalyst. At the hydrogen/propane ratio of 1: 1, the results show that the mass of carbon deposited decreases with increasing the hydrogen in the feed stream but the there are not different in amount of coke on the metal and the support for all catalysts. The higher coke composition on the support is also observed for the Pt/γ-Al_2O_3 catalyst at a lower H/C ratio of 3:1 (Figure 5.17 (c)). Referring back to the H_2 - analyses, it was

shown that there is a higher population of weakly adsorbed hydrogen on the Pt/χ-Al_2O_3. It is proposed that for higher concentrations of hydrogen species on the surface coupled with the relatively high mobility of the hydrogen species, results in the relatively high desorption rate of spillover hydrogen on the χ-Al_2O_3 surface. As a result there is less spillover hydrogen available to hydrogenate the coke precursor hydrocarbons. Therefore a higher hydrogen partial pressure is required for the χ-Al_2O_3 to achieve the observed change in composition of coke described above.

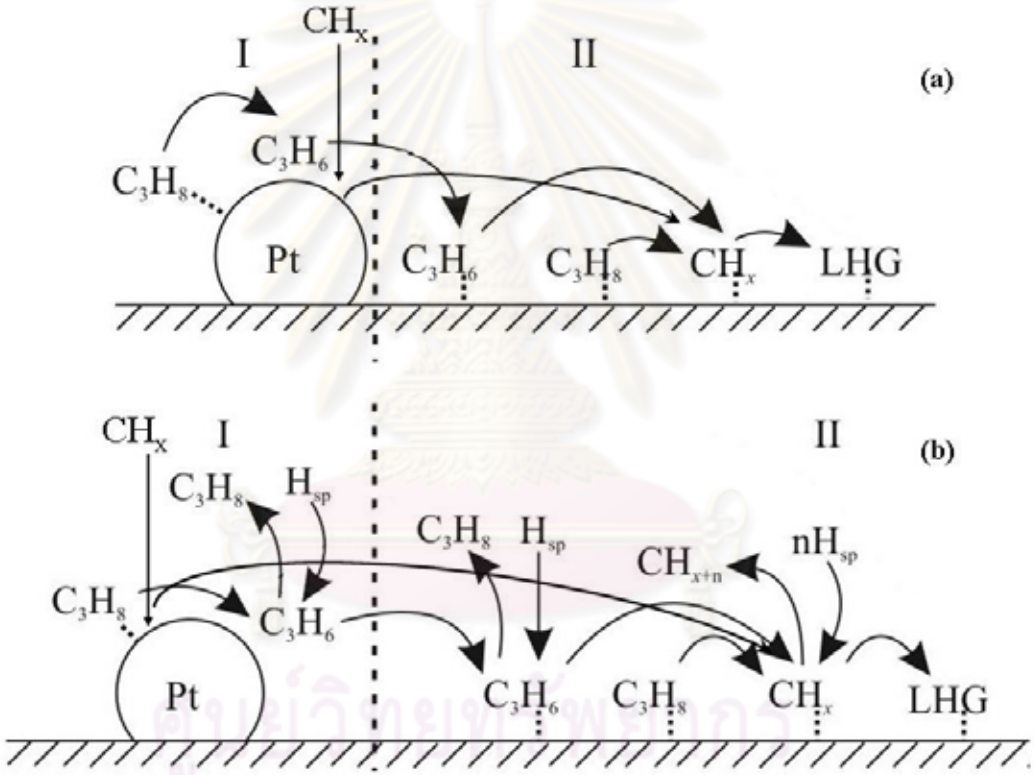

Figure 5.18 Coking and propane conversion mechanism for the Pt/γ-Al_2O_3 and Pt/χ-Al_2O_3 catalysts. (a) H_2/C_3H_8 Ratio = 0 (b) H_2/C_3H_8 Ratio = 1,3

Proposed Mechanism

A mechanism is proposed to help explain the reported experimental observations, as shown in Figure 5.18. The mechanism is split into two main sections I and II. Section I refers to hydrogenation, dehydrogenation and coke deposition processes that take place on the Pt sites. It is assumed majority of the coke is due to the deposition of coke from the substrate. Section II refers to acid catalysed conversion of propylene and propane into oligomers, napthalenes, aromatics, referred to here as CH_x species and carbonaceous species referred to here as low hydrogen content graphitic coke (LHG). Sections II also includes the hydrogenation unsaturated species propylene and CH_x. Beginning in the absence of hydrogen (Figure 5.18 (a)), The dissociative chemisorption of propane adsorbs on a single platinum atom resulting in the formation of propylene in dehydrogenation process. In the long run dehydrogenation reaction, propane and propylene are adsorbed on the metal sites, series of fragmentation lead to low coke formation on the metal and then migrate to the support. Other CH_x species were occurred by the acid catalysed conversion of propylene and propane and then transform to low hydrogen content graphitic coke. With the introduction of hydrogen in Figure 5.18 (b) refers to the hydrogenation, dehydrogenation , after the dehydrogenation reaction propylene can react on the Pt metal with hydrogen species from feed stream and hydrogenate to propane. The propylene and CH_x species on the support in the same way react with the hydrogen species, in this case propane was occurred and saturated CH_x species were produced . The high conversion rate of the $Pt/\chi\text{-}Al_2O_3$ is due to the high mobility of the hydrogen species and spillover hydrogen on Pt metal and the $\chi\text{-}Al_2O_3$ surface. The low coke deposition rate for the $Pt/\chi\text{-}Al_2O_3$ is due to low acidity and the hydrogenation unsaturated species propylene and CH_x.

5.5 The effect of mixed γ - and χ -crystalline phase Al_2O_3 on propane dehydrogenation

The catalytic performances of Pt/C0G100, Pt/C100G0, Pt/C50G50 and Pt/C70G30 catalysts in propane dehydrogenation under H_2/C_3H_8 ratio = 1 and 3 are shown in Figure 5.19. The initial conversion at 5 min of propane dehydrogenation over Pt/C70G30, Pt/C50G50, Pt/C100G0 and Pt/C0G100 catalysts at the ratio H_2/C_3H_8 = 1 were 35.99, 35.93, 31.15 and 24.13 %, respectively. The results show that the higher conversion obtained for the Pt/C70G30, Pt/C50G50. An increase in the ratio of H_2/C_3H_8 to 3 results in a decrease in the conversion for all catalysts at 5 minutes on stream due to an increase hydrogen partial pressure. The Pt on mixed phased Al_2O_3 (Pt/C70G30, Pt/C50G50) still has higher activity than pure phase alumina (χ and γ -Al_2O_3). The differences in catalytic behaviors of Pt/γ-Al_2O_3 and Pt/χ-Al_2O_3 catalysts were previously explained by the hydrogen species mobility and the higher amount of hydrogen spillover on Pt/χ-Al_2O_3 compared to Pt/γ-Al_2O_3. Previous studies have shown that one of the important reasons for platinum-based catalyst during the dehydrogenation of light paraffin is the small ensembles of surface platinum atoms or high dispersion of platinum. From CO-Chemisorption experiments, the metal active sites of platinum supported on Pt/C70G30, Pt/C50G50 were higher than those on the pure phase Al_2O_3 (Pt/C100G0 and Pt/C0G100). In the presence of H_2, the catalytic activity of propane dehydrogenation depended on the platinum dispersion as showed in the high conversion on Pt/C70G30 and Pt/C50G50 in this study.

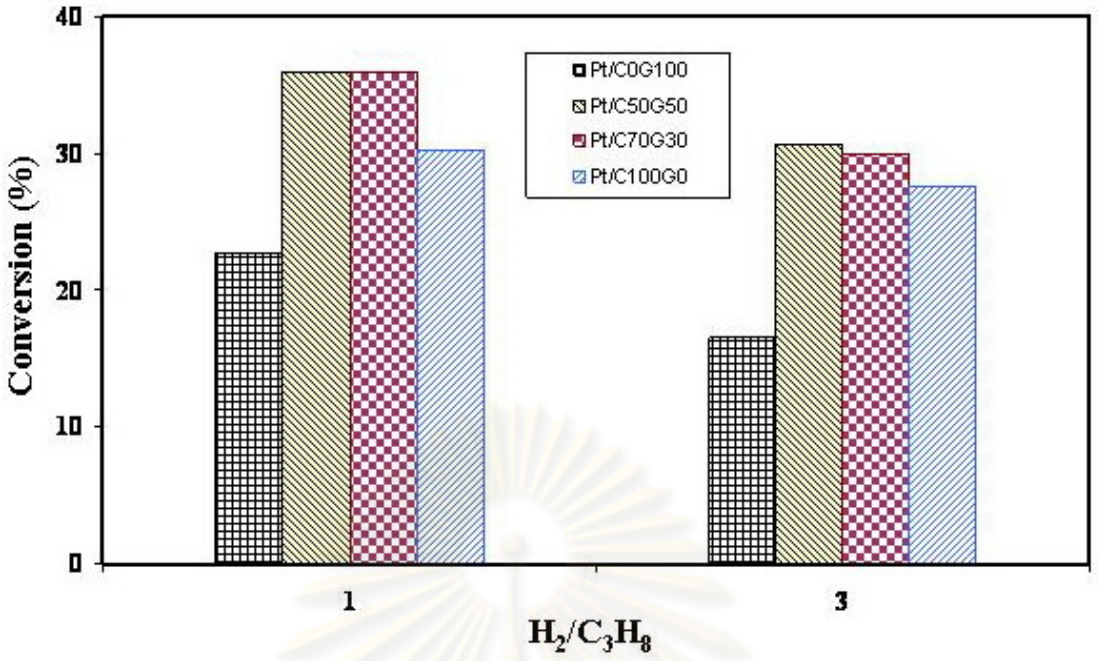

Figure 5.19 Percentage conversion of propane at 5 min. for Pt/C0G100, Pt/C100G0, Pt/C50G50 and Pt/C70G30 catalysts with hydrogen/propane feed gas mixture ratios of 1:1 and 3:1.

ศูนย์วิทยทรัพยากร
จุฬาลงกรณ์มหาวิทยาลัย

CHAPTER VI

CONCLUSIONS AND RECOMMENDATIONS

6.1 Conclusions

The conclusions of the present research are the following:

1. The Pt on mixed phase alumina showed higher activity performances than the gamma and chi alumina through the shift down of the light-off temperature about 50°C on propane oxidation due to the higher platinum dispersion and the interaction between Pt metal and mixed support alumina.

2. Results obtained from H_2 and NH_3-TPD and propane conversion tests indicate that the higher conversion rates and lower coke deposition rates obtained for the Pt/χ-Al_2O_3 catalyst in the presence of hydrogen are attributed to the more highly concentrated active sites, weaker hydrogen adsorption sites. This in turn is considered to be due to a higher proportion of octahedrally coordinated Al atoms at or near the χ-Al_2O_3 surface which confirmed by XPS.

3. The selectivity to propylene was low in Pt/χ-Al_2O_3 catalyst due to the side reactions of cracking and hydrogenolysis were more important for propane dehydrogenation.

4. In the presence of hydrogen, Pt/ mixed phased alumina showed higher initial catalytic activity in propane dehydrogenation than the gamma and chi alumina. This is due to the higher platinum dispersion on mixed phased chi and gamma alumina.

6.2 Recommendations

From this experiment, the recommendations for future works are the following;

1. The low conversion on Pt/chi alumina compare to Pt/ gamma alumina in propane dehydrogenation with the ratio H_2/C_3H_8 = 0. I proposed that the close proximity of the active sites results in a greater crowding and interference with coke deposit. To confirm that I mentioned above, the platinum metal dispersion on the catalysts should be characterized by other advance techniques.

2. The end point of graph line in figure5.14 (TPO data) isn't low enough to calculation the amount of coke therefore; this technique could be improved for coke comparison with TGA data.

3. The use of mix phased χ and γ- Al_2O_3 as supports, it was shown that it is given high active site of Pt and Pt dispersion; however, the evidences are still vague. Hence, it should be uncovered these results.

4. To confirm the lower propene selectivity on Pt/χ- Al_2O_3 in this work, Pt metal location and Pt dispersion on the χ and γ- Al_2O_3 support should be investigate by other advance techniques and test in the hydrogenolysis reaction .

ศูนย์วิทยทรัพยากร
จุฬาลงกรณ์มหาวิทยาลัย

REFERENCES

[1] Gitzen W.H. Alumina as a Ceramic Material. Westerville: Wiley, 1970.

[2] Pajonk G.M., and Teichner, S.J. Proceeding in Physics. Aerogels (1986): 193.

[3] Church J.S., Cant, N.W., and Trimm, D.L. Stabilisation of aluminas by rare earth and alkaline earth ions. Applied Catalysis A: General 101(1993): 105-116.

[4] Farrauto R.J. and C.H. Bartholomew. Fundamentals of Industrial Catalytic Processes. Blackie Academic & Professional (1997): 640-644.

[5] Kim S.D., et al. Effect of γ-alumina content on catalytic performance of modified ZSM-5 for dehydration of crude methanol to dimethyl ether. Applied Catalysis A: General 309(2006): 139-143.

[6] Xia J., Mao, D., Zhang, B., Chen, Q., Zhang, Y., and Tang, Y. Catalytic properties of fluorinated alumina for the production of dimethyl ether. Catalysis Communications 7(2006): 362-366.

[7] Praserthdam P., Inoue, M., Mekasuvandumrong, O., Thanakulrangsan, W., and Phatanasri, S. Effect of organic solvents on the thermal stability of porous silica-modified alumina powders prepared via one pot solvothermal synthesis. Inorganic Chemistry Communications 3(2000): 671-676.

[8] Mekasuwandumrong O., Kominami, H., Praserthdam, P., Inoue, M., and Blendell, J.E. Synthesis of Thermally Stable χ-Alumina by Thermal Decomposition of Aluminum Isopropoxide in Toluene. Journal of the American Ceramic Society 87(2004): 1543-1549.

[9] Mekasuwandumrong O., Pavarajarn,V., Inoue, M., and Praserthdam, P. Preparation and phase transformation behavior of χ -alumina via solvothermal synthesis. Materials Chemistry and Physics 100(2006): 445-450.

[10] Pansanga K., Mekasuwandumrong, O., Panpranot J., and Praserthdam, P. Synthesis of nanocrystalline alumina by thermal decomposition of aluminum isopropoxide in 1-butanol and their applications as cobalt catalyst support. Korean Journal of Chemical Engineering 24(2007): 397-402.

[11] Khom-in J., Praserthdam, P., Panpranot J., and Mekasuwandumrong, O. Dehydration of methanol to dimethyl ether over nanocrystalline Al_2O_3 with mixed [gamma]- and [chi]-crystalline phases. Catalysis Communications 9(2008): 1955-1958.

[12] Inoue M., Kominami H., and T., Inui. Thermal Decomposition of Alkoxides in an Inert Organic Solvent: Novel Method for the Synthesis of Homogeneous Mullite Precursor. Journal of the American Ceramic Society 79(1996): 793-795.

[13] Mekasuwandumrong O., Tantichuwet, P., Chaisuk, C., and Praserthdam, P. Impact of concentration and Si doping on the properties and phase transformation behavior of nanocrystalline alumina prepared via solvothermal synthesis. Materials Chemistry and Physics 107(2008): 208-214.

[14] Meephoka C., Chaisuk, C., Samparnpiboon, P., and Praserthdam, P. Effect of phase composition between nano [gamma]- and [chi]-Al_2O_3 on Pt/Al_2O_3 catalyst in CO oxidation. Catalysis Communications 9(2008): 546-550.

[15] Bera P., Patil K.C., and Hegde, M.S., Oxidation of CH_4 and C_3H_8 over combustion synthesized nanosize metal particles supported on [small alpha]-Al_2O_3. Physical Chemistry Chemical Physics 2(2000): 373-378.

[16] Yazawa Y., Yoshida, H., Takagi, N., Komai, S.-i., Satsuma, A., and Hattori, T. Oxidation state of palladium as a factor controlling catalytic activity of Pd/SiO_2-Al_2O_3 in propane combustion. Applied Catalysis B: Environmental 19(1998): 261-266.

[17] Yazawa Y., Kagi, N., Komai, S.-i., Satsuma, A., Y Murakami., and Hattori, T. Kinetic study of support effect in the propane combustion over platinum catalyst. Catalysis Letters 72(2001): 157-160.

[18] Yazawa Y., Yoshida, H. N., Takagi, Komai,S.-i., Satsuma, A., and Hattori, T. Acid Strength of Support Materials as a Factor Controlling Oxidation State of Palladium Catalyst for Propane Combustion. Journal of Catalysis 187(1999): 15-23.

[19] Yoshida H., Yazawa, Y., and T., Hattori. Effects of support and additive on oxidation state and activity of Pt catalyst in propane combustion. Catalysis Today 87(2003): 19-28.

[20] Corro G., Fierro, J.L.G., and Odilon, V.C. An XPS evidence of Pt^{4+} present on sulfated Pt/Al_2O_3 and its effect on propane combustion. Catalysis Communications 4(2003): 371-376.

[21] Gluhoi A.C., Bogdanchikova, N. and Nieuwenhuys, B.E. Total oxidation of propene and propane over gold-copper oxide on alumina catalysts: Comparison with Pt/Al_2O_3. Catalysis Today 113(2006): 178-181.

[22] Solsona B., Davies, T.E., Garcia, T., Vazquez, I., Dejoz, A., and Taylor, S.H. Total oxidation of propane using nanocrystalline cobalt oxide and supported cobalt oxide catalysts. Applied Catalysis B: Environmental 84(2008): 176-184.

[23] Barias O.A., Holmen, A., and Blekkan, E.A. Propane dehydrogenation over supported platinum catalysts: effect of tin as a promoter. Catalysis Today 24(1995): 361-364.

[24] Barias O.A., Holmen, A., and Blekkan, E.A. Propane dehydrogenation over supported Pt and Pt-Sn catalysts: Catalyst preparation, characterization, and activity measurements. Journal of Catalysis 158(1996): 1-12.

[25] Aguilar-Ros G., et al. Hydrogen interactions and catalytic properties of platinum-tin supported on zinc aluminate. Applied Catalysis A: General 127(1995): 65-75.

[26] Jablonski E.L., Castro, A.A., Scelza, O.A., and Miguel de, S.R. Effect of Ga addition to Pt/Al_2O_3 on the activity, selectivity and deactivation in the propane dehydrogenation. Applied Catalysis A: General 183(1999): 189-198.

[27] Salmones J., Wang, J.-A., Galicia, J.A., and Aguilar-Rios, G. H_2 reduction behaviors and catalytic performance of bimetallic tin-modified platinum catalysts for propane dehydrogenation. Journal of Molecular Catalysis A: Chemical 184(2002): 203-213.

[28] Bednarova L., Lyman, C.E., Rytter, E., and Holmen, A. Effect of Support on the Size and Composition of Highly Dispersed Pt-Sn Particles. Journal of Catalysis 211(2002): 335-346.

[29] Yu C., Ge, Q., Xu, H., and Li, W. Effects of Ce addition on the Pt-Sn/ γ -Al_2O_3 catalyst for propane dehydrogenation to propylene. Applied Catalysis A: General 315(2006): 58-67.

[30] Zhang Y., Zhou, Y., Qiu, A., Wang, Y., Xu, Y., and Wu, P. Propane dehydrogenation on PtSn/ZSM-5 catalyst: Effect of tin as a promoter. Catalysis Communications 7(2006): 860-866.

[31] Yu C., Xu, H., Ge, Q., and Li, W. Properties of the metallic phase of zinc-doped platinum catalysts for propane dehydrogenation. Journal of Molecular Catalysis A: Chemical 266(2007): 80-87.

[32] Barbier J., Marecot, P., Martin, N., Elassal, L., and Maurel,R. Selective Poisoning by Coke Formation on Pt/Al_2O_3. Studies in Surface Science and Catalysis 6(1980): 53-62.

[33] Barbier J., Churin, E., Parera, J.M., and Riviere, J. Characterization of coke by hydrogen and carbon analysis. Reaction Kinetics and Catalysis Letters 29(1985): 323-330.

[34] Beltramini J.N., Martinelli, E.E., Churin, E.J., Figoli, N.S., and Parera, J.M. Pt/Al_2O_3-Cl in pure hydrocarbon reforming. Applied Catalysis 7(1983): 43-55.

[35] Barbier J., Corrom, G., Zhang, Y., Bournonville, J.P., and Franck, J.P. Coke formation on platinum-alumina catalyst of wide varying dispersion. Applied Catalysis 13(1985): 245-255.

[36] Marecot P., Churin, E., and Barbier, J. Coke deposits on Pt/Al_2O_3 catalysts of varying dispersities. Reaction Kinetics and Catalysis Letters 37(1988): 233-237.

[37] Parera J.M., Figoli, N.S., Traffano, E.M., Beltramini, J.N., and Martinelli, E.E. The influence of coke deposition on the functions of a Pt/Al_2O_3-Cl bifunctional catalyst. Applied Catalysis 5(1983): 33-41.

[38] Mongkhonsi T., Prasertdham, P., Saengpoo, A., Pinitniyom, N., and Jaikaew, B. Roles of Pt and alumina during the combustion of coke deposits on propane dehydrogenation catalysts. Korean Journal of Chemical Engineering 15(1998): 486-490.

[39] Xu Z., Zhang, T., Fang, Y., Lin, L., Can, L., and Qin, X. Carbon deposition and migration on Pt and Pt-Sn catalysts. Studies in Surface Science and Catalysis 112(1997): 425-432.

[40] Evans K.A. Chemistry of aluminium gallium indium and thallium. New York: Blackie Academic and Professional, 1993.

[41] Lippens B.C., and Boer, J.H. de. Study of phase transformations during calcination of aluminum hydroxides by selected area electron diffraction. Acta Crystallographica 17(1964): 1312-1321.

ศูนย์วิทยทรัพยากร
จุฬาลงกรณ์มหาวิทยาลัย

[42] Wilson S.J. Phase Transformations and Development of Microstructure in Boehmite-Derived Transition Aluminas. Proceedings of the British Ceramic Society 28(1979): 281-294.

[43] Wefers K., Misra, C. Oxides and Hydroxides of Alumina. In. ALCOA Laboratories. Pennsilvania, (1987): 20

[44] Perego C., and Villa, P.L. The catalytic process from laboratory to the industrail plant. Proceedings of the 3rd Seminar on Catalysis (1994).

[45] Lippens B.D., and Boer, J.H. Study of phase transformations during calcination of aluminum hydroxides by selected area electron diffraction. Acta Crystallographica 17(1964): 1312-1321.

[46] Nagai H., Oshima, Y., Hirano, K., and Kato, A. Sintering Behavior of Aluminum-oxide Derived from Aluminum Hydroxides with Various Morphologies. Journal of the British Ceramic Society 93(1993): 114.

[47] Fierro J.L.G. Metal Oxides: Chemistry and Applications. California: Taylor& Francis Group, 2006.

[48] Saalfeld H. Structure Phases of Dehydrated Gibbsite in Reactivity of solid. Amsterdam: Elsevier, 1961.

[49] Brindley G.W. and J.O., Choe. The Reaction Series, Gibbsite to chi-Alumina to kappa-Alumina to Corundum. American Mineralogist 46(1961): 771-785.

[50] Stiles A.B. Catalyst Supports and Supported Catalyst. Stoneham: Butterworth, 1987.

ศูนย์วิทยทรัพยากร
จุฬาลงกรณ์มหาวิทยาลัย

[51] Dollimore D., Dollimore, J., and Perry, P.D. The Thermal Decomposition of Oxalates. Part VIII. Thermalgravimetric and X-Ray Analysis Study of the Decomposition of Aluminium Oxalate. Journal of the Chemical Society A: Inorganic, Physical, Theoretical (1967): 448-450.

[52] Stumpf H.C., Russell, A.S., Newsome, J.W., and Tucker, C.M. Thermal Transformation of aluminas and Alumina Hydrates. Industrial & Engineering Chemistry Research 42(1950): 1398-1403.

[53] Hicks R.F., Qi, H., Young, M.L., and Lee, R.G. Structure sensitivity of methane oxidation over platinum and palladium. Journal of Catalysis 122(1990): 280-294.

[54] Kooh A.B., Han, W.J., Lee, R.G., and Hicks, R.F. Effect of catalyst structure and carbon deposition on heptane oxidation over supported platinum and palladium. Journal of Catalysis 130(1991): 374-391.

[55] Mouaddib N., Feumi-Jantou, C., Garbowski, E., and Primet, M.. Catalytic oxidation of methane over palladium supported on alumina: Influence of the oxygen-to-methane ratio. Applied Catalysis A: General 87(1992): 129-144.

[56] Muto K.I., Katada, N., and Niwa., M. Complete oxidation of methane on supported palladium catalyst: Support effect. Applied Catalysis A: General 134(1996): 203-215.

[57] Bera P., Patil, K.C., and Hegde, M.S. Oxidation of CH_4 and C_3H_8 over combustion synthesized nanosize metal particles supported on Al_2O_3. Phys Chem Chem Phys 2(2000): 377.

[58] Ertl G.L., and Koch, J. Proceedings of 5th Internatbnal Congress on Catalysis. New York: American Elsevier, 1973.

[59] Campbell C.T., Foyt, D.C., and White, J.M. Oxygen Penetration into the Bulk of Palladium The Journal of Physical Chemistry 81(1977): 491-494.

[60] Yao Y.-F.Y. Oxidation of Alkanes over Noble Metal Catalysts. Industrial & Engineering Chemistry Product Research and Development 19(1980): 293-298.

[61] Burch R., Crittle, D.J., and Hayes, M.J. C-H bond activation in hydrocarbon oxidation on heterogeneous catalysts. Catalysis Today 47(1999): 229-234.

[62] Hiam L., Wise, H., and Khaikin, S. Catalytic oxidation of hydrocarbons on platinum. Journal of Catalysis 10(1968): 272-276.

[63] Cullis. C.F., Keene, D.E., and Trimm, D.L. Studies of the partial oxidation of methane over heterogeneous catalysts. Journal of Catalysis 19(1970): 378-385.

[64] Schwartz A., Holbrook, L.L., and Wlse, H. Catalytic oxidation studies with platinum and palladium. Journal of Catalysis 21(1971): 199-207.

[65] Otto K. Methane oxidation over Pt on γ -alumina: kinetics and structure sensitivity. Langmuir 5(1989): 1364-1369.

[66] Briot P., Auroux, A., Jones, D., and Primet, M. Effect of particle size on the reactivity of oxygen-adsorbed platinum supported on alumina. Applied Catalysis 59(1990): 141-152.

[67] Kooh A.B., Han,W.-J., Lee, R.G., and Hicks, R.F. Effect of catalyst structure and carbon deposition on heptane oxidation over supported platinum and palladium. Journal of Catalysis 130(1991): 374-391.

[68] Baldwin T.R., and Burch, R. Catalytic combustion of methane over supported palladium catalysts: I. Alumina supported catalysts. Applied Catalysis 66(1990): 337-358.

[69] Yazawa Y., Yoshida, H., and Hattori, T. The support effect on platinum catalyst under oxidizing atmosphere: improvement in the oxidation-resistance of platinum by the electrophilic property of support materials. Applied Catalysis A: General 237(2002): 147.

[70] Lee J.H. and Trimm, D.L. Catalytic combustion of methane. Fuel Processing Technology 42(1995): 339-359.

[71] Lisa D. P. Heterogeneous/homogeneous reactions and transport coupling for catalytic combustion systems: a review of model alternatives. Catalysis Today 26(1995):255-265.

[72] Anderson R.B., Stein, K.C., Feenan, J.J., and Hofer, L.J.E. Catalytic oxidation of methane. Journal of Industrial & Engineering Chemistry 53(1961): 809-812.

[73] Arai H., Yamada, K., Eguchi, K., and Seiyama, T. Catalytic combustion of methane over various perovskite-type oxides. Applied Catalysis 26(1986): 265-276.

[74] Sanfilippo D. Dehydrogenation of Paraffins; Key Technology for Petrochemicals and Fuels. Cattech 4(2000): 56-73.

[75] Akporiaye D., et al. A Novel, Highly Efficient Catalyst for Propane Dehydrogenation. Industrial & Engineering Chemistry Research 40(2001): 4741-4748.

[76] Barias O.A., Holmen, A., and Blekkan, E.A. Propane Dehydrogenation over Supported Pt and Pt-Sn Catalysts: Catalyst Preparation, Characterization, and Activity Measurements. Journal of Catalysis 158(1996): 1-12.

[77] Marcilly C. Present status and future trends in catalysis for refining and petrochemicals. Journal of Catalysis 216(2003): 47-62.

[78] Cavani F., Ballarini, N., and Cericola, A. Oxidative dehydrogenation of ethane and propane: How far from commercial implementation. Catalysis Today 127(2007): 113-131.

[79] Tullo A.H. Bringing Good Things to Life. Chemical & Engineering News 81(2003): 15-16.

[80] Egloff G., Thomas, C.L., and Linn, C.B. Pyrolysis of Propane and the Butanes. Industrial & Engineering Chemistry 28(1936): 1283-1294.

[81] Turkevich J., Bonner, F., Schissler, D.O.,and Irsa, P. Stable and unstable isotopes in catalytic research. Discussions of the Faraday Society 8(1950): 348-352.

[82] Satterfield C.N. Heterogeneous Catalysis in Practice. McGraw-Hill Chemical engineering series, United States of America (1980).

[83] Hughes R. Deactivation of Catalyst. Academic Press, London (1984): 265.

[84] Butt J.B., and Eugene, E. P. Activation, Deactivation and Poisoning of catalyst. Academic press, London (1988).

[85] Franck J.P, and Martino, G. Deactivation and Poisoning of Catalyst. Marcel Dekker, New York (1985).

[86] Figoli N.S., Beltramini, J.N., Martinelli, E.E., Sad, M.R., and Parera, J.M. Operational conditions and coke formation on platinum-alumina reforming catalyst. Applied Catalysis 52(1983): 19-32.

[87] Gates B.C., Katzer, J.R., and Schuit, C.A. Chemistry of Catalytic Processes. McGraw-Hill, New York (1979)184.

[88] Cooper B.J.T., Catalyst Deactivation. Elsevier, Amsterdam, Netherlands (1980).

[89] Inoue M., H. Otsu, Kominami, H., and Inui, T. Synthesis of Thermally Stable, Porous Silica-Modified Alumina via Formation of a Precursor in an Organic Solvent. Industrial & Engineering Chemistry Research 35(1996): 295-306.

[90] Miller J.T., Meyers, B.L., Modica, F.S., Lane, G.S., Vaarkamp, M., and Koningsberger, D.C. Hydrogen Temperature-Programmed Desorption (H_2 TPD) of Supported Platinum Catalysts. Journal of Catalysis 143(1993): 395-408.

[91] Joubert J., P. Fleurat-Lessard, Delbecq, F., and Sautet, P. Simulating Temperature Programmed Desorption of Water on Hydrated γ-Alumina from First-Principles Calculations. The Journal of Physical Chemistry B 110(2006): 7392-7395.

[92] Foger K., and Anderson, J.R. Reactions of neopentane and neohexane on platinum/Y-zeolite and platinum/silica catalysts. Journal of Catalysis 54(1978): 318-335.

[93] Dou L.Q., Tan, Y.S., and Lu, D.S. Coated silica as support for platinum catalyst. II. Hydrogen chemisorption and activity for combustion. Applied Catalysis 66(1990): 235-246.

[94] Kramer R., and Andre, M. Adsorption of atomic hydrogen on alumina by hydrogen spillover. Journal of Catalysis 58(1979): 287-295.

[95] He S., Sun, C., Bai, Z., Dai, X., and Wang, B. Dehydrogenation of long chain paraffins over supported Pt-Sn-K/Al_2O_3 catalysts: A study of the alumina support effect. Applied Catalysis A: General 356(2009): 88-98.

[96] Menon P.G., and Froment, G.F. Residual hydrogen in supported platinum catalysts and its influence on their catalytic properties. Applied Catalysis 1(1981): 31-48.

[97] Levy P.J., and Primet, M. States of hydrogen adsorption on platinum-alumina and platinum-ceria catalysts : A temperature-programmed desorption study. Applied Catalysis 70(1991): 263-276.

[98] Ferreira-Aparicio P., Guerrero-Ruiz, A., and Rodriguez-Ramos, I. Hydrogen adsorbed species at the metal/support interface on a Pt/Al_2O_3 catalyst. Journal of the Chemical Society, Faraday Transactions 93(1997): 3563-3567.

[99] Dong W., Wang, X., Wang, H., and Peng, S. TPR and H_2-TPD studies of Pt-$Sn/MgAl_2O_4$ catalysts. Chinese Journal of Catalysis 20(1999): 579-580.

[100] Thomson J., Webb, G., Webster, B.C., and Winfield, J.M. Catalytic properties of γ -alumina. Ab initio molecular orbital studies of clusters of chlorinated γ -alumina. Journal of the Chemical Society, Faraday Transactions 91(1995): 155-161.

[101] Ionescu A., Allouche, A., Aycard, J.P., Rajzmann, M., and Hutschka, F. Study of gamma Alumina Surface Reactivity: Adsorption of Water and Hydrogen Sulfide on Octahedral Aluminum Sites. The Journal of Physical Chemistry B 106(2002): 9359-9366.

[102] Räty J., Suvanto, M., Hirva, P., and Pakkanen, T.A. Adsorption and stepwise decarbonylation of $Re_2(CO)_{10}$ on gamma-alumina: a theoretical study. Surface Science 492(2001): 243-248.

[103] Ahmed F., et al. Dynamics of Hydrogen Spillover on Pt/χ-Al_2O_3 Catalyst Surface: A Quantum Chemical Molecular Dynamics Study. The Journal of Physical Chemistry C 113(2009): 15676-15683.

[104] Kang W., Cheng, B., Li, Q., Zhuang, X., and Ren, Y. A new method for preparing alumina nanofibers by electrospinning technology. Textile Research Journal 81(2011): 148-155.

[105] Vázquez A., López, T., Gómez, R., Bokhimi, Morales, A., and Novaro, O. X-Ray Diffraction, FTIR, and NMR Characterization of Sol-Gel Alumina Doped with Lanthanum and Cerium. Journal of Solid State Chemistry 128(1997): 161-168.

[106] Lavalley J.C., Bensitel, M., Gallas, J.P., Lamotte, J., Busca, G., and Lorenzelli, V. FT-IR study of the [delta](OH) mode of surface hydroxy groups on metal oxides. Journal of Molecular Structure 175(1988): 453-458.

[107] Elmi C., et al. Crystal chemistry, surface morphology and X-ray photoelectron spectroscopy of Fe-rich osumilite from Mt. Arci, Sardinia (Italy). Physics and Chemistry of Minerals 37(2010): 561-569.

[108] Kloprogge J.T., Duong, L.V., Wood, B.J., and Frost, R.L. XPS study of the major minerals in bauxite: Gibbsite, bayerite and (pseudo-)boehmite. Journal of Colloid and Interface Science 296(2006): 572-576.

[109] Delaportas D., et al. γ-Al_2O_3 nanoparticle production by arc-discharge in water: in situ discharge characterization and nanoparticle investigation. Journal of Physics D: Applied Physics 42(2009): 245204.

[110] Barr T. L., Seal, S., Wozniak, K., and Klinowski, J. ESCA studies of the coordination state of aluminium in oxideenvironments. Journal of the Chemical Society, Faraday Transactions 93(1997): 181-186.

[111] Pansanga K., J. Panpranot, O. Mekasuwandumrong, C. Satayaprasert, J.G. Goodwin and Praserthdam, P. Effect of mixed [gamma]- and [chi]-crystalline phases in nanocrystalline Al_2O_3 on the dispersion of cobalt on Al_2O_3. Catalysis Communications 9(2008): 207-212.

[112] Jongsomjit B., T., Wongsalee and Praserthdam, P. Characteristics and catalytic properties of Co/TiO_2 for various rutile:anatase ratios. Catalysis Communications 6(2005): 705-710.

[113] Komhom S., Mekasuwandumrong, O., Praserthdam, P., and Panpranot, J. Improvement of Pd/Al_2O_3 catalyst performance in selective acetylene hydrogenation using mixed phases Al_2O_3 support. Catalysis Communications 10(2008): 86-91.

[114] Grau, J.M., Vera, C.R., and Parera, J.M. Preventing self-poisoning in [Pt/Al_2O_3 + SO^4_2--ZrO_2] mixed catalysts for isomerization-cracking of heavy alkanes by prereduction of the acid function. Applied Catalysis A: General 227(2002): 217-230.

[115] Lin, T.Z. L.W., Zang, J.L., and Xu, Z.S. Dynamic process of carbon deposition on Pt and Pt-Sn catalysts for alkane dehydrogenation Applied Catalysis 67(1990): 11-23.

[116] Bhasin, M.M., McCain, J.H., Vora, B.V., Imai, T., and Pujad, P.R. Dehydrogenation and oxydehydrogenation of paraffins to olefins Applied Catalysis A: General 221(2001): 397-419.

[117] Datka J., Sarbak, Z., and Eischens, R.P. Infrared Study of Coke on Alumina and Zeolite. Journal of Catalysis 145(1994): 544-550.

[118] Chowdhury, M.B.I., Sui, R., Lucky, R.A., and Charpentier, P.A. One-Pot Procedure to Synthesize High Surface Area Alumina Nanofibers Using Supercritical Carbon Dioxide. Langmuir 26(2009): 2707-2713.

[119] Lietz, G., Volter, J., Dobrovolszky, M., and Paul, Z., Initial changes of the catalytic properties of platinum containing catalysts I. Transformations of mono- and bimetallic Pt/Al_2O_3 catalysts by carbonaceous deposits. Applied Catalysis 13(1984): 77-87.

[120] Jovanovic, M.R.P., and Putanov, P. S. Nature and distribution of coke formed on mono-metallic platinum and bimetallic platinum-rhenium catalysts. Applied Catalysis A: General. 159(1997): 1-7.

[121] Shamsi, A., Baltrus, J.P., and Spivey, J.J., Characterization of coke deposited on Pt/alumina catalyst during reforming of liquid hydrocarbons Applied Catalysis A: General 293(2005): 145-152.

ศูนย์วิทยทรัพยากร
จุฬาลงกรณ์มหาวิทยาลัย

APPENDICES

ศูนย์วิทยทรัพยากร
จุฬาลงกรณ์มหาวิทยาลัย

APPENDIX A

CALCULATION OF THE CRYSTALLITE SIZE

Calculation of the crystallite size by Debye-Scherrer equation

The crystallite size was calculated from the half-height width of the diffraction peak of XRD pattern using the Debye-Scherrer equation.

From Scherrer equation:

$$D = \frac{K\lambda}{\beta \cos\theta} \qquad (A.1)$$

where D = Crystallite size, Å

K = Crystallite-shape factor = 0.9

λ = X-ray wavelength, 1.5418 Å for CuKα

θ = Observed peak angle, degree

β = X-ray diffraction broadening, radian

The X-ray diffraction broadening (β) is the pure width of a powder diffraction free from all broadening due to the experimental equipment. α-Alumina is used as a standard sample to observe the instrumental broadening since its crystallite size is larger than 2000 Å. The X-ray diffraction broadening (β) can be obtained by using Warren's formula.

From Warren's formula:

$$\beta = \sqrt{B_M^2 - B_S^2} \qquad (A.2)$$

where B_M = The measured peak width in radians at half peak height.

B_S = The corresponding width of the standard material.

Example: Calculation of the crystallite size of χ-Al_2O_3

The half-height width of peak = 1.153° (from the figure C.1)

= (1.153xπ)/180

= 0.0201 radian

The corresponding half-height width of peak of α-alumina (from the Bs value at the 2θ of 67.44° in figure C.2) = 0.0057 radian

The pure width, $\beta = \sqrt{B_M^2 - B_S^2}$

$= \sqrt{0.0201^2 - 0.0057^2}$

= 0.01927 radian

Scherrer equation:

B = 0.01927 radian

2θ = 67.44°

θ = 33.72°

λ = 1.5418 Å

The crystallite size $= \frac{0.9 \times 1.5418}{0.01927 \cos 33.72}$

= 86.6 Å

= 8.7 nm

ศูนย์วิทยทรัพยากร
จุฬาลงกรณ์มหาวิทยาลัย

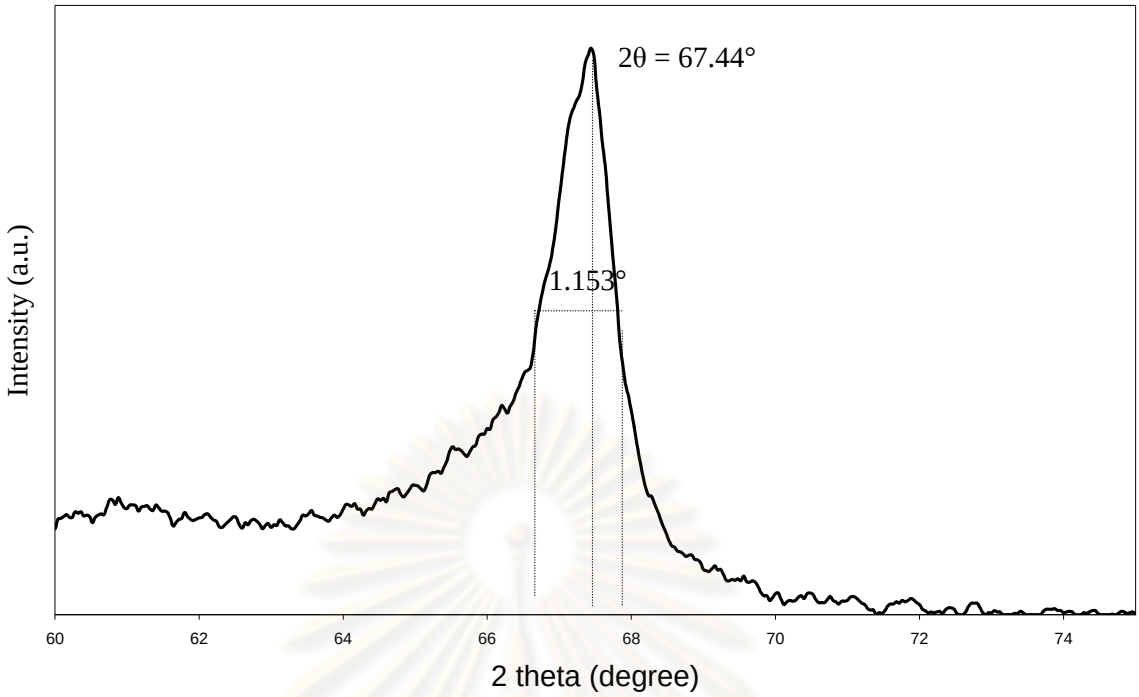

Figure A.1 The diffraction peak of pure chi alumina for calculation of the crystallite size.

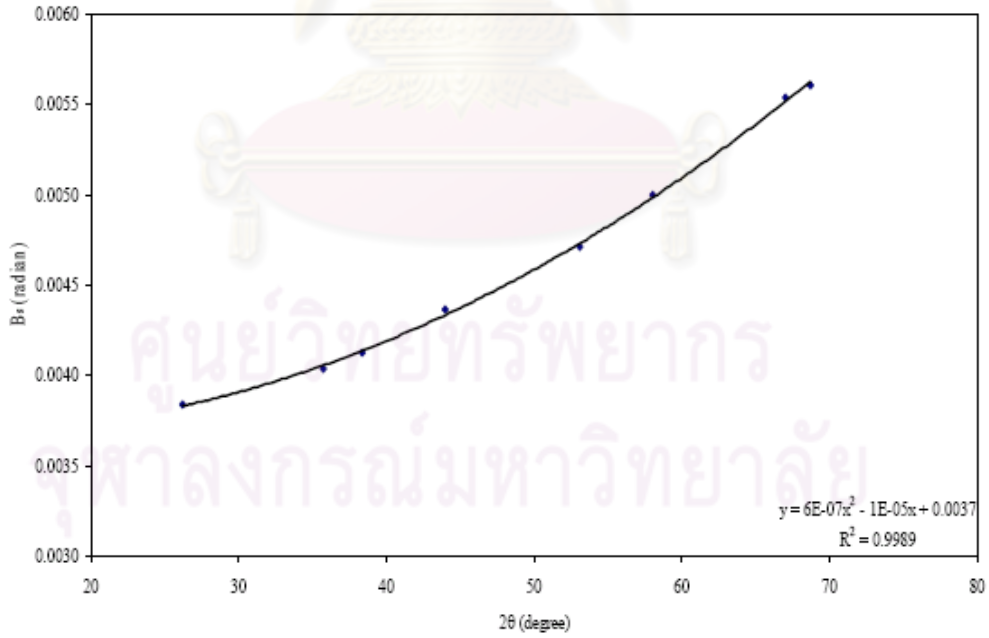

Figure A.2 The plot indicating the value of line broadening due to the equipment. The data were obtained by using α-alumina as a standard.

APPENDIX B

CALCULATION FOR METAL ACTIVE SITES AND DISPERSION

Calculation of the metal active sites and metal dispersion of the catalyst measured by CO adsorption is as follows:

Let the weight of catalyst used	= W	g
Integral area of CO peak after adsorption	= A	unit
Integral area of 50 μl of standard CO peak	= B	unit
Amounts of CO adsorbed on catalyst	= B-A	unit
Volume of CO adsorbed on catalyst	= 50×[(B-A)/B]	μl
Volume of 1 mole of CO at 30^{o}C	= 24.86×10^{6}	μl

Mole of CO adsorbed on catalyst $= \left[\frac{(B-A)}{B}\right]\times\left[\frac{50}{24.86\times10^{6}}\right]$ mole

Molecule of CO adsorbed on catalyst $= \left[1.61\times10^{-6}\right]\times\left[6.02\times10^{23}\right]\times\left[\frac{(B-A)}{B}\right]$ molecules

Metal active sites $= 9.68\times10^{17}\times\left[\frac{(B-A)}{B}\right]\times\left[\frac{1}{W}\right]$ molecules of CO/g of catalyst

Molecules of Pt loaded $= [\%\text{ wt of Pt}]\times\frac{\left[6.02\times10^{23}\right]}{\text{MW of Pt}}$ molecules/g of catalyst

Metal dispersion (%) $= 100\times\left[\frac{\text{molecules of Pt from CO adsorption}}{\text{molecules of Pt loaded}}\right]$

ศูนย์วิทยทรัพยากร
จุฬาลงกรณ์มหาวิทยาลัย

APPENDIX C

The sample of chromatogram and the calibration curve

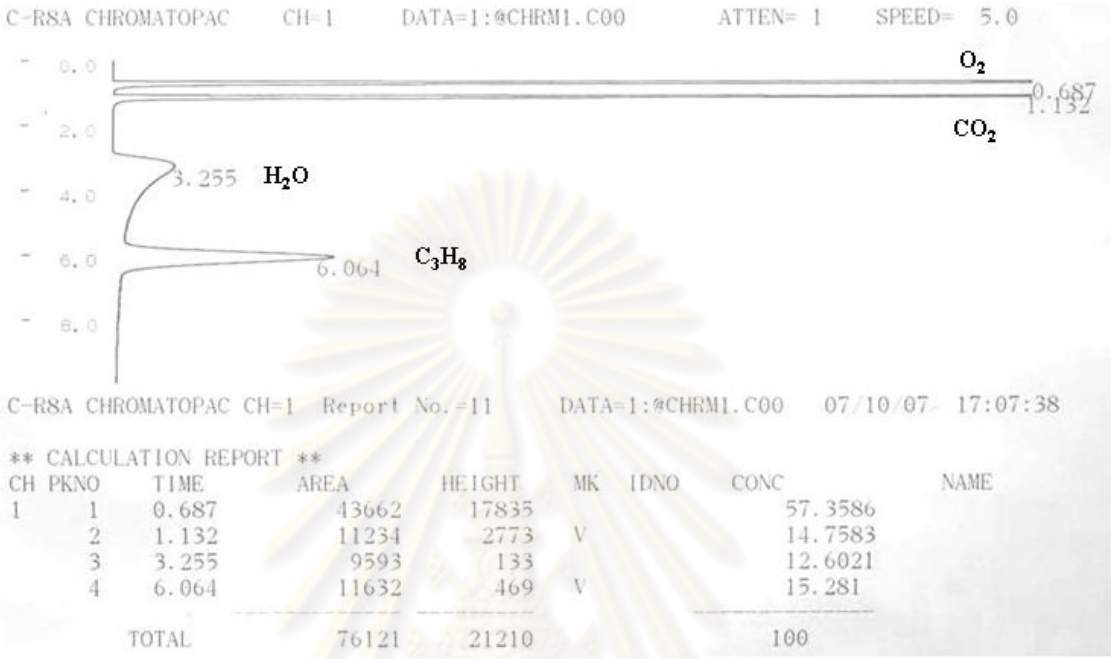

Figure C.1 The sample of chromatogram (Propane oxidation)

The calibration curve of reactant for this study

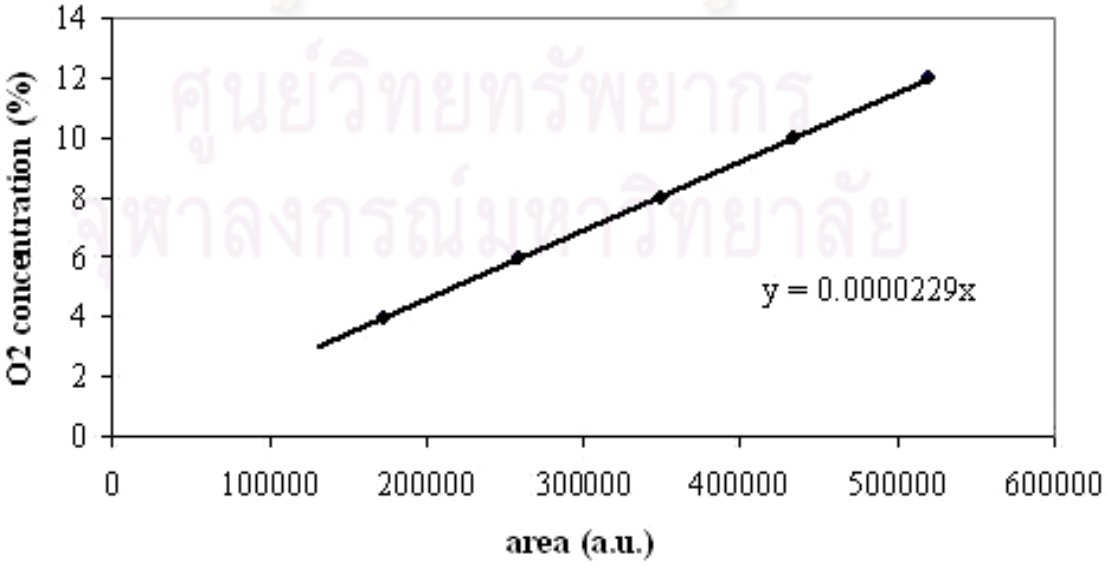

Figure C.2 The calibration curve of oxygen from TCD of GC 8ATP

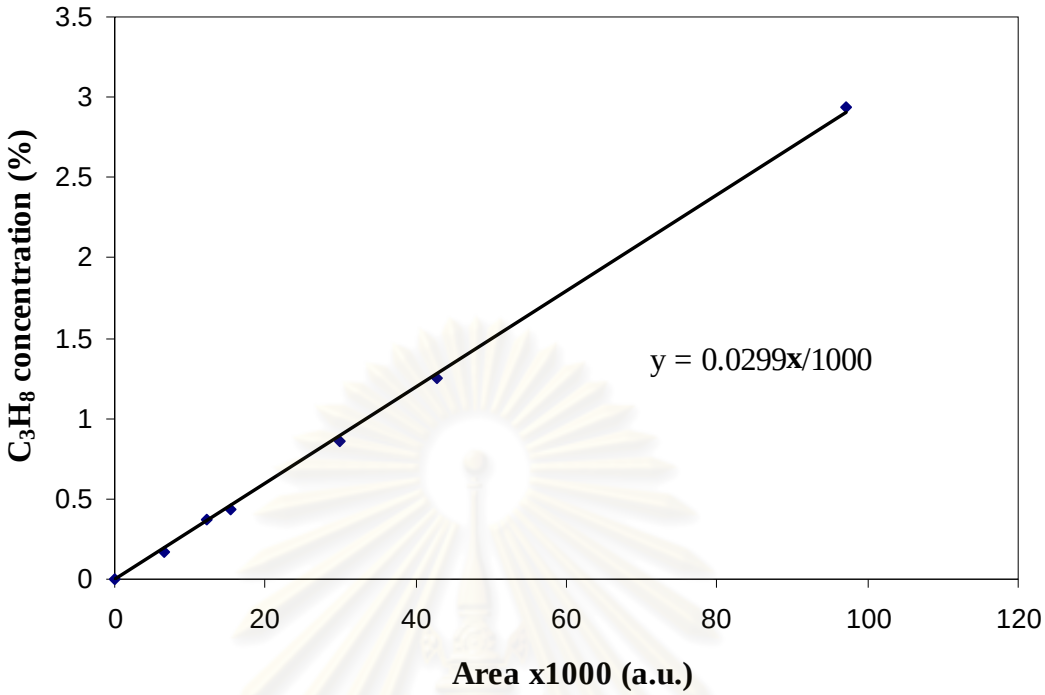

Figure C.3 The calibration curve of C_3H_8 from TCD of GC 8ATP

ศูนย์วิทยทรัพยากร
จุฬาลงกรณ์มหาวิทยาลัย

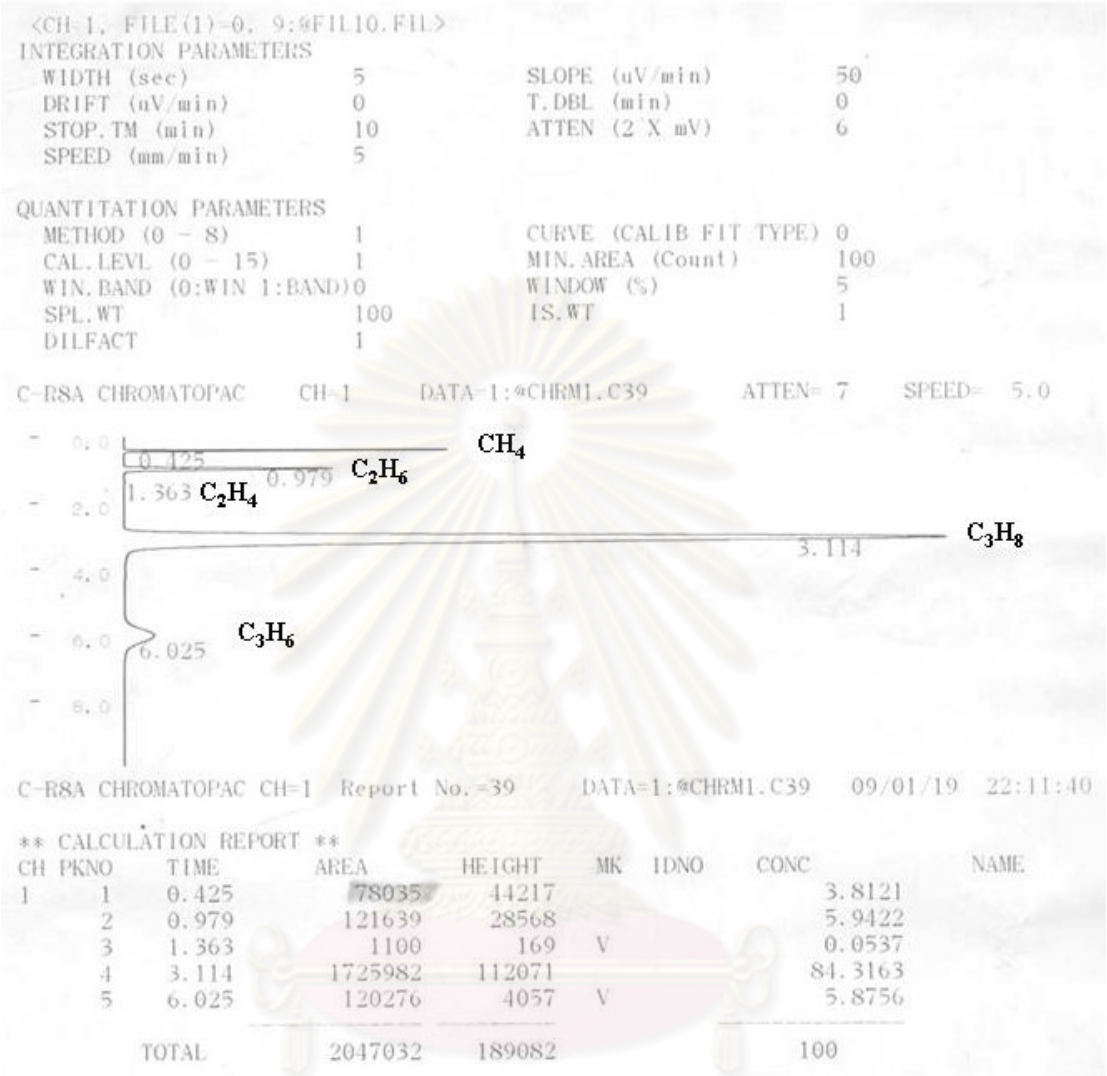

Figure C.4 The sample of chromatogram (Propane dehydrognation)

ศูนย์วิทยทรัพยากร
จุฬาลงกรณ์มหาวิทยาลัย

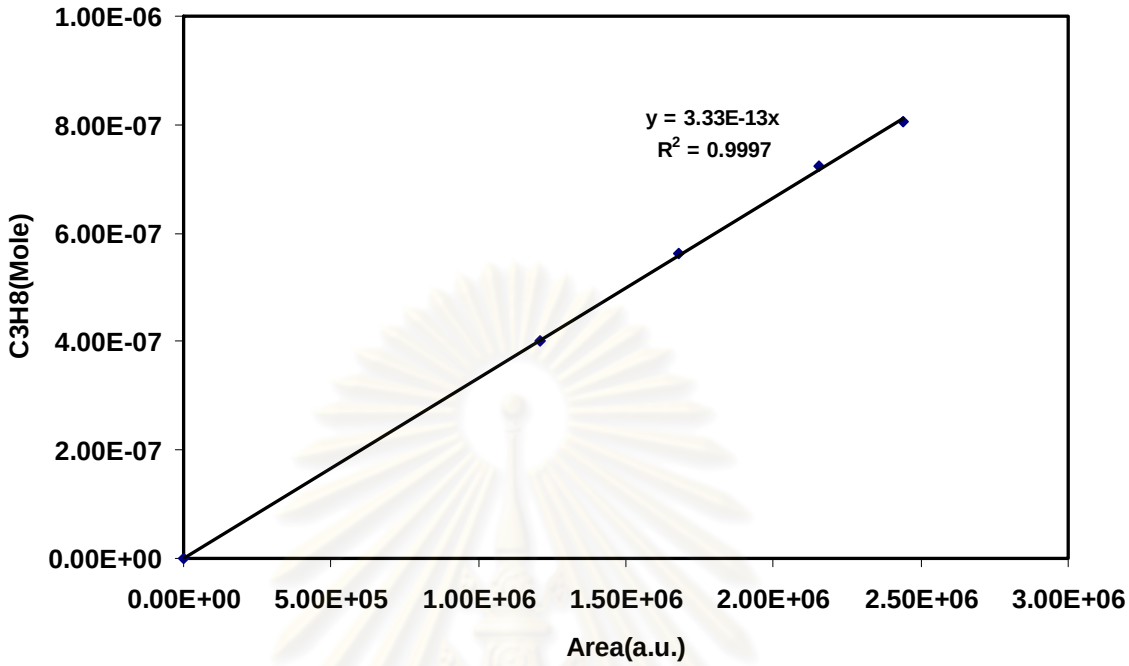

Figure C.5 The calibration curve of C_3H_8 from FID of GC 14B

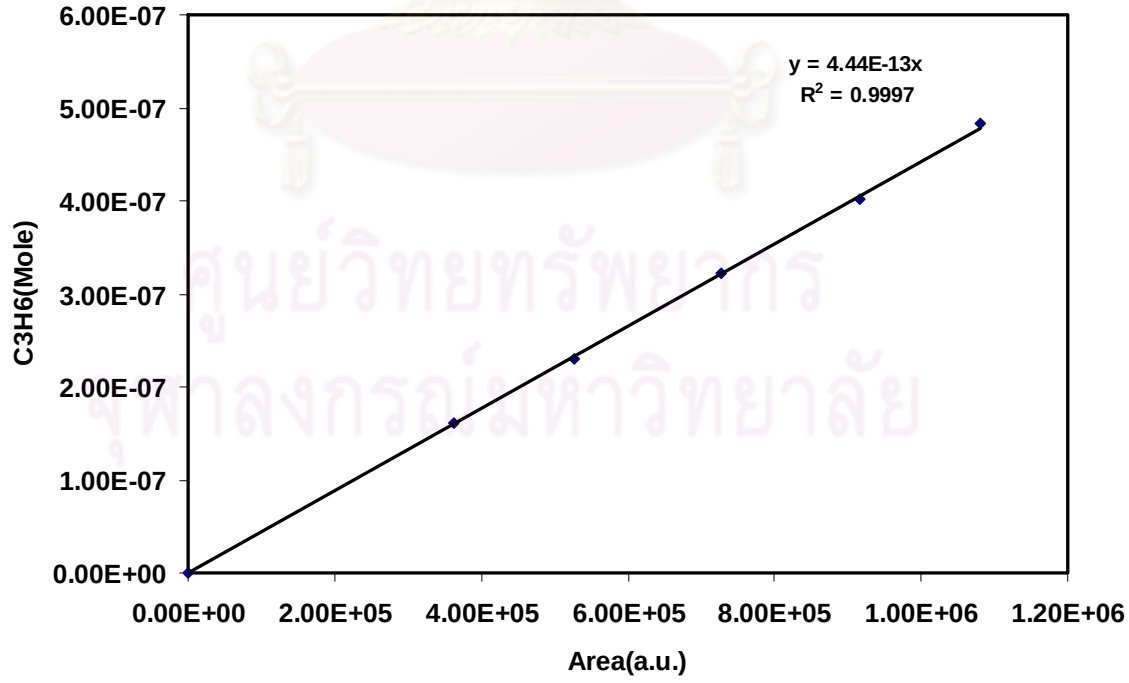

Figure C.6 The calibration curve of C_3H_6 from FID of GC 14B

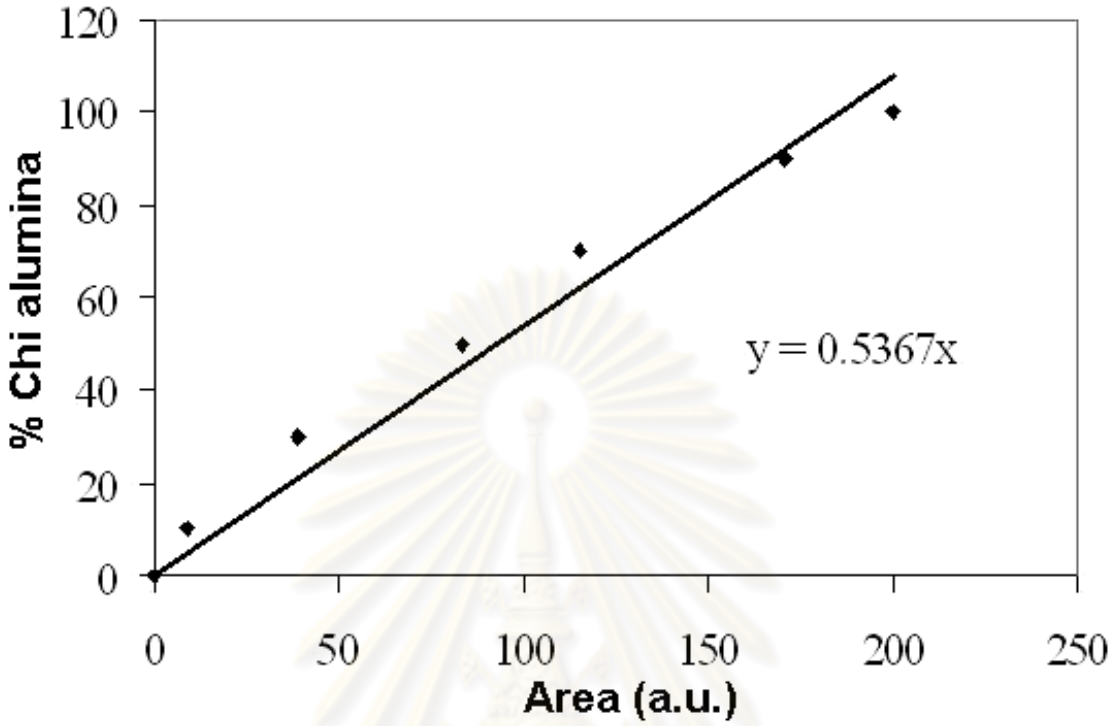

Figure C.7 The calibration curve of %chi alumina phase from XRD data

ศูนย์วิทยทรัพยากร
จุฬาลงกรณ์มหาวิทยาลัย

VITA

Mr Thongchai Glinran was born on January 28, 1973 in Suphanburi, Thailand. He received the Bachelor's Degree in Chemical Engineering from Kasetsart University in March 1997 and Master' s Degree in Chemical Engineering from Kasetsart University in November 2002. After his graduation, he had done his job at Pathumwan Institute of Technology for 4 years. He entered the Doctoral Degree of Engineering in Chemical Engineering at Chulalongkorn University in June 2006.

LIST OF PUBLICATIONS

1. Glinrun T., Mekasuwandumrong O., Panpranot J., Chaisuk C., Praserthdam P. "Improvement of propane oxidation activity over Pt/Al_2O_3 by the use of MIXED γ- and χ-Al_2O_3 Supports". Reaction Kinetics, Mechanisms and Catalysis 2010; 100 (2): 441-448.

2. Glinrun T., Mekasuwandumrong O., Panpranot J., Chaisuk C., Powell J., Praserthdam P. "Evaluation of Catalytic and Coke Formation Behavior of γ- and χ-phase Alumina in the Dehydrogenation of Propane" under revision in publication of Applied Catalysis.

3. Glinrun T., Mekasuwandumrong O., Panpranot J., Chaisuk C., Praserthdam P. "A Comparative Study of Pt Catalysts Supported on χ, γ and MIXED γ- and χ-Al_2O_3 Supports Alumina in the Propane Dehydrogenation" submitted to the publication of The Canadian Journal of Chemical Engineering.